

[Click here to view linked References](#)

1
2
3
4 **An overview on severe plastic deformation: research status, techniques classification,**
5 **microstructure evolution and applications**
6
7

8 **E. Bagherpour¹, N. Pardis¹, M. Reihanian^{*2}, R. Ebrahimi¹**
9

10
11 *1. Department of Materials Science and Engineering, School of Engineering, Shiraz University,*
12 *Shiraz, Iran*

13
14 *2. Department of Materials Science and Engineering, Faculty of Engineering, Shahid Chamran*
15 *University of Ahvaz, Ahvaz, Iran*
16
17
18

19
20 **Abstract**
21

22 The present overview gives a new approach toward developments and recent achievements in
23 severe plastic deformation. The review focuses on several subjects. First, an outline of SPD
24 research status in the world is presented by literature analysis based on the total number of
25 publications, citations and the contribution of the top-ranked countries. Second, the mechanisms
26 of grain refinement and grain growth during SPD processing are discussed by means of the latest
27 concepts. Third, all SPD methods invented so far are classified based on a new approach. Up to
28 now, the growing tendency of researchers to introduce new SPD techniques results in a large
29 number of SPD methods which can be considered as new or modified techniques or a
30 combination of previous ones. Such a reference can help to prevent the future duplication to
31 introduce the SPD processes, which are technically similar. At the end, the practical applications
32 of ultrafine/nanostructured materials and industrial commercialization of SPD methods are
33 summarized.
34
35
36
37
38
39
40
41
42
43
44
45
46
47
48
49
50

51 **Keywords:** Severe plastic deformation; Nanostructured materials; Grain refinement; Research
52 status; Application
53
54
55

56
57
58 *Corresponding author. m.reihanian@scu.ac.ir (M. Reihanian);
59 Tel.: +98 61 33330010 19x5684; fax: +98 61 33336642
60
61

1
2
3
4 **List of abbreviations**
5
6
7

8 ABE Accumulative back extrusion
9
10 ACCB Accumulative Channel-Die Compression Bonding
11
12 AccumEx Accumulated Extrusion
13
14 AE Alternate Extrusion
15
16 AFF Accumulative Fold-Forging
17
18 AFSE Axi-symmetric forward spiral extrusion
19
20 ARB Accumulated roll bonding
21
22 ASB Accumulative Spin Bonding
23
24 C2S2 Continuous Confined Strip Shearing
25
26 CAD Channel Angular Deformation
27
28 CCB Continuous Cyclic Bending
29
30 CCC Cylinder Covered Compression
31
32 CCDF Cyclic Closed-Die Forging
33
34 CEC Cyclic Extrusion-Compression
35
36 CECAP Cyclic Extrusion Compression Angular Pressing
37
38 CECRE C Shape Equal Channel Reciprocating Extrusion
39
40 CEE Cyclic Expansion-Extrusion
41
42 CFS Cyclic Flaring and Sinking
43
44 CG Coarse Grained
45
46 CGP Constrained Groove Pressing
47
48 CP Commercially Pure
49
50 CRB Cyclic Rotating Bending
51
52 CR-ECA Integrated conventional Tandem rolling with ECA deformation
53
54 CSCW Clustered-Small-Cell Wall
55
56 CTE Compound Twist Extrusion
57
58 CVCDE Variable Cross-Section Direct Extrusion
59
60 CVCE Continuous Variable Cross-Section Recycled Extrusion
61
62 DECLE Dual Equal Channel Lateral Extrusion
63
64 DDW Dense-Dislocation Wall
65

1		
2		
3		
4	DTZ	Dislocation Tangle Zone
5		
6	EBS	Electron Back Scatter Diffraction
7		
8	ECAD	Equal Channel Angular Drawing
9		
10	ECAP	Equal Channel Angular Pressing
11		
12	ECAP-FE	Equal Channel Angular Pressing-Forward Extrusion
13		
14	ECATD	Equal Channel Angular Torsion Drawing
15		
16	ECFE	Equal Channel Forward Extrusion
17		
18	ECSEE	Elliptical Cross-Section Spiral Equal-Channel Extrusion
19		
20	EL	Laminar Structure
21		
22	FE-ECAP	Forward Extrusion- Equal Channel Angular Pressing
23		
24	FSP	Friction Stir Processing
25		
26	FSBE	Friction Stir Back Extrusion
27		
28	GNB	Geometrically Necessary Boundary
29		
30	HAGB	High Angle Grain Boundary
31		
32	HCAE	Half Channel Angular Extrusion
33		
34	HPDT	High-Pressure Double Torsion
35		
36	HPT	High Pressure Torsion
37		
38	HPT-CS	High pressure torsion-cylindrical segment
39		
40	HPTT	High Pressure Tube Twisting
41		
42	HS-HPT	High-Speed High Pressure Torsion
43		
44	HTP H-	Tube Pressing
45		
46	IDB	Incidental Dislocation Boundary
47		
48	IDC	Isolated Dislocation Cell
49		
50	I-ECAP	Incremental ECAP
51		
52	LSEM	Large Strain Extrusion Machining
53		
54	MAIFS	Multi-Axial Incremental Forging& Shearing
55		
56	MSB	Micro Shear Band
57		
58	NDMX	Nanodynamics High Performance
59		
60	NP	Number of publication
61		
62	NRE	Nonlinear Rotary Extrusion
63		
64	OIM	Orientation Imaging Microscopy
65		

1		
2		
3		
4	PFM	Plastic Flow Machining
5		
6	PSE	Pure Shear Extrusion
7		
8	PTCAP	Parallel Tubular Channel Angular Pressing
9		
10	PTE	Planar Twist Extrusion
11		
12	RCS	Repetitive Corrugation & Straightening
13		
14	RF	Repetitive forging
15		
16	RT	Rotary Extrusion
17		
18	RUE	Repetitive Upset Extrusion
19		
20	SCAP	Symmetrical channels angular pressing
21		
22	SFE	Stacking Fault Energy
23		
24	SFT	Stacking Fault Tetrahedron
25		
26	Sp-ECAE	Spiral Equal Cannel Angular Extrusion
27		
28	SPD	Severe Plastic Deformation
29		
30	SRAR	Single-Roll Angular-Rolling
31		
32	SSE	Simple Shear extrusion
33		
34	STS	Severe Torsion Straining
35		
36	TCAP	Twist Channel Angular Pressing
37		
38	TCAP	Tube Channel Angular Pressing
39		
40	TCEC	Tube Cyclic Extrusion-Compression
41		
42	TCMAP	Twist channel multi-angular pressing
43		
44	TE	Twist Extrusion
45		
46	T-ECAP	Torsional-equal channel angular pressing
47		
48	TEM	Transmission Electron Microscopy
49		
50	HPS	High-Pressure Shearing
51		
52	TSP	Tube Channel Pressing
53		
54	TST	Tandem Process of Simple Shear Extrusion & Twist Extrusion
55		
56	TWIP	Twinning Induced Plasticity
57		
58	UDW	Uncondensed Dislocation Wall
59		
60	UFG	Ultrafine-Fine Grained
61		
62	VE	Vortex Extrusion
63		
64		
65		

1
2
3
4 **Table of contents**
5

6
7 1. Introduction
8

9 2. The SPD research status in the world
10

11 3. Microstructural evolutions by SPD
12

13
14 3. 1. Grain refinement
15

16 3.1.1. Grain refinement by dislocation activity
17

18 3.1.2. Grain refinement by twinning
19

20
21 3.2. Grain growth
22

23 3.2.1. Grain growth as a consequence of shear strain reversal
24

25 3.2.2. Grain growth in large strains (low grain sizes)
26
27

28 4. Classification of SPD techniques
29

30 5. Application of SPD processed materials
31

32 5.1. SPD processed Al and Cu sputtering targets
33

34 5.2. UFG CP Ti for biomedical application
35

36 5.3. UFG materials for sport applications
37

38 5.4. SPD processed materials for Hydrogen Storage
39
40

41 6. Summary and conclusions
42

43
44 Acknowledgments
45

46
47
48 References
49
50
51
52
53
54
55
56
57
58
59
60
61
62
63
64
65

1
2
3
4 **1. Introduction**
5

6 During the last two decades, severe plastic deformation (SPD) has attracted the increasing
7 attention of the research community due to its potential for the fabrication of bulk nanostructured
8 and ultra-fine grained materials [1]. Several advantages of SPD methods together with the unique
9 physical and mechanical properties inherent to nano/ultra-fined grained materials have caused
10 the specialists' interest to grow remarkably toward the characterization, modification and
11 development of new SPD methods [2,3]. The historical development in SPD processing has been
12 categorized by Langdon into three ages [4]: the ancient age, the scientific age and the
13 microstructural age. According to the Langdon's report, the artisans were the first that utilized
14 the fundamental principles of this type of metal processing in the ancient times. During the Han
15 dynasty around 200 BC, the local artisans in ancient China developed a forging process in order
16 to introduce substantial hardening of steel for use in swords. This technique consisted of a
17 repetitive forging and folding to produce high strength steels. This technique was then expanded
18 to produce Damascus steel in ancient Syria and Wootz steel in ancient India.
19

20
21
22
23
24
25
26
27
28
29
30
31
32
33
34
35
36
37
38 The start of the scientific age goes back to the pioneering work of Bridgman [5]. Bridgman
39 combined the compression and shear deformation to investigate the effects of high pressures on
40 bulk metals [6]. The achievements in this field led to his winning of the Nobel Prize in physics in
41 1946. Further development of this method, presently known as High-Pressure Torsion (HPT) [7],
42 was conducted in formerly Sverdlovsk in the former Soviet Union [8]. Thereafter, in the 1970s
43 and 1980s at an institute in Minsk in the former Soviet Union, Segal and his co-workers
44 introduced a novel forming method, known as equal-channel angular pressing (ECAP), in order
45 to impose high strains into the metal billets by simple shear [9]. Despite the basic innovation
46 during the scientific age, the main attention was directed to the development of material
47
48
49
50
51
52
53
54
55
56
57
58
59
60
61
62
63
64
65

1
2
3
4 processing and little attention was given to the microstructural features of the SPD processed
5
6 metals.
7

8
9 The situation was changed during the microstructural age when new and advanced tools such as
10
11 transmission electron microscopy (TEM), high-resolution TEM, electron back scatter diffraction
12
13 (EBSD), orientation imaging microscopy (OIM) and modern X-ray analysis were innovated. The
14
15 first developments and investigations of nanostructured materials processed by SPD methods
16
17 were fulfilled by Valiev and his co-workers in Ufa in the early 1990's [10]. In fact, through
18
19 several publications, Valiev and his co-workers demonstrated the potential for using SPD
20
21 process to produce nanostructured and ultrafine-grained metals with new and unique properties
22
23 [11]. Subsequently, the microstructural features of nano/ultra-fine grained materials fabricated by
24
25 SPD were progressively of more interest to various scientists around the world outside of Russia
26
27 [12].
28
29
30
31
32

33 At present, besides the numerous published works on microstructural evolution during SPD
34
35 processing, very different and new SPD processes have been developed and evaluated. The most
36
37 common and popular SPD methods are HPT [13,7], ECAP [9,12] and accumulative roll bonding
38
39 (ARB) [14]. Though the growing interest in SPD processing is limited only to the last decade,
40
41 this subject area has made a remarkable impact on published works within the scientific
42
43 community. This is proved by considering the increasing number of publications high numbers
44
45 of citation, numerous specific conferences, workshops and symposia on the subject of SPD
46
47 process. Therefore, the present authors believe that in recent years a new age, named as
48
49 progressive age, has started for SPD processing. This age is characterized by unusual properties
50
51 of processed materials, powder consolidation, composite production and simulation on the one
52
53 hand, and by the development of new SPD methods on the other hand. Regarding the rapid
54
55
56
57
58
59
60
61
62
63
64
65

1
2
3
4 developments during the progressive age of SPD processing, an examination of its impact on the
5 scientific community with emphasis on the contribution of various countries, new achievements
6 and new SPD methods needs to be conducted.
7
8
9

10
11 To date several review papers have been published in this subject area. Some of them
12 characterize the aspects of a particular SPD method such as ECAP [15,12,16-19] and HPT
13 [7,13,20,21], others investigate the nano/ultrafine grained characteristics of SPD methods
14 [7,12,22,15,23-25,3] and the rest consider the new SPD methods that have been developed so far
15 [26]. Regarding several review papers published in this field, the present overview is an attempt
16 to provide some other aspects of SPD methods to which little attention has been paid. These
17 aspects includes the SPD research status in the world, new concepts of grain refinement,
18 collection of all invented SPD methods and new aspects of SPD application. Therefore, in one
19 section, the impact and status of the SPD on the research community are evaluated by
20 considering the contribution of the top-ranked countries. For this purpose, all data are taken from
21 Thomson Reuters ISI Web of Science. In another section, the microstructural evolution during
22 SPD is reviewed by considering several new concepts such as grain refinement by twining, grain
23 growth due to the strain reversal and grain growth because of the large plastic strains. In the next
24 section, all methods of SPD that have been proposed and developed so far are introduced based
25 on a new classification. This section provides a comprehensive source available to cover most of
26 the SPD methods presented up to now. Finally, the potential of SPD methods for practical
27 applications is presented.
28
29
30
31
32
33
34
35
36
37
38
39
40
41
42
43
44
45
46
47
48
49
50
51
52
53
54
55
56
57
58
59
60
61
62
63
64
65

2. The SPD research status in the world

Over the past three decades, producing bulk ultrafine-grained (UFG) and nanostructured materials through the application of SPD methods has attracted a considerable interest in the field of materials science and engineering [17,20]. Based on Thomson Reuters, more than 10000 researchers from 80 countries have contributed to the investigation and development of SPD methods. However, just about 1400 researchers have published more than 5 documents (>0.05%). In addition, in terms of the contribution of different countries, just 32 countries have published more than 40 items (>0.5%). This depicts the importance of SPD in these countries. Fig. 1a shows the ranking of countries according to the total number of publications (NP) in the field of SPD in two different periods of 1990- 2018, and 2008-2018 based on Thomson Reuters ISI Web of Science. According to the total NP up to the end of May 2018, in general, researchers from Russia, China, USA, Japan and Germany have published the highest number of articles. However, the position of countries has changed during the recent decade. China, Russia, USA, Japan and Iran are the first countries during 2008-2018.

The total NP is not a comprehensive measurement to assess the impact and the quality of the publications. To compare the quality and impact of the publications, the *h*-index and the average number of the times a document has been cited for the publication during 2008-2018 (by the first ten countries in the field) are illustrated in Fig. 1b. In accordance to this figure, the highest values of *h*-index are attributed to researches from the USA, Japan, England, Russia, and Germany. On the other hand, according to average citation per article, England, Australia, USA, Japan and Germany are on the top of the list. Considering both the total number of publications and the number of citations (Fig. 1a and Fig. 1b), it is seen that despite the high number of publications from some countries like China, Iran, and India, the *h*-index and the average citation to them are

1
2
3
4 relatively low. This can be attributed to the difference in the visibility and the importance of
5
6 publications due to several reasons.

7
8
9 The visibility of a research arises from two factors including its presentation in the international
10 conferences and collaboration with researchers from other nations. Attending international
11 conferences is an important way for scientists to introduce their new achievements to colleagues
12 from other countries. Therefore, the visibility of the documents can rise by participating and
13 presenting articles in international conferences. In addition, discussions after the presentation,
14 with other colleagues can lead to the improvement of the presented research and also future
15 works. Therefore, the investigation of the total number of documents published in the
16 proceedings is a good measurement to check the visibility.
17
18
19
20
21
22
23
24
25
26
27

28 Based on this argument, the documents are divided into different types including original journal
29 articles, conference proceedings, review articles and book chapters. The fraction of various types
30 of published documents by the researchers for some of the most important countries in SPD is
31 shown in Fig. 2. Interestingly, the highest number of review papers and book chapters has been
32 published by researchers from USA, Russia, Germany and Australia while the Russians and the
33 Japanese have the highest fraction of articles presented in conferences. As shown in Fig. 1b,
34 these countries have the highest value of h -index.
35
36
37
38
39
40
41
42
43
44

45 Another indication of the visibility of the articles that leads to higher numbers of citation is the
46 collaboration with other scientists. The collaboration of various countries in the field of SPD up
47 to the end of 2017 for the top 15 countries in the field of SPD is plotted in Fig. 3. The countries
48 are specified by circles and their collaborations are denoted by the solid lines. The countries of
49 each continent are indicated by a specific color. The size of each circle is an indication of the
50 collaboration of that country with the other countries. The higher number of articles published in
51
52
53
54
55
56
57
58
59
60
61
62
63
64
65

1
2
3
4 collaboration with scientists from other countries causes the circle to be larger. It is obvious that
5
6 England has the highest collaboration and Australia and Germany are ranked after. It should be
7
8 pointed out that England is an exception, because Langdon, who has a high number of
9
10 publications in SPD, has two affiliations with the University of Southern California and the
11
12 University of Southampton. Interestingly, countries like Australia and South Korea with a low
13
14 number of proceedings papers (Fig. 2), have relatively high collaboration (Fig. 3), which may
15
16 result in the high rank of these countries based on citation (Fig. 1b). Another interesting feature
17
18 of this map is the low collaboration of Asian countries.
19
20
21
22

23
24 Since the invention of ECAP in 1981[9], it has attracted the attentions of many from materials
25
26 scientific community that results in more than 5000 published documents. The large number of
27
28 publications in this field has made ECAP the most popular SPD method. Referring to Fig. 4a, the
29
30 USA, China and Russia are the first countries in the world with more than 900, 900 and 700 NP,
31
32 respectively. By limiting the scope of the search to 2008-2018, China becomes the first following
33
34 by Russia and the USA. Interestingly, the highest progress attributes to Iran. While Iran ranks the
35
36 ninth during the total period, it climbs in the list and becomes the fourth in the period of 2008-
37
38 2018. A closer look at the variation of NP during this period indicates that in the USA, Japan,
39
40 South Korea and Germany, the NP in the field of ECAP decreased from 2008 to 2018 and the
41
42 NP remained approximately constant in Russia, China and Czech Republic. Iran is the only
43
44 country that retains its progress and its NP increased gradually from 2008 to 2018. To compare
45
46 the quality and impact of the publications in the field of ECAP, the rank of countries according
47
48 to the h-index and the average number of times an item has been cited for the total number of
49
50 documents during 2008-2018 is shown in Fig. 4b. Studies conducted in England, the USA,
51
52 Germany, Australia and Japan have received more attention.
53
54
55
56
57
58
59
60
61
62
63
64
65

1
2
3
4 The second popular method of SPD is HPT with more than 2800 published documents up to
5 now. In HPT, a specimen is subjected to torsional shear straining under a high hydrostatic
6 pressure [13,20,21]. HPT is usually applied to the disk-shaped specimens [20], though HPT
7 processing of the cylindrical [27,28] and the sheet samples [29] has been reported outstandingly.
8
9 The HPT method was first introduced by Bridgman in 1935 [13]. However, the importance of
10 HPT in SPD community mainly comes from the report of Valiev and his co-workers in 1988
11 [30]. According to Web of Science, from that time to 2018, most of the researches in this field
12 have been performed in Russia, USA, China, Japan and England (Fig. 4c). As shown in Fig. 4c,
13 the same trend is seen in the recent decade (2008-2018). An interesting feature of this figure is
14 that, by comparing this figure with Figs. 1a and Fig. 4a, the first-ranked countries in SPD and
15 also in ECAP and HPT are the same but they appear in a different order. The rank of countries
16 according to the *h*-index and the average number of times an item has been cited for the total
17 number of documents in HPT are shown in Fig. 4d. As can be seen, publications from USA,
18 Japan, England, Russia, and China have the highest *h*-index. Regarding the average number of
19 citation to an article, England, the USA, and Australia are the firsts in the ranking. This confirms
20 the high quality of the researches conducted in Australia, despite the low number of publication
21 in this field.
22
23
24
25
26
27
28
29
30
31
32
33
34
35
36
37
38
39
40
41
42
43
44

45 In addition to ECAP and HPT, ARB (invented in 1998) [14] is another popular method of SPD.
46 Up to now, more than 900 documents have been published in the field of ARB. As illustrated in
47 Fig. 4e, Iran and Japan have the first and second rank in the world with 247 and 202 records in
48 ARB, respectively. The third position is held by China with approximately half the number of
49 the publications of Iran and Japan. This indicates that ARB has attracted considerable attention
50 from Iranians considering the fact that ARB in Iran began 10 years after the first efforts of the
51
52
53
54
55
56
57
58
59
60
61
62
63
64
65

1
2
3
4 Japanese in this field. The rank of countries in ARB does not change significantly during the
5 recent ten years. Compared with ECAP and HPT, it is seen that Russians are not interested in
6 ARB in spite of their high tendency to the other methods. In Contrast, several researchers from
7 other countries that have a contribution in field of ECAP and HPT, are interested in ARB too.
8
9 For instance, researchers from Canada and Denmark have published considerable number of
10 articles in the field. Looking to the average citations and *h*-index of the publication during 2008-
11 2018 (Fig. 4f), it is observed that the publications from Iran, USA, Japan, Germany and Australia
12 could attract the most attention through the scientific community.
13
14
15
16
17
18
19
20
21
22
23
24

25 **3. Microstructural evolutions by SPD**

26
27 The SPD induced structural evolution and the corresponding deformation mechanisms have been
28 investigated extensively. Not only did the studies confirm the grain refinement in SPD products,
29 but also they expressed the occurrence of grain growth depending on the grain sizes at the time
30 of the deformation and the deformation conditions. In this section, the mechanisms of grain
31 refinement and grain growth by SPD processing are discussed.
32
33
34
35
36
37
38
39
40
41

42 **3.1. Grain refinement**

43
44 A large number of works and review papers have been published to describe the mechanisms of
45 grain refinement in SPD processing. Therefore, this paper presents only some generalized
46 mechanisms to complete the academic history of the current work. The mechanism of grain
47 refinement during SPD is controlled mainly by two main factors: process parameters including
48 the strain, strain rate, temperature and deformation path and materials parameters such as initial
49 grain size and stacking fault energy (SFE).
50
51
52
53
54
55
56
57
58
59
60
61
62
63
64
65

1
2
3
4 Tao and Lu [31] have shown that grain refinement through dislocation glide and twinning are two
5
6 competitive mechanisms of grain refinement in FCC metals. They state that the strain rate and
7
8 temperature are two important process variables that control the mechanism of microstructural
9
10 refinement during plastic deformation. In order to combine the effect of temperature T and that
11
12 of the strain rate $\dot{\epsilon}$ they used Zener-Hollomon parameter, $Z = \dot{\epsilon} \exp(-Q/RT)$ where R is the
13
14 gas constant and Q is the activation energy for deformation. Their results showed that by
15
16 increasing Z (i.e., increasing strain rate and/or decreasing temperature) the refinement by
17
18 twinning mechanism becomes more dominant. They also indicated that at a critical Z^* , which
19
20 designates a critical strain rate and/or a critical temperature, a transition in the dominating
21
22 refinement mechanism from slip by dislocations to twinning occurs. The critical Z^* depends on
23
24 the SFE, a material parameter, that crucially determines whether the deformation occurs by slip
25
26 or twinning. The deformation by twinning is dominated at low to medium SFE even at low strain
27
28 rates or at high temperatures. In contrast, the deformation mode in high SFE materials is
29
30 controlled by slip even at relatively high strain rates and/or at low temperatures. Therefore, it can
31
32 be concluded that Z^* increases with increasing SFE (Fig. 5). For low SFE metals, the structural
33
34 refinement is dominated by twinning even under low Z conditions, for medium SFE metals the
35
36 twinning mechanism may be active just under high Z values and for high or very high SFE metals
37
38 the grain refinement occurs through dislocation activity even at high Z conditions.

39
40 In addition to SFE, the initial grain size can also affect the mode of deformation and determines
41
42 the mechanism of grain refinement. It has been shown that by changing the microstructure from
43
44 coarse grain to ultrafine or nano-structure, the possibility of deformation by twinning becomes
45
46 more effective. In other words, by reducing the grain size, the mechanism of grain refinement
47
48
49
50
51
52
53
54
55
56
57
58
59
60
61
62
63
64
65

1
2
3
4 through twinning is more likely to be dominant. It has been concluded that the variation in Z^*
5
6 with SFE (i.e., Z^* -SFE line in Fig. 5) can be shifted to the right when the grain size is reduced.
7
8
9

10 11 **3.1.1. Grain refinement by dislocation activity** 12

13
14 Dislocation activity that results in grain refinement is mainly categorized as dislocation gliding,
15
16 accumulation, interaction, tangling and spatial rearrangement. There have been a number of
17
18 models such as Sach's zero constraint [32], relaxed constraint [33], and Taylor's full constraint
19
20 [34] models. However, the most pronounced one, particularly for equiaxed grains, is Taylor's
21
22 model in which strain compatibility is achieved through simultaneous operation of at least five
23
24 slip systems [34,35]. With the acknowledgment of Taylor's model, the so-called grain
25
26 subdivision mechanism has been proposed [36]. During plastic deformation, the non-equilibrium
27
28 grain boundaries formed by dislocation accumulation are the key factor for structural
29
30 characterization [1] because at large strains the microstructure contains very high fraction of high
31
32 angle grain boundaries. Fig. 6 illustrates a schematic model for the formation of non-equilibrium
33
34 dislocation boundaries during SPD. During plastic deformation, the non-equilibrium grain
35
36 boundary introduces an excess energy and long range elastic stresses.
37
38
39
40
41

42
43 The progressive accumulation of dislocations into dislocation boundaries results in the formation
44
45 of two types of dislocation boundaries with different structure and morphologies [37]. One is the
46
47 incidental dislocation boundaries (IDBs) that are formed by mutual trapping of glide dislocations
48
49 subdivide the grains into cells. These boundaries have mainly a tangled dislocation structure.
50
51 Geometrically necessary boundaries (GNBs) are another type of dislocation boundaries that are
52
53 formed due to the activation of different slip system in adjacent grains or due to partitioning of
54
55 total shear strain among a set of slip planes. These types of boundaries subdivide the grains into
56
57
58
59
60
61
62
63
64
65

1
2
3
4 cellblocks and are nearly planar boundaries with a regular dislocation structure. With increasing
5
6 the plastic strain, the boundary spacing of both IDBs and GNBs decreases whereas their
7
8 misorientation angle increases. However, the rate of change of boundary spacing and
9
10 misorientaion angle of GNBs is higher than that of IDBs. At large strains, a high fraction of
11
12 dislocation boundaries, particularly GNBs, change their misorientation into the high angle grain
13
14 boundaries and an ultrafine-grained structure is formed. The gradual change of the dislocation
15
16 boundaries produced at low strains into the high angle boundaries at large strains is called the in-
17
18 situ or continuous dynamic recrystallization [38]. The characteristics of this type of mechanism
19
20 are that at large plastic strains the microstructure contains a wide distribution of misorientation
21
22 angles and the low and high angle grain boundaries are spatially mixed throughout the structure.
23
24 TEM image of the microstructure of pure Al after six cycles of ARB is presented in Fig. 7 as an
25
26 example [39]. The misorientation map of the framed area is also included.
27
28
29
30
31
32

33 Another key factor in the grain refinement is the initial grain orientations. Based on a mechanism
34
35 proposed by Xue et al. [40] for the grain refinement of OFHC Cu in the first pass of ECAP, the
36
37 initial orientation of the grains affects the grain refinement (as shown in Fig. 8). This model
38
39 explains that the microstructural changes in the first ECAP pass usually contains four stages:
40
41 “dislocation generation” (Fig. 8b), “dislocation cell construction” (Fig. 8b), “self-organized
42
43 gliding along the main slip planes and an elongated laminar structures (ELS) formation (Fig.
44
45 8c)”, and the “possible formation of a second set of ELS and/or secondary microbands” (Fig.
46
47 8d). They concluded that all the ELSs were found to develop on $\{1\ 1\ 1\}$ planes. They often
48
49 appeared to have their boundaries either nearly parallel or perpendicular to the micro shear bands
50
51 (MSBs).
52
53
54
55
56
57
58
59
60
61
62
63
64
65

1
2
3
4 Moreover, it is well discovered that the final dimension of refined grains is directly associated
5 with some initial substructure characteristics prior to reaching the MSP. According to the model
6 proposed by Sakai et al. [38,39,41,42] (Fig. 9), MSBs develop and cross each other to form
7 equiaxed structure at intersections and later along the bands. Further processing increases the
8 density of MSBs to reach an equiaxed structure with ultrafine grain size. In fact, the minimum
9 grain size achieved by a specific SPD process is determined through the development of a
10 dynamic balance between dislocation generation and dislocation recovery [7].
11
12
13
14
15
16
17
18
19
20

21 The authors would like to refer the readers to the fact that IDBs and GNBs are general terms and
22 if one likes to investigate the boundaries in more detail, he/she should consider five dislocation
23 structures that have been detected in severely deformed materials by Huang et al. [35]. These
24 include clustered-small-cell wall (CSCW), uncondensed dislocation wall (UDW), isolated
25 dislocation cell (IDC), dense-dislocation wall (DDW), and dislocation tangle zone (DTZ). A
26 TEM image of nanostructured Cu subjected to RCS process containing various types of
27 boundaries is shown in Fig. 10. Usually DDWs, UDWs and CSCWs are observed in GNBs. The
28 CSCWs are similar to the micro shear bands defined by Hansen *et al* [43,44]. Although DDWs
29 and CSCWs have been detected in both rolled and severely deformed microstructures, IDCs,
30 UDW and DTZs have not been observed in rolled microstructures. It should be pointed out that
31 UDWs and DTZs have been detected in fatigued polycrystalline copper [45] as well.
32
33
34
35
36
37
38
39
40
41
42
43
44
45
46
47
48
49

50 **3.1.2. Grain refinement by twinning**

51 This mechanism is important in metals with low to medium SFE particularly at high strain rates
52 and/or at low temperatures when the critical shear stress for twinning is lower than that of
53 dislocation glide. According to this mechanism, plastic deformation causes the formation of
54
55
56
57
58
59
60
61
62
63
64
65

1
2
3
4 several deformation twins within the coarse grains. The average spacing between adjacent twin
5 boundaries may be in the nanometer scale and twin/matrix (T/M) lamellae with a nanoscale
6 thickness [46].
7
8
9

10
11 Based on the development of deformation twin structures in various FCC metals, Tao and Lu
12 [31] proposed four different mechanisms for grain refinement through twinning. These
13 mechanisms are twin/lamellae (T/M) fragmentation, formation of twins, twin/twin intersection
14 and shear banding of T/m lamellae. Fig. 11 illustrates the schematic models and the
15 corresponding TEM images of four structural refinement mechanisms. According to the first
16 mechanism, the T/M layers are fragmented by the accumulation of dislocations and formation of
17 IDBs within them (Ia). With increasing the strain, the misorientation angle of the IDBs increases
18 and at the same time, twin boundaries lose their coherency due to the absorption of more
19 dislocations (Ib). This mechanism has been observed in Cu deformed through surface
20 mechanical attrition treatment process at ambient temperature (Ic) [47]. In the second
21 mechanism, the formation of the secondary twins within the T/M lamellae plays a significant
22 role in twin layer subdivision (IIa) and as before the interaction of dislocations with twin
23 boundaries results in incoherency across the refine volumes (IIb). The formation of secondary
24 twins within the T/M lamellae has been observed in the surface layer of a surface mechanical
25 grinding treatment Cu sample (IIc) [48]. The third mechanism can occur in the FCC metals that
26 have low SFE. According to this model, the formation of multiple twins inside the T/M lamellae
27 (IIIa) subdivides the twin layers into smaller blocks (IIIb) with high misorientation. A typical
28 TEM image of multiple twin formation after surface mechanical attrition treatment of 304 type
29 stainless steel is shown in (IIIc) [49]. According to the fourth model, the localized deformation in
30 the form of shear banding takes place across the T/M lamellae (IV a and b). The formation of
31
32
33
34
35
36
37
38
39
40
41
42
43
44
45
46
47
48
49
50
51
52
53
54
55
56
57
58
59
60
61
62
63
64
65

1
2
3
4 nano-sized and equiaxed grain with random orientations in the shear zone is the responsible
5
6 mechanism for grain refinement. The experimental evidence of the formation of shear band
7
8 within the T/M lamellae in a dynamic plastic deformation Cu is shown in IVc [48].
9

10 11 12 13 14 **3.2. Grain growth**

15
16 There is always a minimum average grain size achieved after a specific SPD processing of a
17
18 specific material (usually after several passes). The minimum average grain size is a function of
19
20 process parameters and materials parameters. The minimum grain size is achieved by the
21
22 dynamic balance between the grain refinement process and the grain growth process which is
23
24 evident in SPD processes [50]. In addition to the grain growth due to the large deformation, there
25
26 are a few recent reports that show the grain growth as a consequence of strain reversal during
27
28 SPD processes. In the following, the plastic deformation induced grain growth in two levels of
29
30 deformation is explained, in early stages of SPD in some non-monotonic processes and less than
31
32 a minimum average grain size (in high strains).
33
34
35
36
37
38
39
40

41 **3.2.1. Grain growth as a consequence of shear strain reversal**

42
43 Although the role of strain reversal in softening (Bauschinger effect) and the resulting structure
44
45 have been studied sufficiently for fatigue test conditions, but the plastic strain in fatigue tests is
46
47 lower than 1% and it is of great importance to investigate the effect of strain reversal in SPD
48
49 processes. A few articles have studied the effect of shear strain reversal on microstructural
50
51 evolution during various SPD processes. For example, the effect of strain reversal during HPT
52
53 was investigated by Horita and Langdon [51] in 2005, Wetscher and Pippan [52] in 2006 and
54
55 Orlov et al. in 2009 [53]. One of the most comprehensive studies on the effect of shear strain
56
57
58
59
60
61
62
63
64
65

1
2
3
4 reversal on the microstructure and texture of SPD processed samples has been published in a set
5 of publications during 2016-2018 by Bagherpour et al. [54-58]. They deformed pure Cu samples
6 by a single pass of simple shear extrusion (SSE) process, which interestingly contained shear
7 strain reversal. Using TEM, STEM and EBSD investigations, they calculated the grain size,
8 texture and dislocation density of the samples during the process in regions of both forward and
9 reverse shear and proposed a model for the microstructural changes during shear strain reversal.
10
11
12
13
14
15
16
17
18

19 The proposed model for the microstructural evolution during SSE processing can be generalized
20 to every process such as TE and ECAP in route C in which shear strain reversal is inherent (non-
21 monotonic processes). The model is an extension to rotational (in-situ) recrystallization [59] in
22 the presence of shear strain reversal. Fig. 12 illustrates a schematic of the model. As it was
23 discussed in the previous sections, the grain subdivision is the main mechanism in the forward
24 shear and consequently elongated cells with interconnecting subgrains are formed gradually
25 during forward shear. By reversing the shear, the dislocation fluxes are reversed leading to the
26 reduction of the stored excessive dislocations introduced in the boundaries by the activation
27 imbalance and also resulting in disintegration of the misfit dislocations. In addition, the cyclic
28 behavior of the SPD process retarded the formation of HAGBs as a consequence of a kind of
29 Bauschinger effect. For Cu during one pass of SSE, the dislocation density decreased by ~14%,
30 cell wall became thicker by 20% and the lamellar boundary spacing increased by 12%, as a result
31 of shear strain reversal [54]. In general, shear strain reversal during the SPD process have four
32 main consequences: i) the inclination angle between the boundaries and the shear direction
33 increases; ii) the total amount of HAGBs is reduced; iii) the cell walls become thinner and iv) the
34 dislocation density decreases.
35
36
37
38
39
40
41
42
43
44
45
46
47
48
49
50
51
52
53
54
55
56
57
58
59
60
61
62
63
64
65

1
2
3
4 Furthermore, the effect of shear strain reversal on the texture changes of the pure copper during a
5 single pass of SSE has been investigated by finite element analysis [58] and examined
6 experimentally [55]. It has been shown that the simple shear texture is formed gradually in the
7 forward shear. However, the degree of the simple shear texture decreases gradually by shear
8 strain reversal while the major components are still simple shear texture after the end of the
9 process. It must be pointed out that the texture after the end of the processes that contain shear
10 strain reversal depends on the magnitude of both forward and reverse shear.
11
12
13
14
15
16
17
18
19
20

21 It is clear that the mechanism of grain growth by shear strain reversal for fcc metals is well
22 developed. However, for other metals, bcc or hcp ones, the occurrence of grain growth in the
23 presence of shear strain reversal and its mechanism require more investigations.
24
25
26
27
28
29
30

31 **3.2.2. Grain growth in large strains (low grain sizes)**

32 During each SPD method, the grains can be refined to a specific size depending on the stacking
33 fault energy of the material. That is, further processing of the material by SPD method cannot
34 refine the grains anymore. For a specific material, the minimum grain size achievable in a SPD
35 process is controlled by a dynamic equilibrium between the grain refinement and grain growth,
36 which depends on the intrinsic material properties (stacking fault energy, purity, melting
37 temperature, etc.) and extrinsic processing parameters (temperature, strain rate, amount of
38 hydrostatic pressure, deformation mode, etc.) [56]. Plastic deformation- induced grain growth
39 has been widely reported in various SPD methods including HPT [60-63][64-67], ECAP
40 [12,50,64], ARB [65,66] [70,71] and SSE [56,57]. Different mechanisms has been proposed for
41 the strain induced grain growth in nanocrystalline (NC) materials that include the rotation of
42 nano-grains and propagation of shear bands [67], grain boundary migration [68] and stress
43
44
45
46
47
48
49
50
51
52
53
54
55
56
57
58
59
60
61
62
63
64
65

1
2
3
4 coupled grain-boundary migration (a grain grows at the expense of other neighboring grains)
5
6
7 [69].

8
9 One of the promising mechanisms for the strain induced grain growth has been proposed in 2008
10
11 by Wang et al. [60,70] by using a nano-beam electron diffraction investigation of nanocrystalline
12
13 Ni in response to the in-situ tensile deformation under TEM. A schematic of the model, which is
14
15 based on the grain rotation, is illustrated in Fig. 13. Consider a nanostructured material with
16
17 high-angle grain boundaries for the original material, as shown in Fig. 13a. Because of plastic
18
19 deformation, a relative shear between grains 1 and 2 occurs along their boundary through grain
20
21 boundary dislocation glide. At the same time, grain rotation in the neighboring grain 3 takes
22
23 place because of climbing grain boundary dislocations (Fig. 13b). Climb of grain boundary
24
25 dislocations results from the splitting of gliding grain boundary dislocation at triple junction into
26
27 two climbing grain boundary dislocations [71]. By additional deformation, the other grains
28
29 adjacent to grain 3 (e.g., grains 1 and 2) rotate in order to reduce the grain boundary angles and
30
31 to form grain agglomerate (Fig. 13c). As shown in Fig. 13d, with further plastic deformation,
32
33 grain coalescence occurs by merging the neighboring grains into a large grain and this completes
34
35 the grain growth.

36
37
38 After accepting the occurrence of grain growth in nanocrystalline materials when reaching a
39
40 certain grain size, it is essential to find the methods to detect this phenomenon and to define this
41
42 certain grain size. The authors wish to draw attention to the point that the exact detection of the
43
44 growth of a special grain is almost impossible unless for a researcher who has access to the in-
45
46 situ TEM investigations. However, it is generally accepted that there are some other
47
48 microstructure pieces of evidence that would be detected only after achieving the critical grain
49
50 size and at the onset of grain growth or afterward. Therefore, it is legitimate to relate the
51
52
53
54
55
56
57
58
59
60
61
62
63
64
65

1
2
3
4 observation of these evidences to the occurrence of grain size in spite of the fact that they are not
5 necessarily due to the grain growth. Considering this, two main questions are raised in mind,
6 including: i) what are these microstructural pieces of evidence? and ii) what is the minimum
7 average grain size below which grain growth occurs? These ambiguities will be clarified in the
8 following paragraphs.
9

10
11 One indication of grain rotation is the formation of Moiré fringes caused by the small angle
12 misorientation of neighboring grains [60]. A TEM image of a Moiré fringes detected in a pure
13 Cu samples severely deformed by 12 passes of SSE, is shown in Fig. 14a . It should be pointed
14 out that in this sample a grain growth of ~5% is seen in the sample of 12 passes in comparison to
15 8 passes [56]. Another indication of the achievement of the minimum grain size in
16 nanocrystalline fcc metals is the formation of twins, which occurs for these materials at room
17 temperature and low strain rates. This phenomena has been described by three distinguished
18 mechanisms including consecutive “partial dislocation emission from grain boundaries (GBs)
19 and GB junctions” [72,73], “dynamic overlapping of stacking faults results in nucleation of twins
20 inside grains” [74] and “twin lamella formation via the dissociation and migration of GB
21 segments” [75]. However, a large amount of plastic deformation is the prerequisite to initiation
22 of twinning. Fig. 14b shows an example of such a deformation twins with twin boundary spacing
23 (λ) measured as ~12 nm. It is initiated from GBs and extended via partial dislocation emission
24 from the neighbor (111) slip plane in Cu samples severely deformed by 12 passes of SSE.
25

26
27 The other sign of attaining the minimum grain size is indicated by stacking fault tetrahedra
28 (SFT), a common type named vacancy clustered defects, which is believed to be formed by the
29 Silcox-Hirsch mechanism [76]. SFTs with sizes of 4–14 nm and an average value of about 7 nm
30 in a grain of Cu detected in a severely deformed sample of 12 passes of SSE are shown in Fig.
31
32
33
34
35
36
37
38
39
40
41
42
43
44
45
46
47
48
49
50
51
52
53
54
55
56
57
58
59
60
61
62
63
64
65

1
2
3
4 14c. Bagherpour et al. [56] found SFTs only in grains that are confined by well-developed sharp
5
6 grain boundaries. These kind of boundaries have been observed in dynamically recovered or
7
8 even partially recrystallized grains and raised from substantial stress relief.
9

10
11 One method to predict the onset of growth is to predict the certain grain size (d_c) below which
12
13 the nano twins can be formed. Huang et al. [77] proposed a relationship for the d_c as

$$d_c = \frac{2\alpha G(nb-b_1)b_1}{\gamma_{SFE}} \quad (1)$$

14
15 where n is a stress concentration factor, b is the Burgers vector of the full dislocation, b_l is the
16
17 Burgers vector modulus of the Shockley partial dislocation, G is the shear modulus, γ_{SFE} is the
18
19 SFE of the metal and α is a parameter reflecting the character of the dislocation. However, it is
20
21 not always easy to measure the SFE for the specific material. In 2017, Bagherpour and his
22
23 coworkers [56] proposed a relationship between γ_{SFE} and the maximum size of SFTs (l_{max}) as
24
25
26
27
28
29
30
31

$$\gamma_{SFE} = \frac{2G(b_3^2-2b_2^2)}{\sqrt{3}l_{max}} \quad (2)$$

32
33 in which b_2 is the Burgers vector modulus of stair-rod dislocations (with Burgers vector of
34
35 $a/6[110]$) and b_3 is the Burgers vector modulus of Frank loop ($a/3\langle 111 \rangle$) dislocations. They
36
37 derived this equation using the energy balance between the total energy of the tetrahedral defect
38
39 and the total energy of the triangular Frank loop and determined the critical grain size to achieve
40
41 nano twins as below
42
43
44
45
46

$$d_c = \frac{\sqrt{3}l_{max}(nb-b_1)b_1}{(b_3^2-2b_2^2)} \quad (3)$$

4. Classification of SPD techniques

47
48 Due to the interesting properties of ultrafine-grained/nanostructured metals processed by SPD
49
50 techniques, many investigations have been dedicated to new roots for processing materials by
51
52 SPD as well as the modifications of the current available techniques. These developments have
53
54
55
56
57
58
59
60
61

1
2
3
4 made it possible to conduct SPD by different deformation modes on metallic materials with
5
6 different shapes/geometries (rods, bars, billets, tubes and sheets).
7

8
9 So far, there have been many reports on different SPD techniques and some review papers have
10
11 been dedicated to this topic [7,12,22,15,23,26,24,25,3]. However, these papers have covered
12
13 only a group of SPD techniques and there is no comprehensive source available to cover most of
14
15 the SPD methods presented so far. Therefore, several duplications have occurred in a field in
16
17 which a unique technique is presented with different names and by different groups of
18
19 researchers. This can happen because the authors, for instance, have not been aware of the
20
21 presence of such a technique before. Therefore, this section tries to fill this gap by providing a
22
23 comprehensive source of SPD techniques and their modifications over the course of years as well
24
25 as the very recent ones. This can lead to a useful reference for researchers working in this field.
26
27
28
29

30
31 Due to the numerous number of SPD techniques presented so far, these techniques are presented
32
33 in separate tables, which are categorized based on the processing method as follows:
34
35

- 36 1- SPD techniques based on equal channel angular pressing/ECAP
- 37
- 38 2- SPD techniques based on torsion/shear under high pressure
- 39
- 40
- 41 3- SPD techniques based on direct/indirect extrusion
- 42
- 43 4- SPD techniques based on pressing/forging
- 44
- 45 5- SPD techniques based on rolling
- 46
- 47 6- Combined SPD techniques
- 48
- 49

50
51 In this section, the authors try to collect (in the following tables) all conventional, modified and
52
53 combined techniques that have been introduced as SPD method so far. The presented references
54
55 can guide the readers to follow each technique/modification and consequently find more
56
57 information/references on that topic.
58
59
60
61

1
2
3
4 By investigating the first publications on each method, the countries, which have contributed to
5 the introduction of each method, can be found. In table 1, all the collaborations of the countries
6 in the mentioned categories are summarized by counting the number of the contributions for each
7 country. Although 19 countries are involved, more than 70% of the innovations come from only
8 7 countries including Iran, Japan, China, the USA, South Korea, the UK and Poland. As shown
9 in Fig. 15, Iran, Japan and china with 20%, 14% and 14% of the total contributions, respectively,
10 are the first countries in this regard. Iran is the only country that has contributed to all the
11 categories.
12
13

14 Table 2 provides different techniques which are presented for SPD processing using the
15 principles of equal channel angular pressing (ECAP). In most cases the main objectives for
16 presenting these various techniques are:
17
18

- 19 1- Providing the possibility of continuous processing of samples (for long samples).
- 20 2- Increasing the grain refinement efficiency of ECAP.
- 21 3- Performing ECAP on samples with various shapes/geometries.

22 In addition, some modifications have been carried out in the design of ECAP to increase the
23 process efficiency by decreasing the processing load or increasing the homogeneity of the
24 processed samples. Some examples are presented in the same table. As can be concluded, most
25 of these modifications have been done in Japan and UK.
26
27

28 The authors would like to draw the attentions of the readers to the fact that the mode of
29 deformation in all of the mentioned methods in the Table 2 is similar to that of ECAP. This can
30 be concluded by a close look to the geometry of the dies and tools in almost all of the methods.
31 However, the similarity of the process of "large strain machining" to ECAP is not as clear as the
32 rest of the methods. To clarify this, a more detail investigation of the deformation mechanism
33
34
35
36
37
38
39
40
41
42
43
44
45
46
47
48
49
50
51
52
53
54
55
56
57
58
59
60
61
62
63
64
65

1
2
3
4 through the process is of great advantage. The plane-strain machining is considered by a sharp,
5
6 wedge-shaped tool that is used to remove a specific depth of a material. This is achieved by the
7
8 movement of the tool in a direction perpendicular to its cutting edge. In the orthogonal cutting
9
10 process, material is severely deformed at a very narrow zone in front of the tool tip. In 1945,
11
12 Merchant [78] proposed that the whole shear strain is imposed on a certain plane called a “shear
13
14 plane”. Fig. 16a, illustrates the position of the shear plane in addition to the general deformation
15
16 model for orthogonal cutting. As observed, the shear plane in the "large strain machining" is
17
18 similar to that of ECAP, which can be found in Fig. 16b. This is the main reason that the authors
19
20 put the process of "large strain machining" in the category of the methods based on ECAP.
21
22
23

24
25 Since tubes are the most practical essentials in aerospace, automobile, building construction,
26
27 petroleum industries, etc. [122], it is sensible to pay further attention to fabricate tubular UFG
28
29 materials. Whereas most of the techniques in Table 2 are capable to process billets or bars, some
30
31 of them, including ECAP are used for processing of tubular samples [114,115]. tubular channel
32
33 angular pressing (TCAP) [121], tube channel pressing (TCP) [122,123], and parallel tubular
34
35 channel angular pressing (PTCAP) [124], are designed to fabricate the nanostructured tubes from
36
37 the initial tubular work pieces. The considerable Iranians’ attention to tubular UFG samples may
38
39 come from the fact that Iran is in the second place in the production of natural gas. Furthermore,
40
41 petrochemical industries are the biggest companies in Iran. Hence, researches in the development
42
43 of tubular sections can attract more funds from both companies and government. Another
44
45 promising aspect of the methods based on ECAP, is its ability to continuous processing of the
46
47 pieces. These methods are conshearing process [82], continuous confined strip shearing (C2S2)
48
49 [83-86], ECAP–Conform [87], Multi ECAP Conform [91], and continuous frictional angular
50
51 extrusion [90]. Therefore, the continuity of the process and its ability to process work pieces
52
53
54
55
56
57
58
59
60
61
62
63
64
65

1
2
3
4 with different shapes and geometries are some of the key factors that make ECAP as a good
5
6 candidate for industrial uses.
7

8
9 Considering the high efficiency of high pressure torsion (HPT) in grain refinement, many efforts
10
11 have been conducted to scale up the sample size as well as the application of a similar
12
13 deformation mode on samples with various geometries (other than disks) like tubes, rings, rods
14
15 and bars. Table 3 summarizes some of these techniques. Similar to the methods based on ECAP,
16
17 researchers from Japan are pioneers in the methods based on high pressure (Table 1).
18
19

20
21 In the SPD techniques illustrated in Table 4, the work piece is pushed to pass through a die with
22
23 special design/geometry with a direct/indirect extrusion channel. However, after the process, the
24
25 sample retrieves its initial geometry, which makes it possible to repeat the process for several
26
27 times. Therefore, a high level of strain can be accumulated within the sample, and consequently,
28
29 a significant structure evolution happens. Most of these techniques can be easily installed on any
30
31 available pressing/direct extrusion facilities. Iranian scholars with more than 30% of the
32
33 contributions in these methods are the first in the world.
34
35
36

37
38 Among all of the methods based on extrusion, twist extrusion (TE) and simple shear extrusion
39
40 (SSE) attracted most attention. For instance, the microstructural changes and mechanical
41
42 behavior of pure aluminum [146-148], pure copper [54-57,149], twinning induced plasticity
43
44 (TWIP) steel [150,151,149,152] and pure magnesium [153-155] after SSE processing was
45
46 studied experimentally. Besides, a number of studies have simulated the process by finite
47
48 element (FE) analysis and/or crystal plasticity FE [156,146,147,58,157,158].
49
50

51
52 The SPD techniques, which can be considered as open/closed die forging techniques, are
53
54 summarized in Table 5. These techniques are designed for giant straining of samples, generally,
55
56 by repeating the process (pressing/forging) on different sides of the sample. A few numbers of
57
58
59
60
61

1
2
3
4 countries including China, the USA and Iran have contributed to these methods and have been
5
6 the most active ones. Accumulative roll bonding (ARB) [14] is a well-known effective technique
7
8 for SPD processing of sheet materials. However, there are other alternatives for SPD processing
9
10 of sheet materials by rolling, which are presented in Table 6.
11
12
13

14 To increase the efficiency in SPD processing, some SPD/forming techniques have been
15
16 combined in a single die / set-up which are presented here as “combined SPD techniques” (Table
17
18 7). These methods benefit from the simultaneous application of different deformation modes in
19
20 addition to the high strain value accumulated within the sample during processing using the
21
22 combined techniques. Therefore, these techniques can generally result in a structure with smaller
23
24 grain size and with a more homogeneous grain size distribution compared to the results, which
25
26 could be obtained after processing by each process alone. These methods attracted the attention
27
28 of Iranian researchers rather than that of the others (Table 1).
29
30
31
32

33 Although SPD techniques are generally designed in a way to retrieve the initial geometry of the
34
35 samples, the initial geometry of the processed sample is not retained after processing by single
36
37 pass SPD techniques. Single pass SPD techniques, however, are capable of introducing relatively
38
39 large plastic strains by combining different modes of deformation that can result in smaller
40
41 grains with a high fraction of HAGBs compared to those of the conventional forming operations
42
43 (like extrusion or rolling). The single pass methods, which can be found in Tables 2-7, are : non-
44
45 equal channel angular pressing /channel angular deformation (CAD) [116,117], double change
46
47 channel angular pressing [118], ECAP forward extrusion (ECAP-FE) [231], forward extrusion
48
49 ECAP (FE-ECAP) [232], incremental angular splitting [119], torsion extrusion [240,241], vortex
50
51 Extrusion (VE) [188,189], variable cross-section direct extrusion (CVCDE) [190,191],
52
53 gradation extrusion [192,193], integrated extrusion [194], compound extrusion [195], compound
54
55
56
57
58
59
60
61
62
63
64
65

1
2
3
4 twist extrusion/C-TE (TE+Ext.)[243], alternate extrusion (AE) [196], large strain machining
5
6 [120] and large strain extrusion machining (LSEM) [245]. It is noted that among all SPD
7
8 method, friction stir processing (FSP) [144,145] can be categorized as a single-pass or multi-pass
9
10 process.
11
12
13
14

15 16 **5- Application of SPD- processed materials** 17

18
19 Despite the extraordinary multifunctional properties of the UFG materials processed by SPD
20
21 such as high strength, good strength to weight ratio, long fatigue life and the possibility of
22
23 fabricating cutting-edge products with efficient methods by UFG materials [248], commercial
24
25 uses of UFG material products are currently rare. As shown in the previous section around 120
26
27 variants of SPD methods have been introduced, which shows the great potential of SPD for
28
29 industrialization. Some market reports documented more than 100 specific market areas for
30
31 nanostructured metals including automobile, aerospace, electronic devices and defensive and
32
33 biomedical applications [249,250]. Seventy patents have been issued from 1997 to 2017 in the
34
35 field of SPD. However, there is still a long way ahead to offer SPD products in the market. The
36
37 important steps required to achieve this goal are the capability to reduce both, the cost of
38
39 products and the amount of the waste material, and the ability to produce larger samples (scale-
40
41 up). The number of patents related to SPD in each year from 1997 to 2017 is shown in Fig. 17. A
42
43 drastical increase in the number of patents is seen in 2013 and 2014; most of them are about the
44
45 application of SPD to new materials like Mg, Ti and reinforced metals. On the other hand, the
46
47 first patents frequently focused on the design parameters with emphasis on ECAP. In this section
48
49 some of various applications of SPD in commercial uses have been reviewed.
50
51
52
53
54
55
56
57
58
59
60
61
62
63
64
65

5.1. SPD-processed Al and Cu sputtering targets

The first commercial application of bulk UFG metals returns to 2003 when the sputtering targets for physical vapor deposition were successfully fabricated by scaling up the ECAP technique in Honeywell Electronic Materials [251] in the USA. Honeywell started the scale-up efforts of ECAE in 1997 with the construction of the first production die which has led to several large-scale die sets for different standard sizes of Al, Cu and pure Ti using presses with the capacity of 1000 and 4000 tons (Fig. 18). Most of these dies have been in use on a weekly basis for 6 year [252]. It may be interesting for the readers that the term ECAE (sometimes used instead of ECAP) is a registered trademark of Honeywell International, Inc [12,251]. They offer UFG Al and Cu sputtering targets with a diameter up to 300 mm and a mass up to 32.7 kg. These are produced from plates by ECAP (Fig. 19) monolithically. The monolithic sputtering targets (where the entire target is a mono-block) are used for metallization of silicon wafers in the production of semiconductors. In comparison to the traditional targets (which consists of a target material bonded or soldered to a backing plate made from strong materials like Al 6061 or CuCr), the UFG sputtering targets offers higher lifetime and more uniform deposited coating due to the stronger material and the reduced arcing, respectively, and a better kit utilization. Furthermore, Praxair Electronics by their facilities in the USA, France and South Korea, presents UFG Al and Cu targets (200mm and 300mm in size) with better sputter performance and 65-75% reduction in the ownership cost of such targets [253,15].

5.2. UFG CP Ti for biomedical application

Globally, the rapid growth in the rate of the human population results in the continues increase in the number of elderly people, which in turn leads to the increase in the need for the artificial

1
2
3
4 implantable devices to replace the failed tissues. Therefore, one of the most suitable areas for the
5
6 application of the UFG materials is in the field of medical implants such as hip, knee and dental
7
8 implants as well as various screws, plates and meshes used in orthopaedic applications. Popular
9
10 materials usually used in these applications are cobalt-chrome alloys, stainless steel and titanium
11
12 alloys. The high strength, good formability, and excellent fatigue and fracture performance of
13
14 metallic biomaterials (mainly titanium and cobalt chrome alloys) result in the extensive demand
15
16 of them for surgical implants. In addition to the mentioned properties, high corrosion resistance
17
18 and low toxicity of the alloys systems that are expected to be used in the physiological
19
20 conditions, are the favorable properties of them. Therefore, Ti and its alloys have been used
21
22 widely in implantable devices, which had been forecasted by a US Industry Study [254]. The
23
24 main advantages of Ti alloys are high corrosion resistance, due to the formation of a very stable
25
26 passive layer of TiO_2 on the alloy surface, intrinsic biocompatibility, low Young's modulus
27
28 (twofold lower compared to stainless steel and Co–Cr), resulting in less stress shielding and
29
30 lower density and producing fewer artifacts on computer tomography and magnetic resonance
31
32 imaging [255,256]. However, commercially pure (CP) Ti has low mechanical and fatigue
33
34 strength which is not sufficient for the load bearing implants (orthopedic application) and
35
36 restricts its application only to dental implants [257]. Alloying by Al and V allows a significant
37
38 improvement in the mechanical properties, and currently the Ti–6Al–4V alloy is the most
39
40 extensively used surgical Ti alloy. However, the alloying elements carry the risk of the alloy
41
42 being toxic for human body as a result of their excessive liberation and accretion in the tissues
43
44 [255]. To prevail the problem of destructive ion release, enhancement of the mechanical
45
46 properties of pure titanium by nano-scale grain refinement is an alternative to alloying notion
47
48 [257,256,255].

1
2
3
4 Nanostructured titanium has been advanced through the labors of over 160 scientists, engineers,
5
6 and medical professionals around the world. In 1999, Webster et al. provided the first evidence
7
8 that osteoblast (bone-forming cells) adhesion and bone formation increases significantly on
9
10 nanostructured titania compared with conventional titania [258]. Studies of UFG titanium and its
11
12 special nanoscale structure were begun in 2003 at Purdue University [259] in the USA, and
13
14 afterward were replicated at research institutions worldwide, each reliably authenticating the
15
16 positive result that bone cells more rapidly attach to and more readily adhere to UFG titanium
17
18 than the coarse grain (CG) counterpart. Generally, both *in vitro* and *in vivo* studies have
19
20 obviously established that nanostructured Ti increases osteoblast cell functions and enhances
21
22 Osseo integration while at the same time, decreasing bacterial attachment onto the implant
23
24 compared with CG Ti [260].
25
26
27
28
29
30

31 To achieve ultra-fine grained structure in CP Ti, both ‘bottom-up’ and ‘top-down’ approaches
32
33 have been used. Since the current work focuses on SPD methods, which are categorized in top-
34
35 down methods, we do not consider the bottom-up methods and only focus on the grain
36
37 refinement during SPD processes; mostly, ECAP [261-264] and HPT [265-267] were used for
38
39 this purpose. However, there are limited works on the direct application of UFG Ti for medical
40
41 applications. One of the good examples of such products is a new generation of dental implants
42
43 under the trademark Nanoimplant (Timplant), which is fabricated in the company Timplant
44
45 (Ostrava, Czech Republic) and shown in Fig. 20. The processing route consists of ECAP-C for
46
47 grain refinement and secondary processing of drawing for shaping and additional strengthening
48
49 following the final process of grinding in order to produce the required surface quality and
50
51 tolerance [268,256]. As a result, long rods with lengths up to 3 m (Fig. 21), diameters of 4–8
52
53 mm, accuracy grade h8 suitable for automation of implant machining, and a uniform
54
55
56
57
58
59
60
61
62
63
64
65

1
2
3
4 nanostructure with a subgrain size of 150–200 nm can be produced. These new generation
5
6 implants are smaller in diameter (2.4 mm) than conventional implants (3.5 mm) (Fig. 22). The
7
8 smaller size of the dental implants has two main advantages. Firstly, they can be successfully
9
10 inserted into thin jawbones where larger implants are not feasible. Secondly, they introduce less
11
12 damage during the surgery. Presently, these implants have been certified according to the
13
14 European standard EN ISO 13485:2003 [248]. In another project in the framework of VINAT
15
16 funded by European Commission and the Ministry of Education and Science of Russian
17
18 Federation, another implant prototype with the diameter of 2.0 mm with the ultimate tensile
19
20 strength of 1330 MPa was developed (Fig. 22) [256]. As shown in Fig. 22, this small implant
21
22 was installed into the jawbone of an 18 years old patient between teeth 11 and 13. Another
23
24 implant with the diameter of 2.4 mm was inserted to the right side position of tooth 12. This
25
26 surgery has been successful and the final metal-ceramic crowns were fixed on the implants after
27
28 six weeks.
29
30
31
32
33

34
35
36 Another example for the use of UFG CP Ti in biomedical applications is in trauma cases, plates
37
38 (Fig. 23a) and screws (Fig. 23b), which are planned to be widely used for fixing bones. Very
39
40 high compressive and bending strength and sufficient ductility are the required properties for
41
42 these plates. Besides, a special conic screw (Fig. 23c) and a unique device for the correction and
43
44 fixation of spinal column (Fig. 23d), with high static and fatigue strength have been successfully
45
46 fabricated from UFG Ti by ECAP.
47
48
49
50
51
52
53
54
55
56
57
58
59
60
61
62
63
64
65

5.3. UFG materials for sport applications

In the sport facilities, particularly where the high strength to weight ratio is need, UFG materials can play an important role. Bulk nanostructured metallic materials could find applications in different fields such as golf, tennis, bicycling, scuba diving, archery, back packing, rock climbing and more. Some of the examples are nanodynamics high performance (NDMX) golf balls, Metallix and Airflow racquets (PowerMetal Technologies and HEAD) [253]. However, none of the products are made by SPD methods. The hollow nanostructured titanium core of the NDMX golf balls is manufactured using the UFG chip machining technology licensed by Purdue University and the Metallix racquets have been made by carbon fibers and Integran's electro deposition technology. Therefore, it seems that using SPD in sport industry needs more effort from the researchers in this field to find new application for SPD products in sport utilities and to present the great potential of the UFG products in the fabrication of light, strong and long life parts.

5.4. SPD-processed materials for Hydrogen Storage

It was well documented that SPD processing can lead to substantial improvements in the kinetics of hydrogen storage in metallic materials particularly in Mg-based alloys. Most of studies in Hydrogen storage are focused on the methods to use H₂ as lightweight, compact energy carrier for mobile applications. Various approaches have been used to store hydrogen including high pressures, cryogenics, and chemical compounds in which hydrogen is released upon heating. The light weight and low cost of Mg alloys for hydrogen storage made them an attractive choice for on-board mobile applications [271]. However, high thermodynamic stability, high hydrogen desorption temperature and relatively poor hydrogen absorption–desorption kinetics of Mg alloys

1
2
3
4 are big challenges in this regard [20,248]. One way to improve the hydrogen storage properties
5
6 of Mg-alloys is grain refinement. Skripnyuk et al. [272] in 2004, are the first researchers who
7
8 study the effect of SPD on the hydrogen storage properties of Mg alloy hydrides using ECAP.
9
10 They showed that the UFG Mg alloy ZK60 achieved after 8 passes of ECAP by rout A at 250
11
12 °C and 300 °C and one additional pass at environmental temperature has a higher hydrogen
13
14 storage property in means of the hydrogen capacity and the pressure hysteresis in comparison
15
16 with its CG counterpart. The exact mechanism for grain size that affects Mg hydride's hydrogen
17
18 storage property still remains unexplained. So far, it is generally documented that the finer grain
19
20 size, the larger the surface area, which in turn leads to the easier diffusion of dissociated H atoms
21
22 into the Mg matrix [273]. Furthermore, ECAP processed materials can contain a large fraction
23
24 of high-angle grain boundaries. The impact of grain boundary on hydrogenation kinetics has
25
26 been intensively studied. Reports showed that hydrogen could diffuse much faster along the
27
28 grain boundaries. Besides, the ECAP process generates defects such as vacancies and
29
30 dislocations which produce a constructive effect on the diffusion kinetics. Many details of the
31
32 effect of different parameters on the hydrogen storage of ECAP processed Mg-alloys and the
33
34 mechanisms involved in this phenomenon can be found in the recent critical review paper of
35
36 Wang et al. [273]. In some other studies, the effect of HPT on the hydrogen storage properties of
37
38 Mg ZK60 [274] and Mg₂Ni have been investigated. In general, HPT enhanced the hydrogen
39
40 sorption kinetics due to a high density of planar lattice defects, such as crystallite boundaries and
41
42 stacking faults, induced by HPT [248,20]. It is reasonable to conclude that SPD processes in
43
44 general and HPT and ECAP processes in particular have the great potential to be used in the
45
46 production of the nanocrystalline elements. ECAP can cheaply use for the fabrication of
47
48 cylindrical hydrogen batteries while HPT could be used for the construction of metal hybrid
49
50
51
52
53
54
55
56
57
58
59
60
61
62
63
64
65

1
2
3
4 tablets. Moreover, the applicability of the use of other methods like TE and SSE that have a great
5
6 potential for commercialization, and are cheaper and easier than the other methods, would be of
7
8 great interest in this field.
9

10 11 12 13 14 **6. Summery and conclusions**

15
16 During the last three decades, severe plastic deformation has progressed as a novel method to
17
18 achieve nano/ultra-fine grained structure in a wide range of metallic materials. To the end of
19
20 2016, SPD processing has attracted the significant attention of more than 4700 researchers from
21
22 69 countries. The bulk of the work is based on the characterization of microstructure and
23
24 mechanical properties of SPD processed materials. The microstructural characterization mainly
25
26 focuses on the study of grain size, examination of the grain boundary and dislocation structure
27
28 and the texture evaluation. In spite of being three decades old and the extensive works on
29
30 microstructure and mechanical properties, SPD constitutes a field, which is still young and
31
32 demands considerable challenges. The reason can be explained by several points of view. First,
33
34 compared with common aspects of SPD processed materials, several features such as magnetic
35
36 properties, weldability and powder consolidation have attracted less attention. Second, the
37
38 achievements in some aspects of SPD processed materials such as wear behavior; corrosion
39
40 resistance and the simultaneous increase in the strength and ductility are contradictory and still
41
42 need further investigations. Third, limited efforts have been directed toward production of
43
44 materials other than metallic alloys by SPD process. Although extensive works have been done
45
46 to produce composite materials by ARB, the fabrication of composites as well as hard to deform
47
48 materials, polymers and ceramics (at low or moderate temperature) by various SPD methods is
49
50 still a challenge. Finally, it is worth nothing that up to now, more than 90% of the publications in
51
52
53
54
55
56
57
58
59
60
61
62
63
64
65

1
2
3
4 this field comprises just three conventional SPD methods including ECAP, HPT and ARB.
5
6 However, about 120 methods with different deformation modes and different shapes/geometries
7
8 including rods, bars, billets, tubes and sheets have been introduced as new SPD processes.
9
10 Among many types of conventional and new SPD techniques, the efforts to scale up and
11
12 commercialization have focused on the ECAP process. Therefore, the practical applications of
13
14 SPD processed materials demands the commercialization of other SPD methods and requires
15
16 further investigations in the future.
17
18
19
20
21
22

23 **Acknowledgments**

24 The financial support of Shahid Chamran University of Ahvaz and Shiraz University is
25
26 gratefully appreciated.
27
28
29
30

31 **Compliance with Ethical Standards**

32 Conflict of Interest: The authors declare that they have no conflict of interest.
33
34
35
36
37

38 **References**

- 39
40
41
42
43 1. Valiev RZ, Islamgaliev RK, Alexandrov IV (2000) Bulk nanostructured materials from severe
44 plastic deformation. *Progress in materials science* 45 (2):103-189
45
46 2. Valiev R, Estrin Y, Horita Z, Langdon T, Zehetbauer M, Zhu Y (2016) Fundamentals of
47 superior properties in bulk nanoSPD materials. *Materials Research Letters* 4 (1):1-21
48
49 3. Azushima A, Kopp R, Korhonen A, Yang D, Micari F, Lahoti G, Groche P, Yanagimoto J,
50 Tsuji N, Rosochowski A (2008) Severe plastic deformation (SPD) processes for metals. *CIRP*
51 *Annals* 57 (2):716-735
52
53 4. Langdon TG Processing by severe plastic deformation: Historical developments and current
54 impact. In: *Materials Science Forum*, 2010. vol 667. p 9
55
56 5. Bridgman P (1943) On torsion combined with compression. *Journal of Applied Physics* 14
57 (6):273-283
58
59
60
61
62
63
64
65

- 1
2
3
4 6. Bridgman PW (1952) Studies in large plastic flow and fracture, vol 177. McGraw-Hill New
5 York,
6
- 7
8 7. Zhilyaev AP, Langdon TG (2008) Using high-pressure torsion for metal processing:
9 Fundamentals and applications. Progress in Materials Science 53 (6):893-979
10
- 11 8. Smirnova N, Levit V, Pilyugin V, Kuznetsov R, Davydova L, Sazonova V (1986) Evolution
12 of the fcc single-crystal structure during severe plastic-deformations. Fizika Metallov i
13 Metallovedenie 61 (6):1170-1177
14
- 15
16 9. Segal V, Reznikov V, Dobryshevshiy A, Kopylov V (1981) Plastic working of metals by
17 simple shear. Russian Metallurgy (Metally) (1):99-105
18
- 19
20 10. Valiev RZ, Krasilnikov N, Tsenev N (1991) Plastic deformation of alloys with submicron-
21 grained structure. Materials Science and Engineering: A 137:35-40
22
- 23
24 11. Valiev R, Korznikov A, Mulyukov R (1993) Structure and properties of ultrafine-grained
25 materials produced by severe plastic deformation. Materials Science and Engineering: A 168
26 (2):141-148
27
- 28
29 12. Valiev RZ, Langdon TG (2006) Principles of equal-channel angular pressing as a processing
30 tool for grain refinement. Progress in materials science 51 (7):881-981
31
- 32
33 13. Bridgman PW (1935) Effects of high shearing stress combined with high hydrostatic
34 pressure. Physical Review 48 (10):825
35
- 36
37 14. Saito Y, Tsuji N, Utsunomiya H, Sakai T, Hong R (1998) Ultra-fine grained bulk aluminum
38 produced by accumulative roll-bonding (ARB) process. Scripta materialia 39 (9):1221-1227
39
- 40
41 15. Furukawa M, Horita Z, Nemoto M, Langdon T (2001) Processing of metals by equal-channel
42 angular pressing. Journal of materials science 36 (12):2835-2843
43
- 44
45 16. Kawasaki M, Langdon TG (2016) achieving superplastic properties in ultrafine-grained
46 materials at high temperatures. Journal of materials science 51 (1):19-32
47
- 48
49 17. Valiev RZ, Estrin Y, Horita Z, Langdon TG, Zechetbauer MJ, Zhu YT (2006) Producing
50 bulk ultrafine-grained materials by severe plastic deformation. Jom 58 (4):33-39
51
- 52
53 18. Beyerlein IJ, Tóth LS (2009) Texture evolution in equal-channel angular extrusion. Progress
54 in Materials Science 54 (4):427-510
55
- 56
57 19. Figueiredo RB, Langdon TG (2012) Fabricating ultrafine-grained materials through the
58 application of severe plastic deformation: a review of developments in Brazil. Journal of
59 Materials Research and Technology 1 (1):55-62
60
- 61
62 20. Valiev RZ, Estrin Y, Horita Z, Langdon TG, Zehetbauer MJ, Zhu Y (2016) Producing Bulk
63 Ultrafine-Grained Materials by Severe Plastic Deformation: Ten Years Later. JOM 68 (4):1216-
64 1226. doi:10.1007/s11837-016-1820-6
65

- 1
2
3
4 21. Edalati K, Horita Z (2016) A review on high-pressure torsion (HPT) from 1935 to 1988.
5 Materials Science and Engineering: A 652:325-352
6
7
8 22. Estrin Y, Vinogradov A (2013) Extreme grain refinement by severe plastic deformation: a
9 wealth of challenging science. *Acta materialia* 61 (3):782-817
10
11 23. Toth LS, Gu C (2014) Ultrafine-grain metals by severe plastic deformation. *Materials*
12 *Characterization* 92:1-14
13
14
15 24. Rosochowski A Processing metals by severe plastic deformation. In: *Solid State Phenomena*,
16 2005. Trans Tech Publ, pp 13-22
17
18 25. Verlinden B (2005) Severe plastic deformation of metals. *Metalurgija* 11 (3):165-182
19
20 26. Wang C, Li F, Wang L, Qiao H (2012) Review on modified and novel techniques of severe
21 plastic deformation. *Science China Technological Sciences* 55 (9):2377-2390
22
23 27. Hohenwarter A (2015) Incremental high pressure torsion as a novel severe plastic
24 deformation process: processing features and application to copper. *Materials Science and*
25 *Engineering: A* 626:80-85
26
27
28 28. Sakai G, Nakamura K, Horita Z, Langdon TG (2005) Developing high-pressure torsion for
29 use with bulk samples. *Materials Science and Engineering: A* 406 (1-2):268-273
30
31
32 29. Edalati K, Horita Z (2010) Continuous high-pressure torsion. *Journal of materials science* 45
33 (17):4578-4582
34
35 30. Valiev R, Kuznetsov O, Musalimov RS, Tsenev N Low-temperature superplasticity of
36 metallic materials. In: *Soviet Physics Doklady*, 1988. p 626
37
38
39 31. Tao N, Lu K (2009) Nanoscale structural refinement via deformation twinning in face-
40 centered cubic metals. *Scripta Materialia* 60 (12):1039-1043
41
42 32. Sachs G (1928) Zur Ableitung einer Fließbedingung. *Z Ver Dtsch Ing* 72:734-736
43
44 33. Kocks UF, Tome CN, Wenk H-R (1998) *Texture and Anisotropy. Preferred Orientations in*
45 *Polycrystals and Their Effect on Material Properties*. Cambridge University Press, ISBN
46 521465168:12-30
47
48
49 34. Taylor GI (1938) Plastic strain in metals. *J Inst Metals* 62:307-324
50
51 35. Huang JY, Zhu YT, Jiang H, Lowe TC (2001) Microstructures and dislocation configurations
52 in nanostructured Cu processed by repetitive corrugation and straightening. *Acta Materialia* 49
53 (9):1497-1505. doi:10.1016/S1359-6454(01)00069-6
54
55
56 36. Hughes DA, Hansen N (1997) High angle boundaries formed by grain subdivision
57 mechanisms. *Acta Materialia* 45 (9):3871-3886. doi:10.1016/S1359-6454(97)00027-X
58
59
60
61
62
63
64
65

- 1
2
3
4 37. Hansen N, Mehl RF (2001) New discoveries in deformed metals. *Metallurgical and materials*
5 *transactions A* 32 (12):2917-2935
6
7
8 38. Sakai T, Belyakov A, Kaibyshev R, Miura H, Jonas JJ (2014) Dynamic and post-dynamic
9 recrystallization under hot, cold and severe plastic deformation conditions. *Progress in Materials*
10 *Science* 60:130-207
11
12 39. Kamikawa N, Tsuji N, Huang X, Hansen N (2006) Quantification of annealed
13 microstructures in ARB processed aluminum. *Acta materialia* 54 (11):3055-3066
14
15
16 40. Xue Q, Beyerlein I, Alexander D, Gray Iii G (2007) Mechanisms for initial grain refinement
17 in OFHC copper during equal channel angular pressing. *Acta Materialia* 55 (2):655-668
18
19
20 41. Kamikawa N, Sakai T, Tsuji N (2007) Effect of redundant shear strain on microstructure and
21 texture evolution during accumulative roll-bonding in ultralow carbon IF steel. *Acta Materialia*
22 55 (17):5873-5888
23
24
25 42. Sakai T, Belyakov A, Miura H (2008) Ultrafine grain formation in ferritic stainless steel
26 during severe plastic deformation. *Metallurgical and Materials Transactions A* 39 (9):2206
27
28
29 43. Hansen N (1990) Cold deformation microstructures. *Materials Science and Technology*
30 (United Kingdom) 6 (11):1039-1047. doi:10.1179/mst.1990.6.11.1039
31
32 44. Bay B, Hansen N, Hughes DA, Kuhlmann-Wilsdorf D (1992) Overview no. 96 evolution of
33 f.c.c. deformation structures in polyslip. *Acta Metallurgica Et Materialia* 40 (2):205-219.
34 doi:10.1016/0956-7151(92)90296-Q
35
36 45. Liu CD, Bassim MN, You DX (1994) Dislocation structures in fatigued polycrystalline
37 copper. *Acta Metallurgica Et Materialia* 42 (11):3695-3704. doi:10.1016/0956-7151(94)90435-9
38
39
40 46. Lu K, Hansen N (2009) Structural refinement and deformation mechanisms in nanostructured
41 metals. *Scripta Materialia* 60 (12):1033-1038
42
43
44 47. Wang K, Tao N, Liu G, Lu J, Lu K (2006) Plastic strain-induced grain refinement at the
45 nanometer scale in copper. *Acta Materialia* 54 (19):5281-5291
46
47
48 48. Li W, Tao N, Lu K (2008) Fabrication of a gradient nano-micro-structured surface layer on
49 bulk copper by means of a surface mechanical grinding treatment. *Scripta Materialia* 59 (5):546-
50 549
51
52 49. Zhang H, Hei Z, Liu G, Lu J, Lu K (2003) Formation of nanostructured surface layer on AISI
53 304 stainless steel by means of surface mechanical attrition treatment. *Acta materialia* 51
54 (7):1871-1881
55
56 50. Victoria-Hernández J, Suh J, Yi S, Bohlen J, Volk W, Letzig D (2016) Strain-induced
57 selective grain growth in AZ31 Mg alloy sheet deformed by equal channel angular pressing.
58 *Materials Characterization* 113:98-107. doi:10.1016/j.matchar.2016.01.002
59
60
61
62
63
64
65

- 1
2
3
4 51. Horita Z, Langdon TG (2005) Microstructures and microhardness of an aluminum alloy and
5 pure copper after processing by high-pressure torsion. *Materials Science and Engineering A* 410-
6 411:422-425. doi:10.1016/j.msea.2005.08.133
7
8
9 52. Wetscher F, Pippan R (2006) Cyclic high-pressure torsion of nickel and Armco iron.
10 *Philosophical Magazine* 86 (36):5867-5883. doi:10.1080/14786430600838288
11
12 53. Orlov D, Todaka Y, Umemoto M, Tsuji N (2009) Role of strain reversal in grain refinement
13 by severe plastic deformation. *Materials Science and Engineering: A* 499 (1):427-433.
14 doi:<https://doi.org/10.1016/j.msea.2008.09.036>
15
16
17 54. Bagherpour E, Qods F, Ebrahimi R, Miyamoto H (2016) Microstructure evolution of pure
18 copper during a single pass of simple shear extrusion (SSE): role of shear reversal. *Materials*
19 *Science and Engineering: A* 666 (Supplement C):324-338.
20 doi:<https://doi.org/10.1016/j.msea.2016.04.080>
21
22
23 55. Bagherpour E, Qods F, Ebrahimi R, Miyamoto H (2016) Texture Changes during Simple
24 Shear Extrusion (SSE) Processing of Pure Copper. *MATERIALS TRANSACTIONS* 57
25 (9):1386-1391. doi:10.2320/matertrans.MH201501
26
27
28 56. Bagherpour E, Qods F, Ebrahimi R, Miyamoto H (2017) Nanostructured pure copper
29 fabricated by simple shear extrusion (SSE): A correlation between microstructure and tensile
30 properties. *Materials Science and Engineering: A* 679 (Supplement C):465-475.
31 doi:<https://doi.org/10.1016/j.msea.2016.10.068>
32
33
34 57. Bagherpour E, Qods F, Ebrahimi R, Miyamoto H Strain reversal in simple shear extrusion
35 (SSE) processing: Microstructure investigations and mechanical properties. In: *AIP Conference*
36 *Proceedings*, 2018. vol 1. AIP Publishing, p 020007
37
38
39 58. Sheikh H, Ebrahimi R, Bagherpour E (2016) Crystal plasticity finite element modeling of
40 crystallographic textures in simple shear extrusion (SSE) process. *Materials & Design* 109
41 (Supplement C):289-299. doi:<https://doi.org/10.1016/j.matdes.2016.07.030>
42
43
44 59. Derby B (1991) The dependence of grain size on stress during dynamic recrystallisation.
45 *Acta Metallurgica et Materialia* 39 (5):955-962. doi:[https://doi.org/10.1016/0956-](https://doi.org/10.1016/0956-7151(91)90295-C)
46 [7151\(91\)90295-C](https://doi.org/10.1016/0956-7151(91)90295-C)
47
48
49 60. Wang YB, Ho JC, Liao XZ, Li HQ, Ringer SP, Zhu YT (2009) Mechanism of grain growth
50 during severe plastic deformation of a nanocrystalline Ni-Fe alloy. *Applied Physics Letters* 94
51 (1):011908. doi:10.1063/1.3065025
52
53
54 61. Korznikov AV, Tyumentsev AN, Ditenberg IA (2008) On the limiting minimum size of
55 grains formed in metallic materials produced by high-pressure torsion. *Physics of Metals and*
56 *Metallography* 106 (4):418-423. doi:10.1134/S0031918X08100128
57
58
59 62. Korznikova EA, Dmitriev SV (2014) Mechanisms of deformation-induced grain growth of a
60 two-dimensional nanocrystal at different deformation temperatures. *Physics of Metals and*
61 *Metallography* 115 (6):570-575. doi:10.1134/S0031918X14060088
62
63
64
65

- 1
2
3
4 63. Edalati K, Ito Y, Suehiro K, Horita Z (2009) Softening of high purity aluminum and copper
5 processed by high pressure torsion. *International Journal of Materials Research* 100 (12):1668-
6 1673. doi:10.3139/146.110231
7
8
9 64. Agnew SR, Weertman JR (1998) Cyclic softening of ultrafine grain copper. *Materials*
10 *Science and Engineering A* 244 (2):145-153. doi:10.1016/S0921-5093(97)00689-8
11
12 65. Alvandi H, Farmanesh K (2015) Microstructural and mechanical properties of nano/ultra-fine
13 structured 7075 aluminum alloy by accumulative roll-bonding process. *Proceedings of the 5th*
14 *International Biennial Conference on Ultrafine Grained and Nanostructured Materials*, *Procedia*
15 *Materials Science* 11:17-23
16
17
18 66. Tamimi S, Ketabchi M, Parvin N, Sanjari M, Lopes A (2014) Accumulative roll bonding of
19 pure copper and IF steel. *Int J Met* 2014:9
20
21
22 67. Sansoz F, Dupont V (2006) Grain growth behavior at absolute zero during nanocrystalline
23 metal indentation. *Applied Physics Letters* 89 (11). doi:10.1063/1.2352725
24
25
26 68. Farkas D, Frøseth A, Van Swygenhoven H (2006) Grain boundary migration during room
27 temperature deformation of nanocrystalline Ni. *Scripta Materialia* 55 (8):695-698.
28 doi:10.1016/j.scriptamat.2006.06.032
29
30 69. Legros M, Gianola DS, Hemker KJ (2008) In situ TEM observations of fast grain-boundary
31 motion in stressed nanocrystalline aluminum films. *Acta Materialia* 56 (14):3380-3393.
32 doi:10.1016/j.actamat.2008.03.032
33
34
35 70. Wang YB, Li BQ, Sui ML, Mao SX (2008) Deformation-induced grain rotation and growth
36 in nanocrystalline Ni. *Applied Physics Letters* 92 (1):011903. doi:10.1063/1.2828699
37
38 71. Gutkin MY, Ovid'ko IA, Skiba NV (2003) Crossover from grain boundary sliding to
39 rotational deformation in nanocrystalline materials. *Acta Materialia* 51 (14):4059-4071.
40 doi:10.1016/S1359-6454(03)00226-X
41
42
43 72. Chen M, Ma E, Hemker KJ, Sheng H, Wang Y, Cheng X (2003) Deformation twinning in
44 nanocrystalline aluminum. *Science* 300 (5623):1275-1277. doi:10.1126/science.1083727
45
46
47 73. Liao XZ, Zhou F, Lavernia EJ, Srinivasan SG, Baskes MI, He DW, Zhu YT (2003)
48 Deformation mechanism in nanocrystalline Al: Partial dislocation slip. *Applied Physics Letters*
49 83 (4):632-634. doi:10.1063/1.1594836
50
51 74. Liao XZ, Zhao YH, Srinivasan SG, Zhu YT, Valiev RZ, Gunderov DV (2004) Deformation
52 twinning in nanocrystalline copper at room temperature and low strain rate. *Applied Physics*
53 *Letters* 84 (4):592-594. doi:10.1063/1.1644051
54
55
56 75. Yamakov V, Wolf D, Phillpot SR, Mukherjee AK, Gleiter H (2002) Dislocation processes in
57 the deformation of nanocrystalline aluminium by molecular-dynamics simulation. *Nature*
58 *Materials* 1:45. doi:10.1038/nmat700
59 <https://www.nature.com/articles/nmat700#supplementary-information>
60
61
62
63
64
65

- 1
2
3
4 76. Kiritani M (1997) Story of stacking fault tetrahedra. *Materials Chemistry and Physics* 50
5 (2):133-138. doi:[https://doi.org/10.1016/S0254-0584\(97\)80250-7](https://doi.org/10.1016/S0254-0584(97)80250-7)
6
7
8 77. Huang CX, Wang K, Wu SD, Zhang ZF, Li GY, Li SX (2006) Deformation twinning in
9 polycrystalline copper at room temperature and low strain rate. *Acta Materialia* 54 (3):655-665.
10 doi:<https://doi.org/10.1016/j.actamat.2005.10.002>
11
12 78. Merchant ME (1945) Mechanics of the metal cutting process. I. Orthogonal cutting and a
13 type 2 chip. *Journal of Applied Physics* 16 (5):267-275. doi:10.1063/1.1707586
14
15 79. Kanani M, Sohrabi S, Ebrahimi R, Paydar MH (2014) Continuous and ultra-fine grained chip
16 production with large strain machining. *Journal of Materials Processing Technology* 214
17 (8):1777-1786. doi:<https://doi.org/10.1016/j.jmatprotec.2014.03.028>
18
19
20 80. Nakashima K, Horita Z, Nemoto M, Langdon TG (2000) Development of a multi-pass
21 facility for equal-channel angular pressing to high total strains. *Materials Science and*
22 *Engineering: A* 281 (1):82-87
23
24
25 81. Berbon PB, Furukawa M, Horita Z, Nemoto M, Langdon TG (1999) Influence of pressing
26 speed on microstructural development in equal-channel angular pressing. *Metallurgical and*
27 *Materials Transactions A: Physical Metallurgy and Materials Science* 30 (8):1989-1997.
28 doi:10.1007/s11661-999-0009-9
29
30
31 82. Utsunomiya H, Hatsuda K, Sakai T, Saito Y (2004) Continuous grain refinement of
32 aluminum strip by conshearing. *Materials Science and Engineering: A* 372 (1):199-206
33
34
35 83. Lee J-C, Seok H-K, Han J-H, Chung Y-H (2001) Controlling the textures of the metal strips
36 via the continuous confined strip shearing(C2S2) process. *Materials Research Bulletin* 36 (5-
37 6):997-1004. doi:[http://dx.doi.org/10.1016/S0025-5408\(01\)00557-8](http://dx.doi.org/10.1016/S0025-5408(01)00557-8)
38
39
40 84. Lee J-C, Seok H-K, Suh J-Y (2002) Microstructural evolutions of the Al strip prepared by
41 cold rolling and continuous equal channel angular pressing. *Acta Materialia* 50 (16):4005-4019
42
43
44 85. Han J-H, Seok H-K, Chung Y-H, Shin M-C, Lee J-C (2002) Texture evolution of the strip
45 cast 1050 Al alloy processed by continuous confined strip shearing and its formability
46 evaluation. *Materials Science and Engineering: A* 323 (1):342-347
47
48
49 86. Lee J-C, Seok H-K, Han J-H, Chung Y-H (2001) Controlling the textures of the metal strips
50 via the continuous confined strip shearing (C2S2) process. *Materials research bulletin* 36
51 (5):997-1004
52
53
54 87. Xu C, Schroeder S, Berbon PB, Langdon TG (2010) Principles of ECAP–Conform as a
55 continuous process for achieving grain refinement: Application to an aluminum alloy. *Acta*
56 *Materialia* 58 (4):1379-1386
57
58
59 88. Zisman A, Rybin V, Van Boxel S, Seefeldt M, Verlinden B (2006) Equal channel angular
60 drawing of aluminium sheet. *Materials Science and Engineering: A* 427 (1):123-129
61
62
63
64
65

- 1
2
3
4 89. León J, Luis-Pérez C Analysis of stress and strain in the equal channel angular drawing
5 process. In: Materials science forum, 2006. Trans Tech Publ, pp 19-24
6
7
8 90. Huang Y, Prangnell P (2007) Continuous frictional angular extrusion and its application in
9 the production of ultrafine-grained sheet metals. Scripta materialia 56 (5):333-336
10
11 91. Fakhretdinova E, Raab GI, Ganiev M Development of a Force Parameter Model for a New
12 Severe Plastic Deformation Technique–Multi-ECAP-Conform. In: Applied Mechanics and
13 Materials, 2015. Trans Tech Publ, pp 386-390
14
15
16 92. Zhu X, Xu XJ, Zhao Z, Chong K, Cheng C, Cheng XN The novel continuous large
17 deformation technology integrating conventional rolling with equal-channel angular technology.
18 In: Materials Science Forum, 2011. Trans Tech Publ, pp 127-132
19
20
21 93. Chen B, Lin DL, Zeng XQ, Lu C Single Roll Drive Equal Channel Angular Process—a
22 Potential Severe Plastic Deformation (SPD) Process for Industrial Application. In: Materials
23 Science Forum, 2006. Trans Tech Publ, pp 557-560
24
25
26 94. Rosochowski A, Olejnik L (2008) Finite element analysis of two-turn Incremental ECAP.
27 International journal of material forming 1 (1):483-486
28
29 95. Rosochowski A, Olejnik L, Richert MW Double-billet incremental ECAP. In: Materials
30 Science Forum, 2008. Trans Tech Publ, pp 139-144
31
32
33 96. Olejnik L, Rosochowski A, Richert MW Incremental ECAP of plates. In: Materials Science
34 Forum, 2008. Trans Tech Publ, pp 108-113
35
36 97. Bruder E, GÃ¼rtan MO, Groche P, MÃ¼ller C Severe Plastic Deformation by Equal Channel
37 Angular Swaging. In: Materials Science Forum, 2010. Trans Tech Publ, pp 103-107
38
39
40 98. Raab G (2005) Plastic flow at equal channel angular processing in parallel channels.
41 Materials Science and Engineering: A 410:230-233
42
43 99. Rosochowski A, Olejnik L, Richert M (2007) 3D-ECAP of square aluminium billets. In:
44 Advanced Methods in Material Forming. Springer, pp 215-232
45
46
47 100. Olejnik L, Rosochowski A (2005) Methods of fabricating metals for nano-technology.
48 Technical Sciences 53 (4)
49
50 101. Talebanpour B, Ebrahimi R, Janghorban K (2009) Microstructural and mechanical
51 properties of commercially pure aluminum subjected to Dual Equal Channel Lateral Extrusion.
52 Materials Science and Engineering: A 527 (1):141-145
53
54
55 102. Yoon SC, Seo MH, Krishnaiah A, Kim HS (2008) Finite element analysis of rotary-die
56 equal channel angular pressing. Materials Science and Engineering: A 490 (1):289-292
57
58
59
60
61
62
63
64
65

- 1
2
3
4 103. Nishida Y, Arima H, Kim J-C, Ando T (2001) Rotary-die equal-channel angular pressing of
5 an Al – 7 mass% Si – 0.35 mass% Mg alloy. *Scripta Materialia* 45 (3):261-266.
6 doi:[http://dx.doi.org/10.1016/S1359-6462\(01\)00985-X](http://dx.doi.org/10.1016/S1359-6462(01)00985-X)
7
8
9 104. Nagasekhar AV, Kim HS (2008) Analysis of T-shaped equal channel angular pressing using
10 the finite element method. *Metals and Materials International* 14 (5):565-568
11
12 105. Rao VS, Kashyap BP, Prabhu N, Hodgson PD (2008) T-shaped equi-channel angular
13 pressing of Pb–Sn eutectic and its tensile properties. *Materials Science and Engineering: A* 486
14 (1–2):341-349. doi:<http://dx.doi.org/10.1016/j.msea.2007.09.004>
15
16
17 106. Nagasekhar AV, Kim HS (2008) Plastic deformation characteristics of cross-equal channel
18 angular pressing. *Computational Materials Science* 43 (4):1069-1073
19
20
21 107. Chou C-Y, Lee S-L, Lin J-C, Hsu C-M (2007) Effects of cross-channel extrusion on the
22 microstructures and superplasticity of a Zn–22 wt.% Al eutectoid alloy. *Scripta Materialia* 57
23 (10):972-975. doi:<http://dx.doi.org/10.1016/j.scriptamat.2007.04.029>
24
25
26 108. Rosochowski A, Olejnik L, Richert J, Rosochowska M, Richert M (2013) Equal channel
27 angular pressing with converging billets—Experiment. *Materials Science and Engineering: A*
28 560 (0):358-364. doi:<http://dx.doi.org/10.1016/j.msea.2012.09.079>
29
30
31 109. Guo W, Wang Q, Ye B, Liu M, Peng T, Liu X, Zhou H (2012) Enhanced microstructure
32 homogeneity and mechanical properties of AZ31 magnesium alloy by repetitive upsetting.
33 *Materials Science and Engineering: A* 540:115-122
34
35
36 110. Kim K, Yoon J (2013) Evolution of the microstructure and mechanical properties of AZ61
37 alloy processed by half channel angular extrusion (HCAE), a novel severe plastic deformation
38 process. *Materials Science and Engineering: A* 578:160-166
39
40
41 111. Ruzs S, Malanik K, Dutkiewicz J, Cizek L, Skotnicova I, Hluchnik J (2009) Influence of
42 change of direction of deformation at ECAP technology on achieved UFG in AlMn1Cu alloy.
43 *Journal of Achievements in Materials and Manufacturing Engineering* 35 (1):21-28
44
45
46 112. Mathieu J-P, Suwas S, Eberhardt A, Toth L, Moll P (2006) A new design for equal channel
47 angular extrusion. *Journal of Materials Processing Technology* 173 (1):29-33
48
49
50 113. Yamane T, Kondou R, Makabe C Grain refinement and strengthening of a cylindrical pure-
51 Aluminum specimen by using modified equal-channel angular pressing technique. In: *Key*
52 *Engineering Materials*, 2007. Trans Tech Publ, pp 937-942
53
54
55 114. Nagasekhar A, Chakkingal U, Venugopal P (2006) Candidature of equal channel angular
56 pressing for processing of tubular commercial purity-titanium. *Journal of materials processing*
57 *technology* 173 (1):53-60
58
59
60 115. Djavanroodi F, Zolfaghari AA, Ebrahimi M, Nikbin K (2014) Route effect on equal channel
61 angular pressing of copper tube. *Acta Metallurgica Sinica (English Letters)* 27 (1):95-100
62
63
64
65

- 1
2
3
4 116. Lee DN (2000) An upper-bound solution of channel angular deformation. *Scripta materialia*
5 43 (2):115-118
6
7
8 117. Tóth LS, Lapovok R, Hasani A, Gu C (2009) Non-equal channel angular pressing of
9 aluminum alloy. *Scripta Materialia* 61 (12):1121-1124
10
11 118. Lu L, Liu T, Chen Y, Wang L, Wang Z (2012) Double change channel angular pressing of
12 magnesium alloys AZ31. *Materials & Design* 35:138-143
13
14
15 119. Rosochowski A, Rosochowska M, Olejnik L (2012) New SPD Process of Incremental
16 Angular Splitting. *Key Engineering Materials* 504:569-574
17
18 120. Swaminathan S, Brown T, Chandrasekar S, McNelley T, Compton W (2007) Severe plastic
19 deformation of copper by machining: Microstructure refinement and nanostructure evolution
20 with strain. *Scripta materialia* 56 (12):1047-1050
21
22
23 121. Faraji G, Mashhadi MM, Kim HS (2011) Tubular channel angular pressing (TCAP) as a
24 novel severe plastic deformation method for cylindrical tubes. *Materials Letters* 65 (19):3009-
25 3012
26
27
28 122. Zangiabadi A, Kazeminezhad M (2011) Development of a novel severe plastic deformation
29 method for tubular materials: Tube Channel Pressing (TCP). *Materials Science and Engineering:*
30 *A* 528 (15):5066-5072
31
32
33 123. Farshidi MH, Kazeminezhad M, Miyamoto H (2014) Microstructural evolution of
34 aluminum 6061 alloy through tube channel pressing. *Materials Science and Engineering A*
35 615:139-147. doi:10.1016/j.msea.2014.07.061
36
37
38 124. Faraji G, Babaei A, Mashhadi MM, Abrinia K (2012) Parallel tubular channel angular
39 pressing (PTCAP) as a new severe plastic deformation method for cylindrical tubes. *Materials*
40 *Letters* 77:82-85
41
42 125. Lee HH, Yoon JI, Kim HS (2018) Single-roll angular-rolling: A new continuous severe
43 plastic deformation process for metal sheets. *Scripta Materialia* 146:204-207.
44 doi:<https://doi.org/10.1016/j.scriptamat.2017.11.043>
45
46
47 126. Fadaei A, Farahafshan F, Sepahi-Boroujeni S (2017) Spiral equal channel angular extrusion
48 (Sp-ECAE) as a modified ECAE process. *Materials & Design* 113:361-368.
49 doi:<https://doi.org/10.1016/j.matdes.2016.10.021>
50
51
52 127. Wadsack R, Pippin R, Schedler B (2003) Structural refinement of chromium by severe
53 plastic deformation. *Fusion Engineering and Design* 66-68:265-269. doi:10.1016/S0920-
54 3796(03)00136-4
55
56
57 128. Tóth LS, Arzaghi M, Fundenberger JJ, Beausir B, Bouaziz O, Arruffat-Massion R (2009)
58 Severe plastic deformation of metals by high-pressure tube twisting. *Scripta Materialia* 60
59 (3):175-177. doi:<http://dx.doi.org/10.1016/j.scriptamat.2008.09.029>
60
61
62
63
64
65

- 1
2
3
4 129. Arzaghi M, Funderberger J, Toth L, Arruffat R, Faure L, Beausir B, Sauvage X (2012)
5 Microstructure, texture and mechanical properties of aluminum processed by high-pressure tube
6 twisting. *Acta materialia* 60 (11):4393-4408
7
8
9 130. Wang M, Shan A (2008) Severe plastic deformation introduced by rotation shear. *Journal of*
10 *Materials Processing Technology* 202 (1):549-552
11
12 131. Wang JT, Li Z, Wang J, Langdon TG (2012) Principles of severe plastic deformation using
13 tube high-pressure shearing. *Scripta Materialia* 67 (10):810-813
14
15
16 132. Harai Y, Ito Y, Horita Z (2008) High-pressure torsion using ring specimens. *Scripta*
17 *Materialia* 58 (6):469-472
18
19
20 133. Edalati K, Lee S, Horita Z (2012) Continuous high-pressure torsion using wires. *Journal of*
21 *Materials Science* 47 (1):473-478. doi:10.1007/s10853-011-5822-z
22
23 134. Fujioka T, Horita Z (2009) Development of high-pressure sliding process for
24 microstructural refinement of rectangular metallic sheets. *Materials transactions* 50 (4):930
25
26
27 135. Bouaziz O, Estrin Y, Kim HS (2009) A New Technique for Severe Plastic Deformation:
28 The Cone–Cone Method. *Advanced Engineering Materials* 11 (12):982-985
29
30 136. Um HY, Yoon EY, Lee DJ, Lee CS, Park LJ, Lee S, Kim HS (2014) Hollow cone high-
31 pressure torsion: Microstructure and tensile strength by unique severe plastic deformation.
32 *Scripta Materialia* 71:41-44
33
34
35 137. Hohenwarter A (2015) Incremental high pressure torsion as a novel severe plastic
36 deformation process: Processing features and application to copper. *Materials Science and*
37 *Engineering: A* 626 (0):80-85. doi:<http://dx.doi.org/10.1016/j.msea.2014.12.041>
38
39
40 138. Kume Y, Kobashi M, Kanetake N (2007) Homogeneity of Grain Refinement of Aluminum
41 Alloy with Compressive Torsion Processing. *Advanced Materials Research* 26:107-110
42
43 139. Jahedi M, Paydar MH, Zheng S, Beyerlein IJ, Knezevic M (2014) Texture evolution and
44 enhanced grain refinement under high-pressure-double-torsion. *Materials Science and*
45 *Engineering: A* 611:29-36
46
47
48 140. Khoddam S (2016) A detailed model of high pressure torsion. *Materials Science and*
49 *Engineering: A*
50
51 141. Khoddam S, Farhoumand A, Hodgson P (2011) Upper-bound analysis of axi-symmetric
52 forward spiral extrusion. *Mechanics of materials* 43 (11):684-692
53
54
55 142. Gurău G, Gurău C, Potecașu O, Alexandru P, Bujoreanu L-G Novel High-Speed High
56 Pressure Torsion Technology for Obtaining Fe-Mn-Si-Cr Shape Memory Alloy Active Elements.
57 *Journal of Materials Engineering and Performance*:1-7
58
59
60
61
62
63
64
65

- 1
2
3
4 143. Nakamura K, Neishi K, Kaneko K, Nakagaki M, Horita Z (2004) Development of severe
5 torsion straining process for rapid continuous grain refinement. *Materials transactions* 45
6 (12):3338-3342
7
8
9 144. Dawes WMTDNCNGMT-SJ (1991) Friction welding.
10
11 145. Mishra RS, Ma ZY (2005) Friction stir welding and processing. *Materials Science and*
12 *Engineering: R: Reports* 50 (1):1-78. doi:<https://doi.org/10.1016/j.msar.2005.07.001>
13
14 146. Pardis N, Ebrahimi R (2009) Deformation behavior in Simple Shear Extrusion (SSE) as a
15 new severe plastic deformation technique. *Materials Science and Engineering: A* 527 (1):355-
16 360. doi:<https://doi.org/10.1016/j.msea.2009.08.051>
17
18 147. Pardis N, Ebrahimi R (2010) Different processing routes for deformation via simple shear
19 extrusion (SSE). *Materials Science and Engineering: A* 527 (23):6153-6156.
20 doi:<https://doi.org/10.1016/j.msea.2010.06.028>
21
22 148. Bagherpour E, Ebrahimi R, Qods F (2015) An analytical approach for simple shear
23 extrusion process with a linear die profile. *Materials & Design* 83 (Supplement C):368-376.
24 doi:<https://doi.org/10.1016/j.matdes.2015.06.023>
25
26 149. Rifai M, Bagherpour E, Yamamoto G, Yuasa M, Miyamoto H (2018) Transition of
27 Dislocation Structures in Severe Plastic Deformation and Its Effect on Dissolution in Dislocation
28 Etchant. *Advances in Materials Science and Engineering* 2018
29
30 150. Bagherpour E, Reihanian M, Ebrahimi R (2012) On the capability of severe plastic
31 deformation of twining induced plasticity (TWIP) steel. *Materials & Design* (1980-2015) 36
32 (Supplement C):391-395. doi:<https://doi.org/10.1016/j.matdes.2011.11.055>
33
34 151. Bagherpour E, Reihanian M, Ebrahimi R (2012) Processing twining induced plasticity steel
35 through simple shear extrusion. *Materials & Design* 40 (Supplement C):262-267.
36 doi:<https://doi.org/10.1016/j.matdes.2012.03.055>
37
38 152. Morshed Behbahani K, Najafisayar P, Abbasi Z, Pakshir M, Ebrahimi R (2016) The Effect
39 of Simple Shear Extrusion on the Corrosion Behavior of Copper. *Iranian Journal of Chemistry*
40 *and Chemical Engineering (IJCCE)* 35 (2):73-78
41
42 153. Tork NB, Pardis N, Ebrahimi R (2013) Investigation on the feasibility of room temperature
43 plastic deformation of pure magnesium by simple shear extrusion process. *Materials Science and*
44 *Engineering: A* 560 (Supplement C):34-39. doi:<https://doi.org/10.1016/j.msea.2012.08.085>
45
46 154. Bayat Tork N, Razavi SH, Saghafian h, Mahmudi R (2016) Superplasticity of a fine-grained
47 Mg–1.5 wt% Gd alloy after severe plastic deformation. *Iranian Journal of Materials Forming* 3
48 (1):65-74. doi:10.22099/ijmf.2016.3711
49
50 155. Bayat Tork N, Razavi SH, Saghafian H, Mahmudi R (2017) Strain-rate sensitivity of Mg–
51 Gd alloys after extrusion and simple shear extrusion. *Materials Science and Technology* 33
52 (18):2244-2252. doi:10.1080/02670836.2017.1374001
53
54
55
56
57
58
59
60
61
62
63
64
65

- 1
2
3
4 156. Bagherpour E, Qods F, Ebrahimi R (2014) Effect of geometric parameters on deformation
5 behavior of simple shear extrusion. IOP Conference Series: Materials Science and Engineering
6 63 (1):012046
7
8
9 157. Kim JG, Latypov M, Pardis N, Beygelzimer YE, Kim HS (2015) Finite element analysis of
10 the plastic deformation in tandem process of simple shear extrusion and twist extrusion.
11 Materials & Design 83:858-865
12
13 158. Sheikh H, Ebrahimi R (2017) Modeling the effect of strain reversal on grain refinement and
14 crystallographic texture during simple shear extrusion. International Journal of Solids and
15 Structures 126:175-186
16
17 159. Beygelzimer Y, Varyukhin V, Synkov S, Orlov D (2009) Useful properties of twist
18 extrusion. Materials Science and Engineering: A 503 (1):14-17
19
20 160. Asghar SA, Mousavi A, Bahador SR (2011) Investigation and numerical analysis of strain
21 distribution in the twist extrusion of pure aluminum. JOM 63 (2):69-76. doi:10.1007/s11837-
22 011-0032-3
23
24 161. Beygelzimer Y, Orlov D, Varyukhin V A new severe plastic deformation method: Twist
25 extrusion. In: TMS Annual Meeting, 2002. pp 297-304
26
27 162. Beygelzimer Y, Varyukhin V, Orlov D, Efros B, Stolyarov V, Salimgareyev H
28 Microstructural evolution of titanium under twist extrusion. In: TMS Annual Meeting, 2002. pp
29 43-46
30
31 163. Beygelzimer Y, Varyukhin V, Synkov S (2008) Shears, vortices, and mixing during twist
32 extrusion. International Journal of Material Forming 1 (SUPPL. 1):443-446.
33 doi:10.1007/s12289-008-0090-4
34
35 164. Beygelzimer YY, Orlov DV (2002) Metal plasticity during the twist extrusion. Defect and
36 Diffusion Forum, vol 208-209.
37
38 165. Kalahroudi FJ, Eviani AR, Jafarian HR, Amouri A, Gholizadeh R (2016) Inhomogeneity in
39 strain, microstructure and mechanical properties of AA1050 alloy during twist extrusion.
40 Materials Science and Engineering A 667:349-357. doi:10.1016/j.msea.2016.04.087
41
42 166. Varyukhin V, Beygelzimer Y, Tkatch V, Maslov V, Synkov S, Synkov A, Nosenko V
43 Consolidation of bulk nanomaterials by twist extrusion of powders. In: TMS Annual Meeting,
44 2006. pp 125-130
45
46 167. Beygelzimer Y, Prilepo D, Kulagin R, Grishaev V, Abramova O, Varyukhin V, Kulakov M
47 (2011) Planar twist extrusion versus twist extrusion. Journal of Materials Processing Technology
48 211 (3):522-529
49
50 168. Eivani A (2014) Towards bulk nanostructured materials in pure shear. Materials Letters
51
52
53
54
55
56
57
58
59
60
61
62
63
64
65

- 1
2
3
4 169. Richert J, Richert M (1986) A new method for unlimited deformation of metals and alloys. Aluminium 62 (8):604-607
5
6
7
8 170. Balasundar I, Raghu T (2013) On the die design for Repetitive Upsetting–Extrusion (RUE)
9 process. International journal of material forming 6 (2):289-301
10
11 171. Balasundar I, Ravi KR, Raghu T (2013) Strain softening in oxygen free high conductivity
12 (OFHC) copper subjected to repetitive upsetting-extrusion (RUE) process. Materials Science and
13 Engineering: A 583 (0):114-122. doi:<http://dx.doi.org/10.1016/j.msea.2013.06.029>
14
15
16 172. Lianxi H, Yuping L, Erde W, Yang Y (2006) Ultrafine grained structure and mechanical
17 properties of a LY12 Al alloy prepared by repetitive upsetting-extrusion. Materials Science and
18 Engineering: A 422 (1–2):327-332. doi:<http://dx.doi.org/10.1016/j.msea.2006.02.014>
19
20
21 173. Zaharia L, Comaneci R, Chelariu R, Luca D (2014) A new severe plastic deformation
22 method by repetitive extrusion and upsetting. Materials Science and Engineering: A 595 (0):135-
23 142. doi:<http://dx.doi.org/10.1016/j.msea.2013.12.006>
24
25
26 174. Aizawa T, Tokumitu K (1999) Bulk mechanical alloying for productive processing of
27 functional alloys. Materials Science Forum 312:13-22
28
29 175. Pardis N, Chen C, Ebrahimi R, Toth L, Gu C, Beausir B, Kommel L (2015) Microstructure,
30 texture and mechanical properties of cyclic expansion–extrusion deformed pure copper.
31 Materials Science and Engineering: A 628:423-432
32
33
34 176. Pardis N, Talebanpour B, Ebrahimi R, Zomorodian S (2011) Cyclic expansion-extrusion
35 (CEE): A modified counterpart of cyclic extrusion-compression (CEC). Materials Science and
36 Engineering: A 528 (25–26):7537-7540. doi:<http://dx.doi.org/10.1016/j.msea.2011.06.059>
37
38
39 177. Pardis N, Chen C, Shahbaz M, Ebrahimi R, Toth L (2014) Development of new routes of
40 severe plastic deformation through cyclic expansion–extrusion process. Materials Science and
41 Engineering: A 613:357-364
42
43 178. Beygelzimer Y, Reshetov A (2006) TWIST EXTRUSIONS PLUS SPREAD EXTRUSION
44 = SPATIAL UNIFORMITY Ultrafine Grained Materials IV 504:119-124
45
46
47 179. Ebrahimi M, Gholipour H, Djavanroodi F (2016) A study on the capability of equal channel
48 forward extrusion process. Materials Science and Engineering: A 650:1-7
49
50
51 180. Zaharia L, Chelariu R, Comaneci R (2012) Multiple direct extrusion: A new technique in
52 grain refinement. Materials Science and Engineering: A 550 (0):293-299.
53 doi:<http://dx.doi.org/10.1016/j.msea.2012.04.074>
54
55
56 181. Muralidharan G, Verlinden B (2015) AccumEx-A New SPD Technique for Fabricating
57 Lamellar Materials. Acta Physica Polonica A 128 (4):523-526
58
59
60
61
62
63
64
65

- 1
2
3
4 182. Wang Q, Chen Y, Lin J, Zhang L, Zhai C (2007) Microstructure and properties of
5 magnesium alloy processed by a new severe plastic deformation method. *Materials Letters* 61
6 (23):4599-4602
7
8
9 183. Fatemi-Varzaneh S, Zarei-Hanzaki A (2009) Accumulative back extrusion (ABE)
10 processing as a novel bulk deformation method. *Materials Science and Engineering: A* 504
11 (1):104-106
12
13
14 184. Alihosseini H, Asle Zaeem M, Dehghani K (2012) A cyclic forward–backward extrusion
15 process as a novel severe plastic deformation for production of ultrafine grains materials.
16 *Materials Letters* 68 (0):204-208. doi:<http://dx.doi.org/10.1016/j.matlet.2011.10.037>
17
18
19 185. Wang C, Li F, Li Q, Wang L (2012) Numerical and experimental studies of pure copper
20 processed by a new severe plastic deformation method. *Materials Science and Engineering: A*
21 548 (0):19-26. doi:<http://dx.doi.org/10.1016/j.msea.2012.03.055>
22
23
24 186. Beygelzimer Y, Kulagin R, Latypov MI, Varyukhin V, Kim HS (2015) Off-axis twist
25 extrusion for uniform processing of round bars. *Metals and Materials International* 21 (4):734-
26 740
27
28 187. Babaei A, Mashhadi M, Jafarzadeh H (2014) Tube Cyclic Extrusion-Compression (TCEC)
29 as a novel severe plastic deformation method for cylindrical tubes. *Materials Science and*
30 *Engineering: A* 598:1-6
31
32
33 188. Shahbaz M, Pardis N, Ebrahimi R, Talebanpour B (2011) A novel single pass severe plastic
34 deformation technique: Vortex extrusion. *Materials Science and Engineering: A* 530:469-472
35
36
37 189. Shahbaz M, Pardis N, Kim J, Ebrahimi R, Kim H (2016) Experimental and finite element
38 analyses of plastic deformation behavior in vortex extrusion. *Materials Science and Engineering:*
39 *A* 674:472-479
40
41
42 190. Li F, Zeng X, Bian N (2014) Microstructure of AZ31 magnesium alloy produced by
43 continuous variable cross-section direct extrusion (CVCDE). *Materials Letters* 135 (0):79-82.
44 doi:<http://dx.doi.org/10.1016/j.matlet.2014.07.116>
45
46
47 191. Li F, Zeng X, Cao GJ (2015) Investigation of microstructure characteristics of the
48 CVCDEed AZ31 magnesium alloy. *Materials Science and Engineering A* 639:395-401.
49 doi:10.1016/j.msea.2015.05.042
50
51
52 192. Neugebauer R, Sterzing A, Selbmann R, Zachäus R, Bergmann M (2012) Gradation
53 extrusion–Severe plastic deformation with defined gradient. *Materialwissenschaft und*
54 *Werkstofftechnik* 43 (7):582-588
55
56
57 193. Landgrebe D, Sterzing A, Schubert N, Bergmann M (2016) Influence of die geometry on
58 performance in gradation extrusion using numerical simulation and analytical calculation. *CIRP*
59 *Annals - Manufacturing Technology* 65 (1):269-272.
60 doi:<http://dx.doi.org/10.1016/j.cirp.2016.04.128>
61
62
63
64
65

- 1
2
3
4 194. Orlov D, Raab G, Lamark TT, Popov M, Estrin Y (2011) Improvement of mechanical
5 properties of magnesium alloy ZK60 by integrated extrusion and equal channel angular pressing.
6 Acta Materialia 59 (1):375-385
7
8
9 195. Chen Q, Zhao Z, Shu D, Zhao Z (2011) Microstructure and mechanical properties of
10 AZ91D magnesium alloy prepared by compound extrusion. Materials Science and Engineering:
11 A 528 (10):3930-3934
12
13
14 196. Li F, Jiang HW, Chen Q, Liu Y (2016) New extrusion method for reducing load and
15 refining grains for magnesium alloy. The International Journal of Advanced Manufacturing
16 Technology:1-7
17
18
19 197. Neugebauer R, Kolbe M, Glass R (2001) New warm forming processes to produce hollow
20 shafts. Journal of Materials Processing Technology 119 (1):277-282
21
22 198. Yu J, Zhang Z, Wang Q, Hao H, Cui J, Li L (2018) Rotary extrusion as a novel severe
23 plastic deformation method for cylindrical tubes. Materials Letters 215:195-199.
24 doi:<https://doi.org/10.1016/j.matlet.2017.12.048>
25
26
27 199. Vu VQ, Beygelzimer Y, Toth LS, Fundenberger J-J, Kulagin R, Chen C (2018) The plastic
28 flow machining: A new SPD process for producing metal sheets with gradient structures.
29 Materials Characterization 138:208-214. doi:<https://doi.org/10.1016/j.matchar.2018.02.013>
30
31 200. Ghosh AK (1988) Method for Producing a Fine Grain Aluminum Alloy Using Three Axes
32 Deformation. United States Patent,
33
34
35 201. Rosochowski A (2004) Processing metals by severe plastic deformation. Solid State
36 Phenomena 101:13-22
37
38
39 202. Wadsack R, Pippin R, Schedler B (2002) Development of Microstructure and Thermal
40 Stability of Nano-Structured Chromium Processed by Severe Plastic Deformation.
41 Nanomaterials by Severe Plastic Deformation:654-659
42
43
44 203. Valiakhmetov OR, Galeev RM, Salishchev GA (1990) Mechanical Properties of the VT8
45 Titanium Alloy with a Submicrocrystalline Structure. Fiz Met Metalloved 10 (10)
46
47
48 204. Salishchev G, Zaripova R, Galeev R, Valiakhmetov O (1995) Nanocrystalline structure
49 formation during severe plastic deformation in metals and their deformation behaviour.
50 Nanostructured Materials 6 (5):913-916. doi:[http://dx.doi.org/10.1016/0965-9773\(95\)00208-1](http://dx.doi.org/10.1016/0965-9773(95)00208-1)
51
52
53 205. Mulyukov RR, Imayev RM, Nazarov AA (2008) Production, properties and application
54 prospects of bulk nanostructured materials. Journal of Materials Science 43 (23-24):7257-7263.
55 doi:10.1007/s10853-008-2777-9
56
57
58 206. Valiev RZ, Estrin Y, Horita Z, Langdon TG, Zehetbauer MJ, Zhu YT (2006) Producing
59 bulk ultrafine-grained materials by severe plastic deformation. JOM 58 (4):33-39.
60 doi:10.1007/s11837-006-0213-7
61
62
63
64
65

- 1
2
3
4 207. Shin DH, Park J-J, Kim Y-S, Park K-T (2002) Constrained groove pressing and its
5 application to grain refinement of aluminum. *Materials Science and Engineering: A* 328 (1–
6 2):98-103. doi:[http://dx.doi.org/10.1016/S0921-5093\(01\)01665-3](http://dx.doi.org/10.1016/S0921-5093(01)01665-3)
7
8
9 208. Yoon SC, Krishnaiah A, Chakkingal U, Kim HS (2008) Severe plastic deformation and
10 strain localization in groove pressing. *Computational Materials Science* 43 (4):641-645
11
12 209. Lee JW, Park JJ (2002) Numerical and experimental investigations of constrained groove
13 pressing and rolling for grain refinement. *Journal of Materials Processing Technology* 130–
14 131:208-213. doi:[http://dx.doi.org/10.1016/S0924-0136\(02\)00722-7](http://dx.doi.org/10.1016/S0924-0136(02)00722-7)
15
16
17 210. Zhao X, Wang J-f, Jing T-f (2007) Gray Cast Iron With Directional Graphite Flakes
18 Produced by Cylinder Covered Compression Process. *Journal of Iron and Steel Research,*
19 *International* 14 (5):52-55. doi:[http://dx.doi.org/10.1016/S1006-706X\(07\)60074-0](http://dx.doi.org/10.1016/S1006-706X(07)60074-0)
20
21
22 211. Hua L, Han X (2009) 3D FE modeling simulation of cold rotary forging of a cylinder
23 workpiece. *Materials & Design* 30 (6):2133-2142
24
25
26 212. Alexander D (2007) New Methods for Severe Plastic Deformation Processing. *Journal of*
27 *Materials Engineering and Performance* 16 (3):360-374. doi:10.1007/s11665-007-9054-y
28
29 213. Babaei A, Faraji G, Mashhadi M, Hamdi M (2012) Repetitive forging (RF) using inclined
30 punches as a new bulk severe plastic deformation method. *Materials Science and Engineering: A*
31 558:150-157
32
33
34 214. Wang QJ, Zhang PP, Liu CR (2012) Principle of the Continuous Variable Cross-Section
35 Recycled Extrusion (CVCE) Process. *Advanced Materials Research* 418:1400-1404
36
37
38 215. Kuziak R, Zalecki W, Węglarczyk S, Pietrzyk M New possibilities of achieving ultrafine
39 grained microstructure in metals and alloys employing MaxStrain technology. In: *Solid State*
40 *Phenomena, 2005*. Trans Tech Publ, pp 43-48
41
42 216. Montazeri-Pour M, H. Parsa M, Mirzadeh H (2015) Multi-Axial Incremental Forging and
43 Shearing as a New Severe Plastic Deformation Processing Technique. *Advanced Engineering*
44 *Materials*:n/a-n/a. doi:10.1002/adem.201400467
45
46
47 217. Kwapisz M Analysis of the Shape of Stamp on the Distribution of Deformation in the
48 Process of Alternate Pressing and Multiaxial Compression. In: *Solid State Phenomena, 2015*.
49 Trans Tech Publ, pp 963-968
50
51
52 218. Sepahi-Boroujeni S, Sepahi-Boroujeni A (2016) Improvements in microstructure and
53 mechanical properties of AZ80 magnesium alloy by means of an efficient, novel severe plastic
54 deformation process. *Journal of Manufacturing Processes* 24:71-77
55
56
57 219. Kamikawa N, Furuhashi T (2013) Accumulative channel-die compression bonding (ACCB):
58 A new severe plastic deformation process to produce bulk nanostructured metals. *Journal of*
59 *Materials Processing Technology* 213 (8):1412-1418
60
61
62
63
64
65

- 1
2
3
4 220. Khodabakhshi F, Gerlich AP (2018) Accumulative fold-forging (AFF) as a novel severe
5 plastic deformation process to fabricate a high strength ultra-fine grained layered aluminum alloy
6 structure. *Materials Characterization* 136:229-239.
7 doi:<https://doi.org/10.1016/j.matchar.2017.12.023>
8
9
10 221. Huang J, Zhu Y, Jiang H, Lowe T (2001) Microstructures and dislocation configurations in
11 nanostructured Cu processed by repetitive corrugation and straightening. *Acta Materialia* 49
12 (9):1497-1505
13
14 222. Mirsepasi A, Nili-Ahmadabadi M, Habibi-Parsa M, Ghasemi-Nanesa H, Dizaji AF (2012)
15 Microstructure and mechanical behavior of martensitic steel severely deformed by the novel
16 technique of repetitive corrugation and straightening by rolling. *Materials Science and*
17 *Engineering: A* 551:32-39
18
19 223. Takayama Y, Uchiyama Y, Arakawa T, Kobayashi M, Kato H (2007) Crystallographic
20 orientation distribution control by means of continuous cyclic bending in a pure aluminum sheet.
21 *Materials transactions* 48 (8):1992-1997
22
23 224. Cui Q, Ohori K (2000) Grain refinement of high purity aluminium by asymmetric rolling.
24 *Materials Science and Technology* 16 (10):1095-1101
25
26 225. Chen YL, Shan AD, Jiang JH, Ding Y Characterizing the shear deformation during
27 asymmetric rolling. In: *Materials Science Forum*, 2008. Trans Tech Publ, pp 327-332
28
29 226. Xu G, Cao X, Zhang T, Duan Y, Peng X, Deng Y, Yin Z (2016) Achieving high strain rate
30 superplasticity of an Al-Mg-Sc-Zr alloy by a new asymmetrical rolling technology. *Materials*
31 *Science and Engineering: A* 672:98-107
32
33 227. Mohebbi M, Akbarzadeh A (2010) A novel spin-bonding process for manufacturing
34 multilayered clad tubes. *Journal of Materials Processing Technology* 210 (3):510-517
35
36 228. Mani B, Jahedi M, Paydar MH (2011) A modification on ECAP process by incorporating
37 torsional deformation. *Materials Science and Engineering: A* 528 (12):4159-4165
38
39 229. Kocich R, Greger M, Kursá M, Szurman I, Macháčková A (2010) Twist channel angular
40 pressing (TCAP) as a method for increasing the efficiency of SPD. *Materials Science and*
41 *Engineering: A* 527 (23):6386-6392
42
43 230. Wang XX, Xue KM, Li P, Wu ZL, Li Q (2010) Equal channel angular pressing and torsion
44 of pure Al powder in tubes. *Advanced Materials Research* 97:1109-1115
45
46 231. Paydar M, Reihanian M, Bagherpour E, Sharifzadeh M, Zarinejad M, Dean T (2009) Equal
47 channel angular pressing–forward extrusion (ECAP–FE) consolidation of Al particles. *Materials*
48 *& Design* 30 (3):429-432
49
50 232. Paydar MH, Reihanian M, Bagherpour E, Sharifzadeh M, Zarinejad M, Dean TA (2008)
51 Consolidation of Al particles through forward extrusion-equal channel angular pressing (FE-
52 ECAP). *Materials Letters* 62 (17-18):3266-3268. doi:10.1016/j.matlet.2008.02.038
53
54
55
56
57
58
59
60
61
62
63
64
65

- 1
2
3
4 233. Kocich R, Macháčková A, Kunčická L (2014) Twist channel multi-angular pressing
5 (TCMAP) as a new SPD process: Numerical and experimental study. *Materials Science and*
6 *Engineering: A* 612:445-455
7
8
9 234. Shamsborhan M, Shokuhfar A (2013) A planar twist channel angular extrusion (PTCAE) as
10 a novel severe plastic deformation method based on equal channel angular extrusion (ECAE)
11 method. *Proceedings of the Institution of Mechanical Engineers, Part C: Journal of Mechanical*
12 *Engineering Science*:0954406213515645
13
14
15 235. Bisadi H, Mohamadi M, Miyanaji H, Abdoli M (2013) A Modification on ECAP Process by
16 Incorporating Twist Channel. *Journal of Materials Engineering and Performance* 22 (3):875-881.
17 doi:10.1007/s11665-012-0323-z
18
19
20 236. Sepahi-Boroujeni S, Fereshteh-Saniee F (2015) Expansion equal channel angular extrusion,
21 as a novel severe plastic deformation technique. *Journal of Materials Science* 50 (11):3908-3919
22
23
24 237. Ivanisenko Y, Kulagin R, Fedorov V, Mazilkin A, Scherer T, Baretzky B, Hahn H (2016)
25 High Pressure Torsion Extrusion as a new severe plastic deformation process. *Materials Science*
26 *and Engineering: A* 664:247-256
27
28 238. Korbel A, Bochniak W (2004) Refinement and control of the metal structure elements by
29 plastic deformation. *Scripta Materialia* 51 (8):755-759
30
31
32 239. Zhang Z, Shao S, Manabe K-i, Kong X, Li Y (2016) Evolution of microstructure and
33 mechanical properties of Al 6061 alloy tube in cyclic rotating bending process. *Materials Science*
34 *and Engineering: A* 676:80-87
35
36
37 240. Mizunuma S Large straining behavior and microstructure refinement of several metals by
38 torsion extrusion process. In: *Materials Science Forum*, 2006. Trans Tech Publ, pp 185-192
39
40 241. Jahedi M, Paydar MH (2011) Three-dimensional finite element analysis of torsion extrusion
41 (TE) as an SPD process. *Materials Science and Engineering: A* 528 (29):8742-8749
42
43 242. Lu L, Liu C, Zhao J, Zeng W, Wang Z (2014) Modification of Grain Refinement and
44 Texture in AZ31 Mg Alloy by a New Plastic Deformation Method. *Journal of Alloys and*
45 *Compounds*
46
47
48 243. Li YZ, Du XF Plastic Deformation Simulation on Compound Twist Extrusion Process for
49 Metal Materials. In: *Applied Mechanics and Materials*, 2013. Trans Tech Publ, pp 2676-2679
50
51 244. Torabzadeh H, Faraji G, Zalnezhad E (2016) Cyclic flaring and sinking (CFS) as a new
52 severe plastic deformation method for thin-walled cylindrical tubes. *Transactions of the Indian*
53 *Institute of Metals* 69 (6):1217-1222
54
55
56 245. Moscoso W, Shankar MR, Mann J, Compton W, Chandrasekar S (2007) Bulk
57 nanostructured materials by large strain extrusion machining. *Journal of materials research* 22
58 (01):201-205
59
60
61
62
63
64
65

- 1
2
3
4 246. Ensafi M, Faraji G, Abdolvand H (2017) Cyclic extrusion compression angular pressing
5 (CECAP) as a novel severe plastic deformation method for producing bulk ultrafine grained
6 metals. *Materials Letters* 197:12-16. doi:<https://doi.org/10.1016/j.matlet.2017.03.142>
7
8
9 247. Pourbashiri M, Sedighi M, Poletti C, Sommitsch C (2017) Enhancing mechanical properties
10 of wires by a novel continuous severe plastic deformation method. *International Journal of*
11 *Materials Research* 108 (9):741-749
12
13
14 248. Sabirov I, Enikeev NA, Murashkin MY, Valiev RZ (2015) Bulk Nanostructured Metals for
15 Innovative Applications. In: Sabirov I, Enikeev NA, Murashkin MY, Valiev RZ (eds) *Bulk*
16 *Nanostructured Materials with Multifunctional Properties*. Springer International Publishing,
17 Cham, pp 101-113. doi:10.1007/978-3-319-19599-5_4
18
19
20 249. Lowe TC (2006) Metals and alloys nanostructured by severe plastic deformation:
21 Commercialization pathways. *JOM* 58 (4):28. doi:10.1007/s11837-006-0212-8
22
23
24 250. Valiev RZ, Zehetbauer MJ, Estrin Y, Höppel HW, Ivanisenko Y, Hahn H, Wilde G, Roven
25 HJ, Sauvage X, Langdon TG (2007) The Innovation Potential of Bulk Nanostructured Materials.
26 *Advanced Engineering Materials* 9 (7):527-533. doi:10.1002/adem.200700078
27
28 251. Ferrasse S, Alford F, Grabmeier S, Düvel A, Zedlitz R, Strothers S, Evans J, Daniels B
29 (2003) ECAE ® Targets with Sub-Micron Grain Structures Improve Sputtering Performance and
30 Cost-of-Ownership. Honeywell International Inc.
31 ([http://www.honeywell.com/sites/docs/doc128e30a-f9d1a68f6a-](http://www.honeywell.com/sites/docs/doc128e30a-f9d1a68f6a-e0df9bfada07602278603c6cb43673fb.pdf)
32 [e0df9bfada07602278603c6cb43673fb.pdf](http://www.honeywell.com/sites/docs/doc128e30a-f9d1a68f6a-e0df9bfada07602278603c6cb43673fb.pdf)), Technology White Paper
33
34
35 252. Ferrasse S, Segal VM, Alford F, Kardokus J, Strothers S (2008) Scale up and application of
36 equal-channel angular extrusion for the electronics and aerospace industries. *Materials Science*
37 *and Engineering: A* 493 (1):130-140. doi:<https://doi.org/10.1016/j.msea.2007.04.133>
38
39
40 253. Azushima A, Kopp R, Korhonen A, Yang DY, Micari F, Lahoti GD, Groche P, Yanagimoto
41 J, Tsuji N, Rosochowski A, Yanagida A (2008) Severe plastic deformation (SPD) processes for
42 metals. *CIRP Annals* 57 (2):716-735. doi:<https://doi.org/10.1016/j.cirp.2008.09.005>
43
44
45 254. (2006). *Biocompatible Materials, US Industry Study with Forecasts to 2010 & 2015, Study*
46 *#2111, the Freedonia Group:264*
47
48 255. Mora-Sanchez H, Sabirov I, Monclus MA, Matykina E, Molina-Aldareguia JM (2016)
49 Ultra-fine grained pure Titanium for biomedical applications. *Materials Technology* 31 (13):756-
50 771. doi:10.1080/10667857.2016.1238131
51
52
53 256. Mishnaevsky L, Levashov E, Valiev RZ, Segurado J, Sabirov I, Enikeev N, Prokoshkin S,
54 Solov'yov AV, Korotitskiy A, Gutmanas E, Gotman I, Rabkin E, Psakh'e S, Dluhoš L, Seefeldt
55 M, Smolin A (2014) Nanostructured titanium-based materials for medical implants: Modeling
56 and development. *Materials Science and Engineering: R: Reports* 81 (Supplement C):1-19.
57 doi:<https://doi.org/10.1016/j.mser.2014.04.002>
58
59
60
61
62
63
64
65

- 1
2
3
4 257. Elias CN, Meyers MA, Valiev RZ, Monteiro SN (2013) Ultrafine grained titanium for
5 biomedical applications: An overview of performance. *Journal of Materials Research and*
6 *Technology* 2 (4):340-350. doi:<https://doi.org/10.1016/j.jmrt.2013.07.003>
7
8
9 258. Webster TJ, Siegel RW, Bizios R (1999) Osteoblast adhesion on nanophase ceramics.
10 *Biomaterials* 20 (13):1221-1227. doi:10.1016/S0142-9612(99)00020-4
11
12 259. Webster TJ, Ejiogor JU Increased, directed osteoblast adhesion at nanophase Ti and
13 Ti6Al4V particle boundaries. In: *Materials Research Society Symposium - Proceedings, 2003.*
14 pp 393-398
15
16
17 260. Durmus NG, Webster TJ (2012) Nanostructured titanium: The ideal material for improving
18 orthopedic implant efficacy? *Nanomedicine* 7 (6):791-793. doi:10.2217/nnm.12.53
19
20
21 261. Stolyarov VV, Zhu YT, Alexandrov IV, Lowe TC, Valiev RZ (2001) Influence of ECAP
22 routes on the microstructure and properties of pure Ti. *Materials Science and Engineering: A* 299
23 (1):59-67. doi:[https://doi.org/10.1016/S0921-5093\(00\)01411-8](https://doi.org/10.1016/S0921-5093(00)01411-8)
24
25
26 262. Sordi VL, Ferrante M, Kawasaki M, Langdon TG (2012) Microstructure and tensile
27 strength of grade 2 titanium processed by equal-channel angular pressing and by rolling. *Journal*
28 *of Materials Science* 47 (22):7870-7876. doi:10.1007/s10853-012-6593-x
29
30
31 263. Gunderov DV, Polyakov AV, Semenova IP, Raab GI, Churakova AA, Gimaltdinova EI,
32 Sabirov I, Segurado J, Sittikov VD, Alexandrov IV, Enikeev NA, Valiev RZ (2013) Evolution
33 of microstructure, macrotexture and mechanical properties of commercially pure Ti during
34 ECAP-conform processing and drawing. *Materials Science and Engineering: A* 562 (Supplement
35 C):128-136. doi:<https://doi.org/10.1016/j.msea.2012.11.007>
36
37
38 264. Roodposhti PS, Farahbakhsh N, Sarkar A, Murty KL (2015) Microstructural approach to
39 equal channel angular processing of commercially pure titanium—A review. *Transactions of*
40 *Nonferrous Metals Society of China* 25 (5):1353-1366. doi:[https://doi.org/10.1016/S1003-](https://doi.org/10.1016/S1003-6326(15)63734-7)
41 [6326\(15\)63734-7](https://doi.org/10.1016/S1003-6326(15)63734-7)
42
43
44 265. Sergueeva AV, Stolyarov VV, Valiev RZ, Mukherjee AK (2001) Advanced mechanical
45 properties of pure titanium with ultrafine grained structure. *Scripta Materialia* 45 (7):747-752.
46 doi:[https://doi.org/10.1016/S1359-6462\(01\)01089-2](https://doi.org/10.1016/S1359-6462(01)01089-2)
47
48
49 266. Wang CT, Fox AG, Langdon TG (2014) Microstructural evolution in ultrafine-grained
50 titanium processed by high-pressure torsion under different pressures. *Journal of Materials*
51 *Science* 49 (19):6558-6564. doi:10.1007/s10853-014-8248-6
52
53
54 267. Islamgaliev RK, Kazyhanov VU, Shestakova LO, Sharafutdinov AV, Valiev RZ (2008)
55 Microstructure and mechanical properties of titanium (Grade 4) processed by high-pressure
56 torsion. *Materials Science and Engineering: A* 493 (1):190-194.
57 doi:<https://doi.org/10.1016/j.msea.2007.08.084>
58
59
60
61
62
63
64
65

- 1
2
3
4 268. Valiev RZ, Semenova IP, Latysh VV, Rack H, Lowe TC, Petruzelka J, Dluhos L, Hrusak D,
5 Sochova J (2008) Nanostructured Titanium for Biomedical Applications. *Advanced Engineering*
6 *Materials* 10 (8):B15-B17. doi:10.1002/adem.200800026
7
8
9 269. Valiev R, Semenova I, Latysh V, Shcherbakov A, Yakushina E (2008) Nanostructured
10 titanium for biomedical applications: New developments and challenges for commercialization.
11 *Nanotechnologies in Russia* 3 (9-10):593-601
12
13
14 270. Valiev R The new SPD processing trends to fabricate bulk nanostructured materials. In:
15 *Solid State Phenomena*, 2006. Trans Tech Publ, pp 7-18
16
17 271. Schlapbach L, Züttel A (2001) Hydrogen-storage materials for mobile applications. *Nature*
18 414:353. doi:10.1038/35104634
19
20
21 272. Skripnyuk VM, Rabkin E, Estrin Y, Lapovok R (2004) The effect of ball milling and equal
22 channel angular pressing on the hydrogen absorption/desorption properties of Mg–4.95 wt% Zn–
23 0.71 wt% Zr (ZK60) alloy. *Acta Materialia* 52 (2):405-414.
24 doi:<https://doi.org/10.1016/j.actamat.2003.09.025>
25
26
27 273. Wang L, Jiang J, Ma A, Li Y, Song D (2017) A Critical Review of Mg-Based Hydrogen
28 Storage Materials Processed by Equal Channel Angular Pressing. *Metals* 7 (9).
29 doi:10.3390/met7090324
30
31 274. Grill A, Horky J, Panigrahi A, Krexner G, Zehetbauer M (2015) Long-term hydrogen
32 storage in Mg and ZK60 after Severe Plastic Deformation. *International Journal of Hydrogen*
33 *Energy* 40 (47):17144-17152. doi:<https://doi.org/10.1016/j.ijhydene.2015.05.145>
34
35
36
37
38
39
40
41
42
43
44
45
46
47
48
49
50
51
52
53
54
55
56
57
58
59
60
61
62
63
64
65

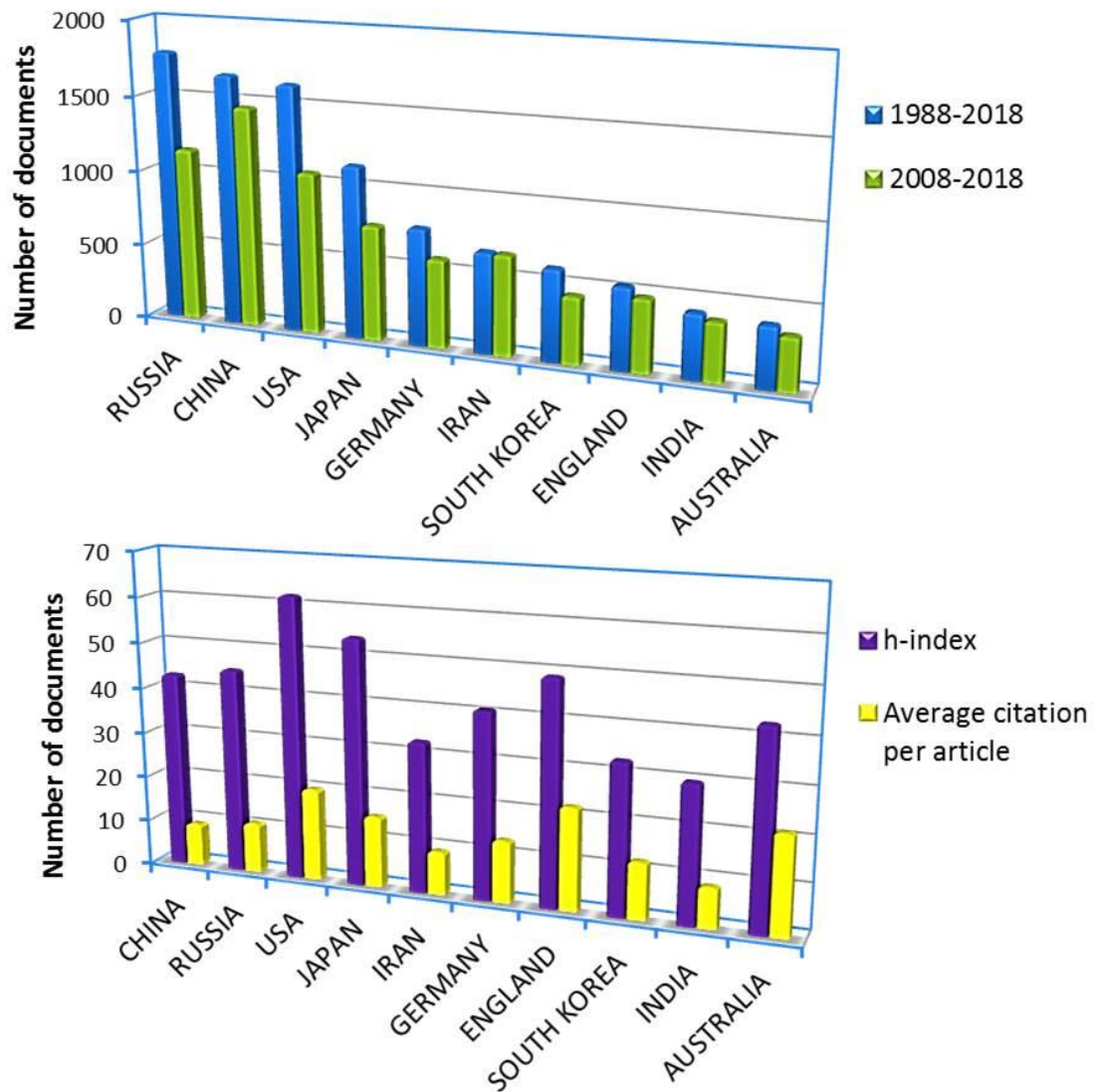


Fig. 1. Rank of the countries according to (a) the total number of publications in the field of SPD, and (b) the citations to the published articles during 2008-2018 based on different criteria

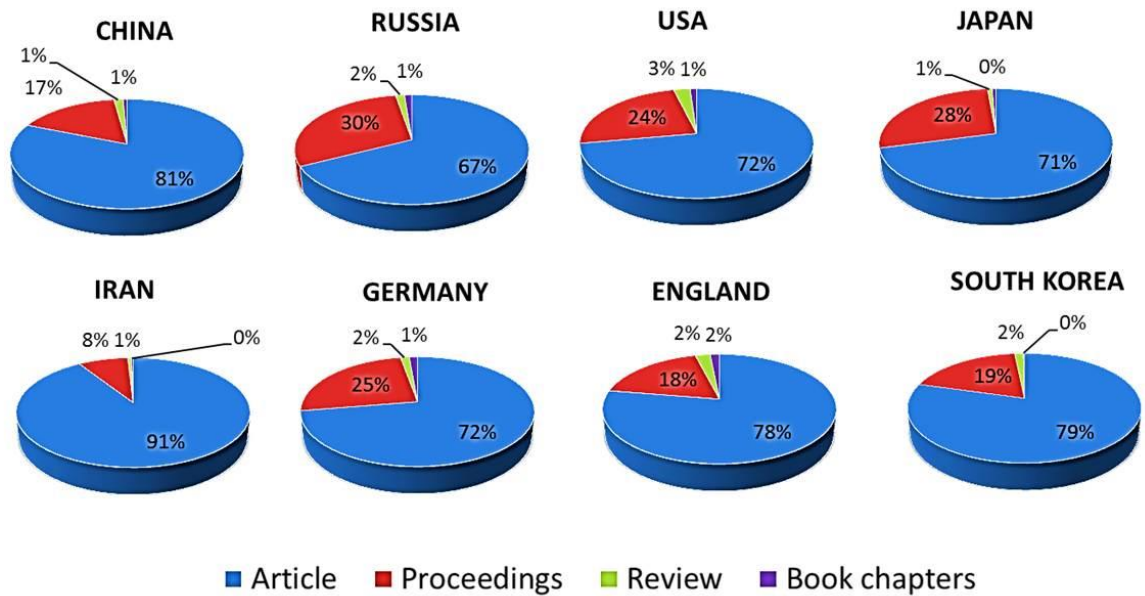


Fig. 2. Fraction of various types of published documents for the most important countries in field of SPD

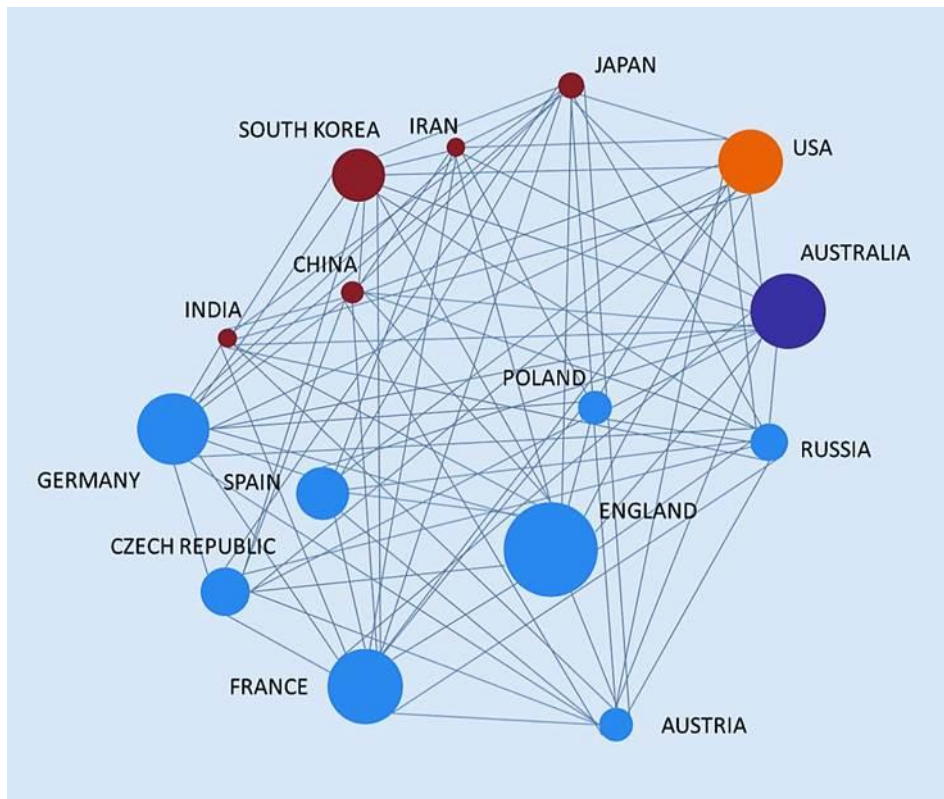


Fig. 3. Collaboration of various countries in the field of SPD up to the beginning of 2016 for the top-ranked countries in the field of SPD; the countries are specified by circles and their collaborations are denoted by the solid lines. The larger the number of articles published in collaboration with scientists from other nations, the larger the circle

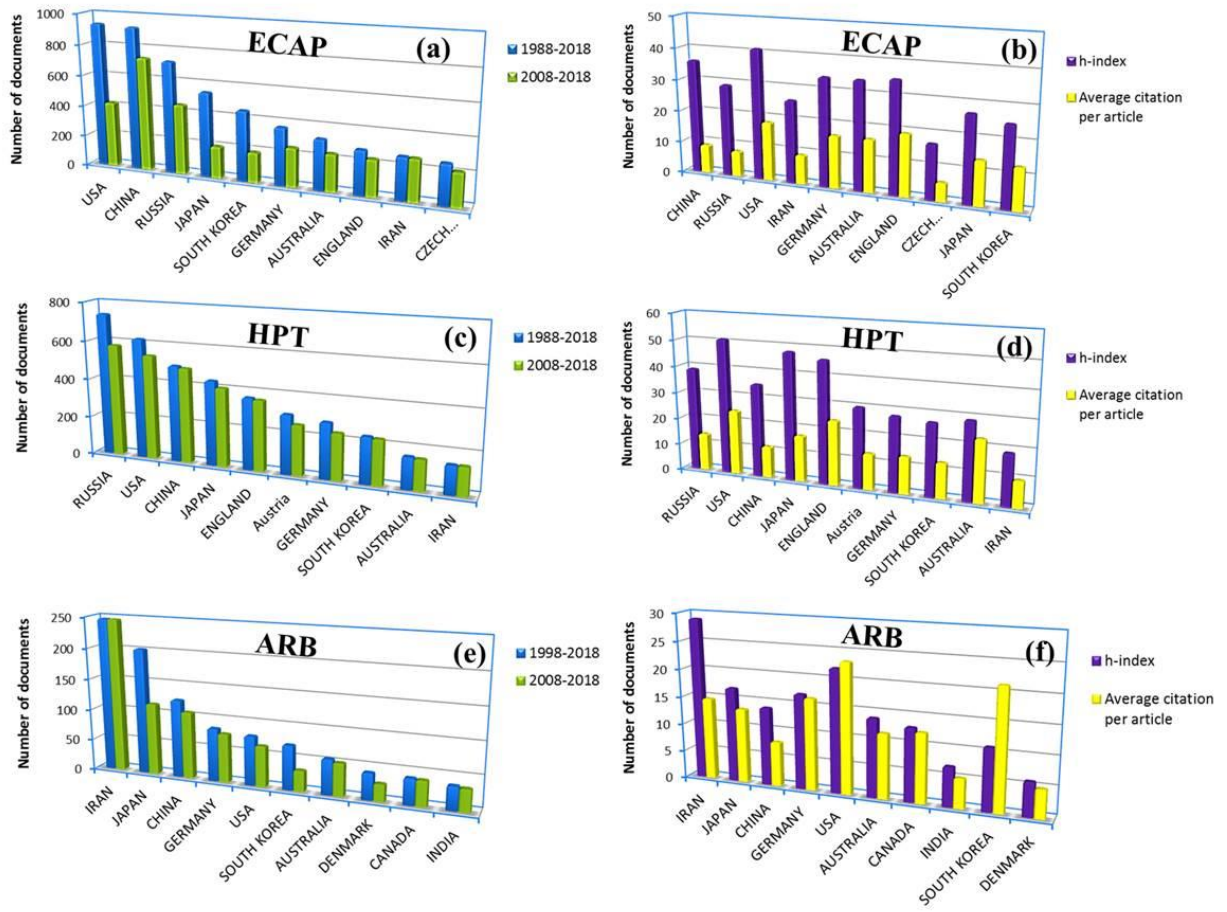


Fig. 4. Rank of the countries in the fields of (a, b) ECAP, (c, d) HPT, and (e, f) ARB, according to (a, c, e) the total number of publications in the field of SPD, and (b, d, f) the citations to the published articles during 2008-2018 based on different criteria

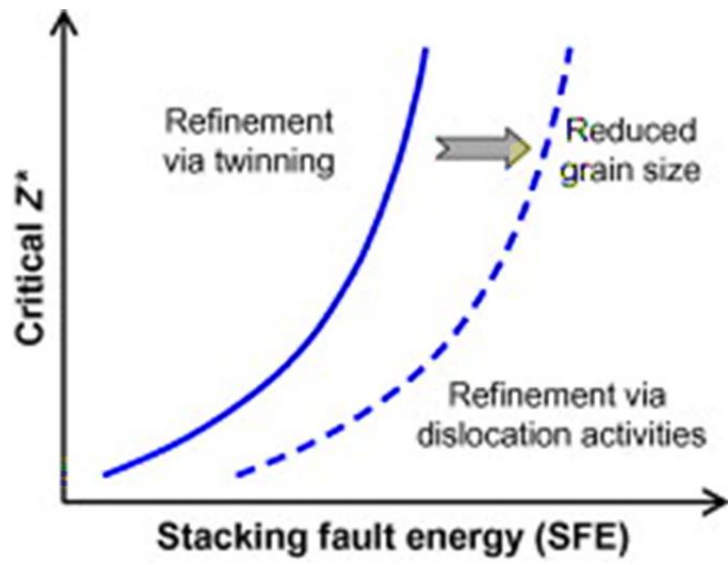


Fig. 5. Effect of the SFE and grain size on the dominating structural refinement mechanism [31]

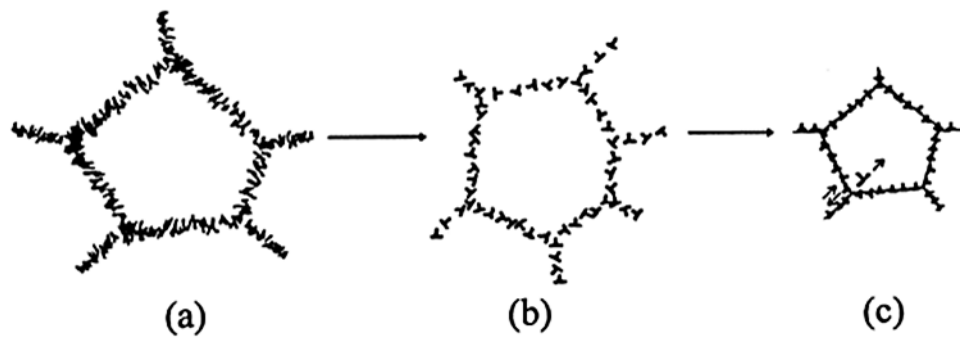


Fig. 6. The proposed model for dislocation substructure at different stages of SPD [1]

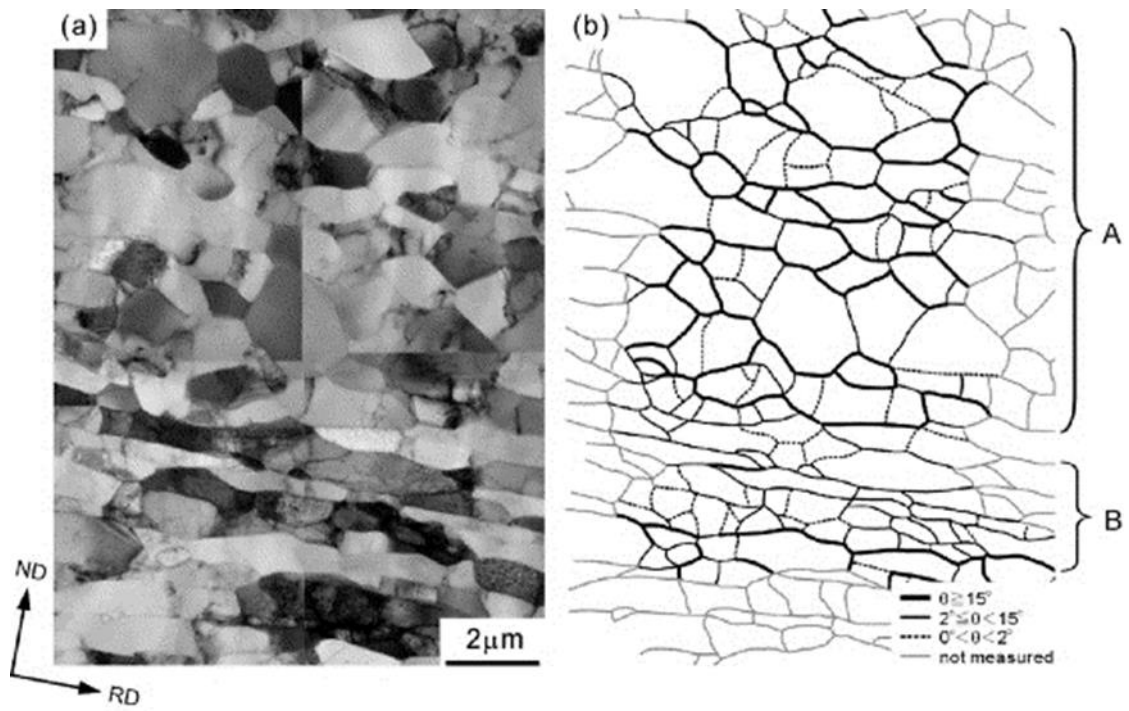


Fig. 7. (a) TEM microstructure and (b) the corresponding grain boundary map of pure Al after six ARB cycles [39]

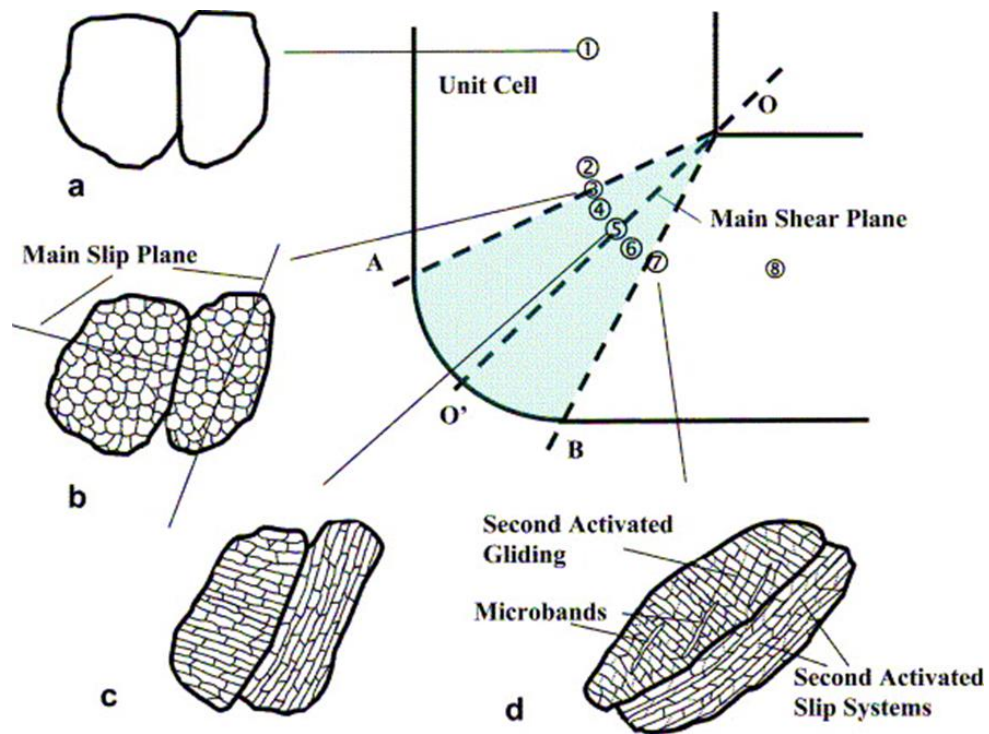


Fig. 8. The process of microstructural evolution during the first pass of ECAP: (a) the initial coarse grains under the shear stress, (b) dislocation generation and construction of dislocation cells (c) self-organized alignment of dislocation walls along slip planes by dislocation gliding and (d) segmentation through secondary slip and microbands [40]

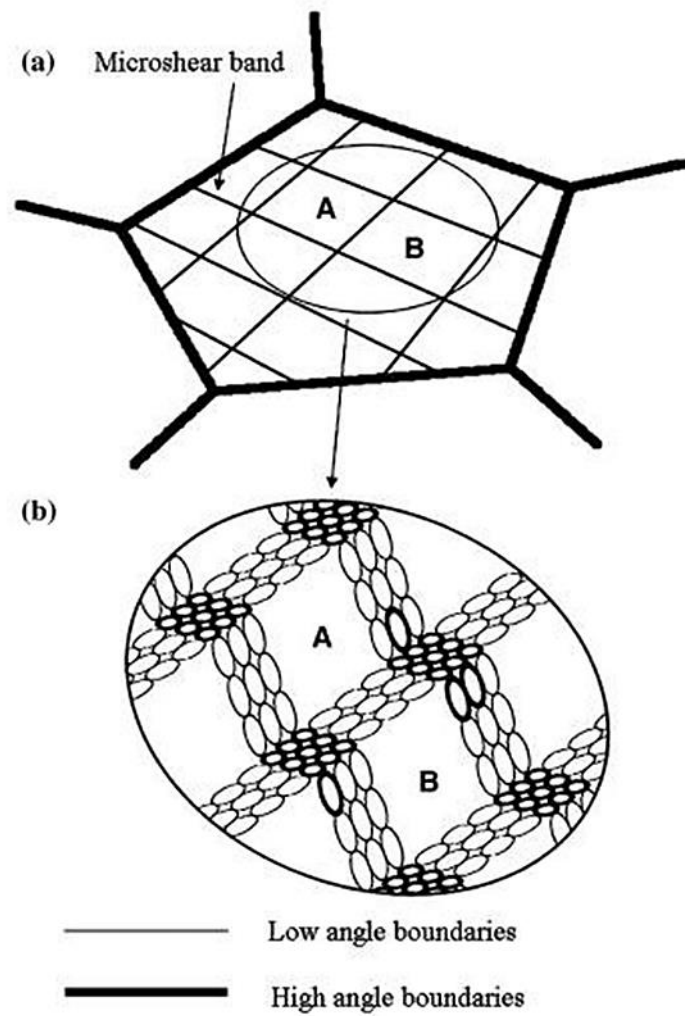


Fig. 9. Schematic illustration of the formation of (a) microshear bands at low strains and (b) subsequent formation of new grains at the intersections and along the microshear bands at large strains [42]

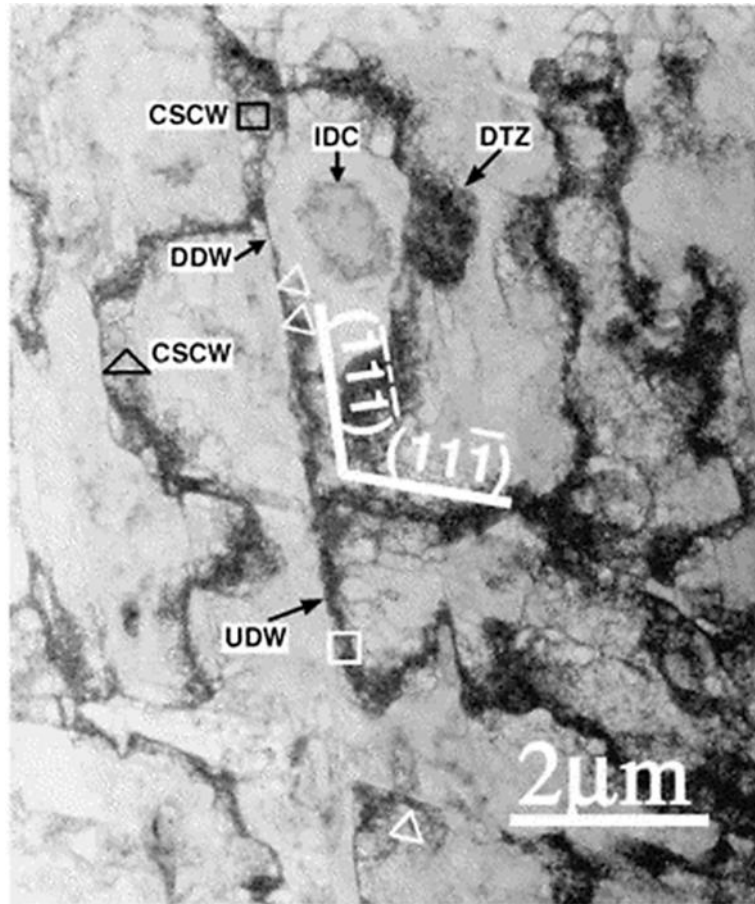


Fig. 10. TEM micrograph showing the different dislocation structures including cells, IDC, CSCWs, DDWs, UDWs and DTZs [35]

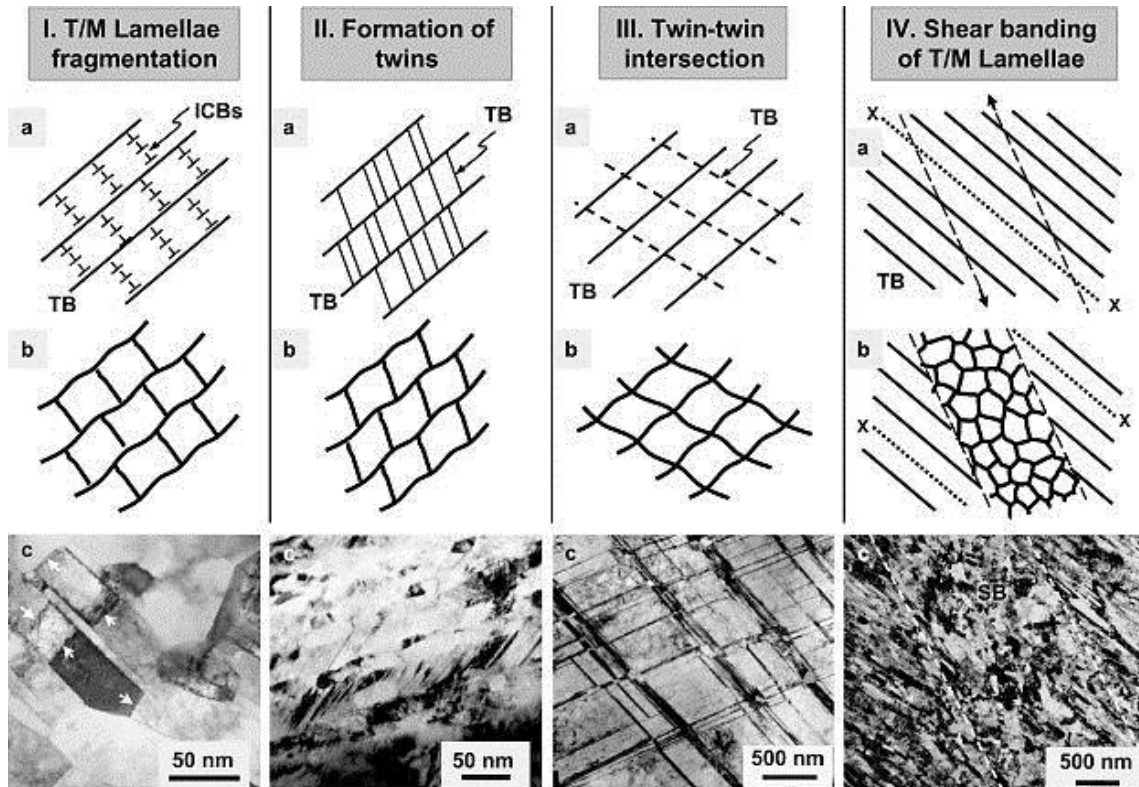


Fig. 11. Schematic illustrations showing four mechanisms of twinning-based grain refinement and the corresponding TEM images [31]

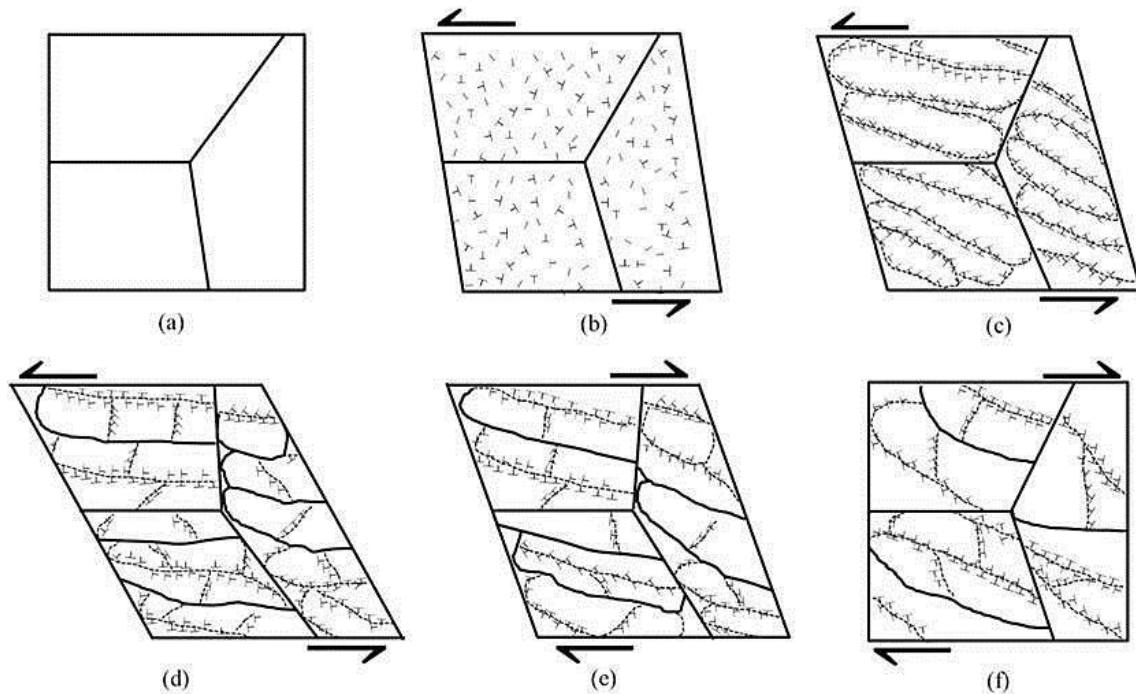


Fig. 12. Schematic illustration of the microstructural evolution during the SPD process that contains forward shear (a-d) and the shear strain reversal (e-f): (a) Initial cell structure, (b) homogeneous distribution of dislocations, (c) elongated cell formation, (d) dislocations blocked by subgrain boundaries and break up of elongated subgrains, (e) diminishing of the misorientation angle and/or eliminating of the dislocation boundaries and (f) final microstructure [54]

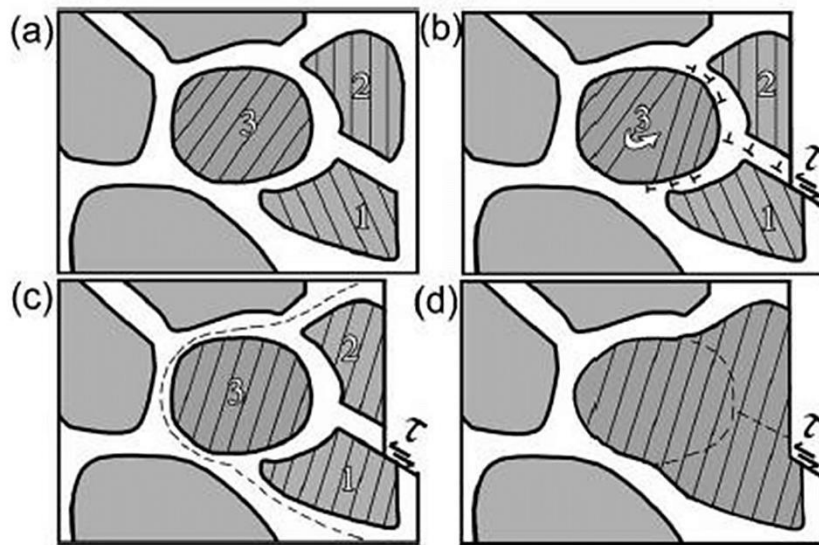


Fig. 13. Schematic illustration of a grain growth model via grain boundary sliding and grain rotation: (a) nano grains with high-angle grain boundaries before plastic deformation, (b) shear of grains 1 and 2 by gliding grain boundary dislocations and subsequent occurrence of rotation of grain 3 by climbing grain boundary dislocations, (c) multiple grain rotations leading to grain agglomeration and (d) A large grain formed with subgrain boundaries (highlighted by dotted line) due to incomplete grain coalescence [70]

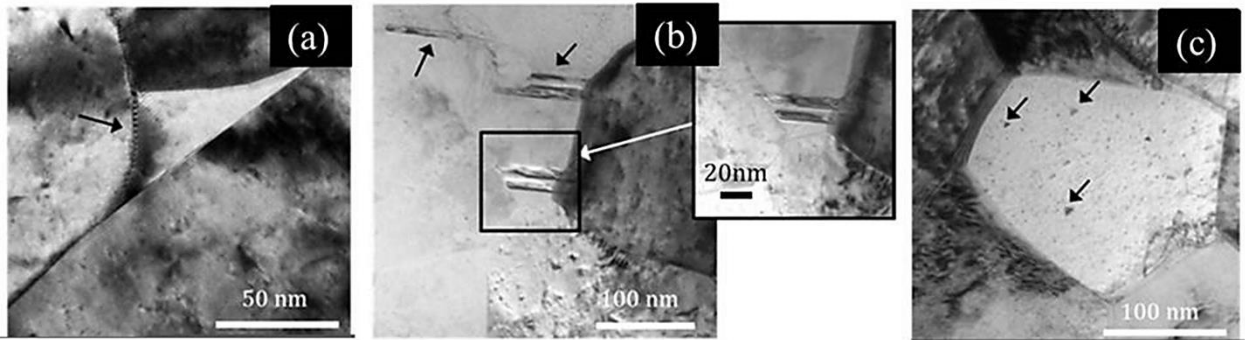


Fig. 14. Microstructural investigations of grain growth in Cu after 12 passes of SSE; (a) Moiré (b) deformation twins and (c) distinct stacking fault tetrahedra (SFT) [56]

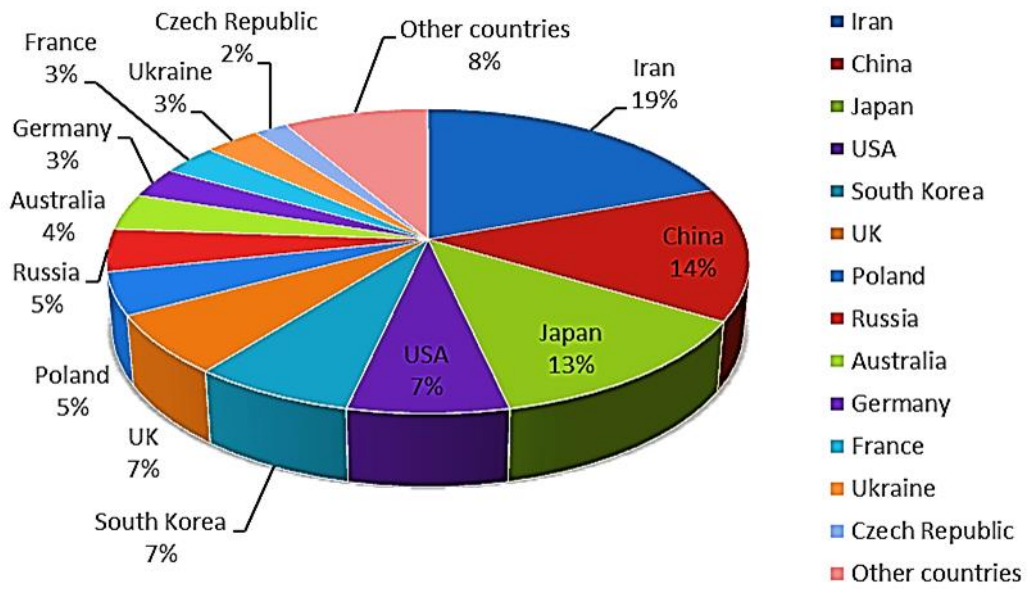
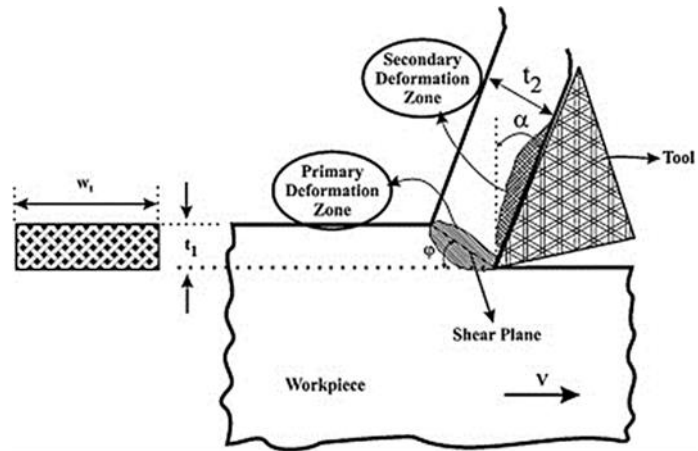
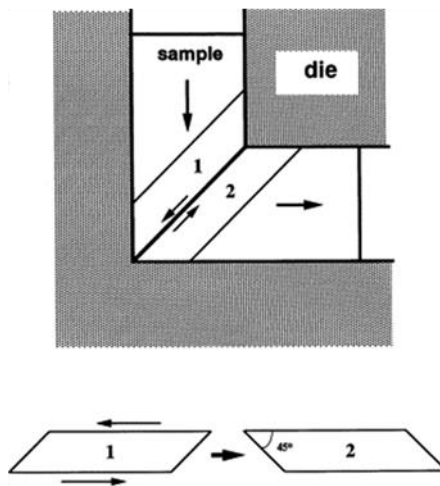


Fig. 15. Contribution of the countries to the introduction of new SPD techniques



(a)



(b)

Fig. 16. Shear plane in the process of (a) "large strain machining" [79], and (b) ECAP [80]

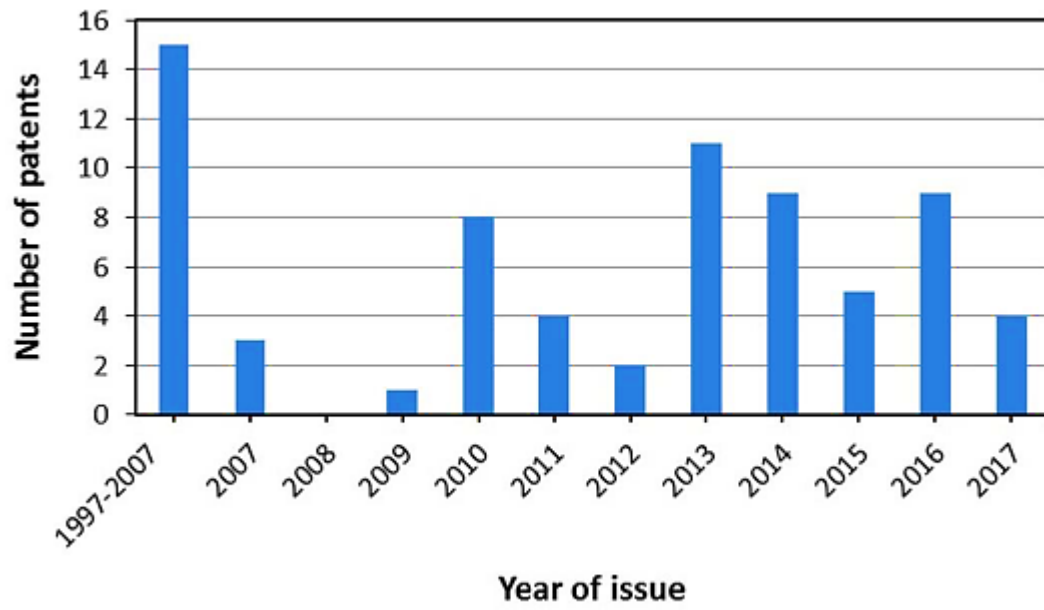


Fig. 17. Number of the patents corresponding to the SPD field in each year



Fig. 18. ECAP die with 4000 tones press capacity [252]

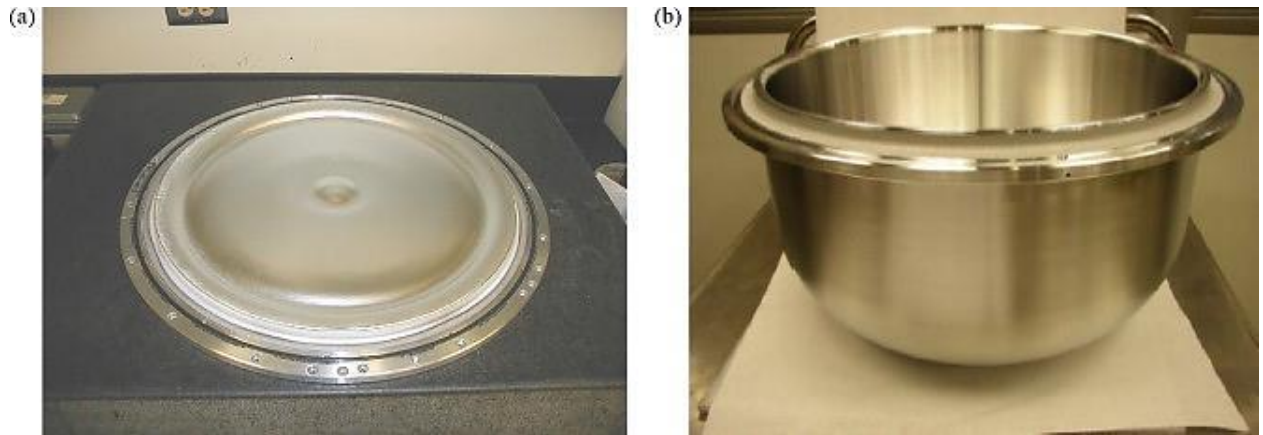


Fig. 19. Flat 300 mm monolithic ECAE Al_{0.5}Cu target with AMAT design and overall dimensions diameter 523.8 mm × 25.4 mm thickness sputtered up to 2738 kWh (+52% life increase) and (b) non-flat and non-sputtered 300 mm monolithic ECAE 6N Cu with HCM Novellus design and overall dimensions diameter 393.7 mm × 25.4 mm thickness × 381 mm height [252]



Fig. 20. A 5 mm diameter Timplant (above) and 2.4 mm diameter Nanoimplant (below) [268]



Fig. 21. View of ultrafine-grained billets with a diameter of 7 and a length of 300 mm from commercially pure grade titanium [269]



A



B



C

Fig. 22. (a) Implant from nanostructured Ti and (b) and (c) X-ray photos after surgery and control photo after incorporation of implants [256]

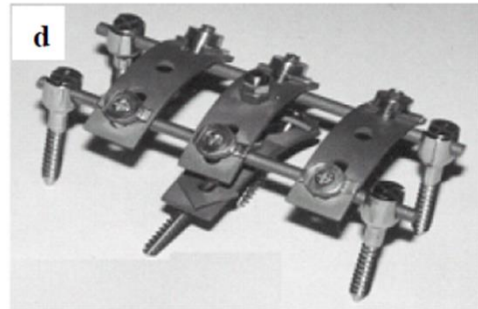
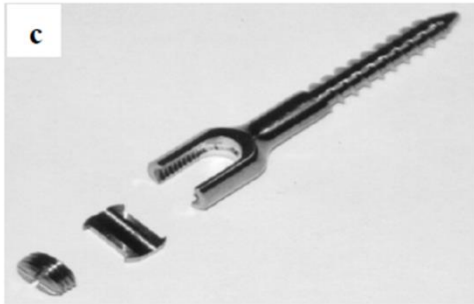
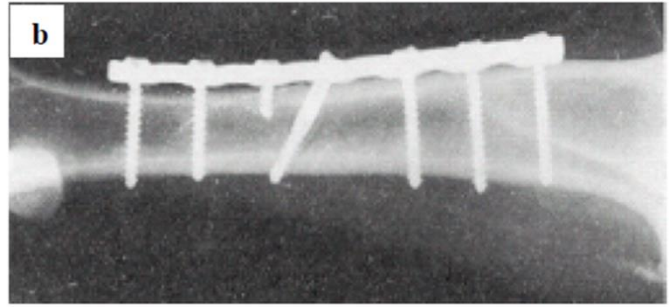
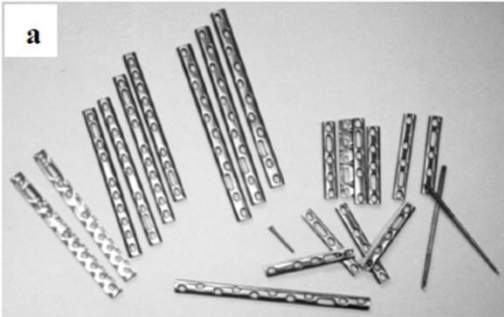


Fig. 23. Medical implants made of nanostructured titanium: (a) and (b) plate implants for osteosynthesis, (c) conic screw for spine fixation and (d) device for correction and fixation of spinal column [270]

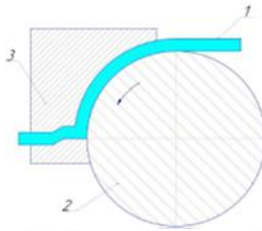
Table 1. Summary of the Contribution of the countries in the different categories of SPD techniques

	Based on ECAP	Based on torsion/shear under high pressure	Based on direct/indirect extrusion	Based on pressing/forging	Based on rolling	Combined techniques	Total
Iran	4	1	8	4	2	11	30
China	4	2	8	3	1	4	22
Japan	5	6	3	-	3	3	20
USA	4	2	-	2	1	2	11
South Korea	6	2	1	1	-	1	11
UK	5	3	-	-	-	2	10
Poland	4	-	1	1	-	1	7
Russia	4	-	1	1	-	1	7
Australia	2	3	1	-	-	-	6
Germany	1	-	3	-	-	1	5
France	1	2	1	-	-	1	5
Ukraine	-	-	4	-	-	1	5
Czech Republic	1	-	-	-	-	2	3
India	2	-	-	-	-	-	2
Belgium	1	-	1	-	-	-	2
Spain	1	-	-	-	-	-	1
Austria	-	1	-	-	-	1	2
Taiwan	1	-	-	-	-	-	1
Norway	-	-	1	-	-	-	1
Canada	-	-	-	1	-	-	1

Table 2. Summary of different SPD techniques based on ECAP

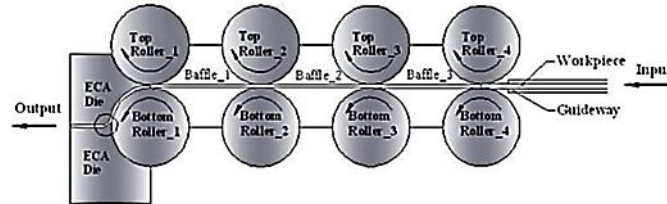
SPD technique	Illustration	[Ref.]
1 Equal-channel angular pressing (ECAP)	<p>The diagram shows a vertical plunger pushing a rectangular sample into a die. The die is a rectangular block with a channel. The sample is being compressed into the channel. A small inset shows the 'pressed sample' with a rectangular cross-section and coordinate axes X, Y, and Z.</p>	[81]
2 Conshearing process	<p>The diagram shows a cross-section of a 'Conshearing process'. A 'Material' strip enters from the left and passes between a 'Central roll' and a 'Satellite roll'. A 'Guide shoe' is positioned above the rolls. The entire assembly is labeled as 'ECA-die' and includes a 'Cover' and an 'Abutment'.</p>	[82]
3 Continuous confined strip shearing (C2S2)	<p>The diagram illustrates the 'Continuous confined strip shearing (C2S2)' process. A 'Thin strip' (1.55 mm thick) enters from the left, passes between a 'Guide roll' and a 'Feeding roll'. The strip then passes through an 'Inlet channel' (1.45 mm) and an 'Outlet channel' (1.55 mm) between the 'Upper die' and 'Lower die'.</p>	[83-86]
4 ECAP-Conform	<p>This diagram provides a detailed view of the 'ECAP-Conform' process. It features a 'Stationary die constructed from steel' with an 'Internal channel' (3.5 mm) and an 'Abrupt abutment to displace sample through $\phi = 90^\circ$'. A 'Rotating inner shaft' (12 cm diameter) is shown with a 'Transition from circular to rectangular cross-section' and a 'Circular cross-section'. The die has an 'Entrance channel' (4.0 mm) and an 'Exit channel'. The overall dimensions of the die are 30 cm by 30 cm.</p>	[87]
5 Equal channel angular drawing (ECAD)	<p>The diagram shows a schematic of 'Equal channel angular drawing (ECAD)' where a sample is drawn through a die. To the right is a photograph of the physical experimental setup, which includes a die and a sample being drawn through it.</p>	[88,89]
6 Continuous frictional angular extrusion	<p>The diagram illustrates 'Continuous frictional angular extrusion'. It shows a sample being extruded through a die. The die has a 'Shear plane' and is labeled with 'TD-ND' and 'ED'. The diagram also shows a cross-section of the die with numbered regions (1, 2, 3, 4, 5, 6) and a 'Shear plane'.</p>	[90]

7 Multi ECAP Conform



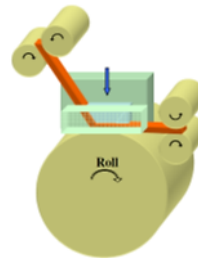
[91]

8 Integrated conventional tandem rolling with ECA deformation (CR-ECA)



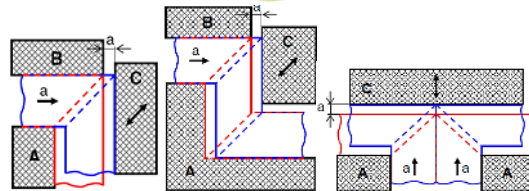
[92]

9 Single roll drive equal channel angular process



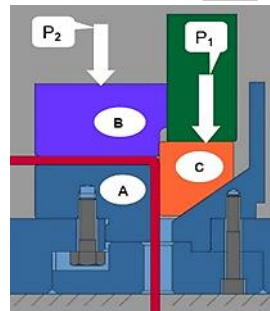
[93]

10 Single/two turn incremental ECAP (I-ECAP); double billet I-ECAP



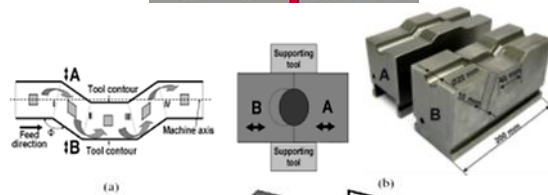
[94,95]

10 Incremental ECAP of plates



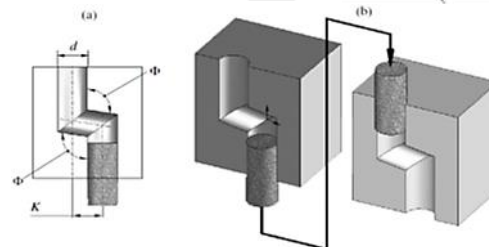
[96]

12 Equal channel angular swaging



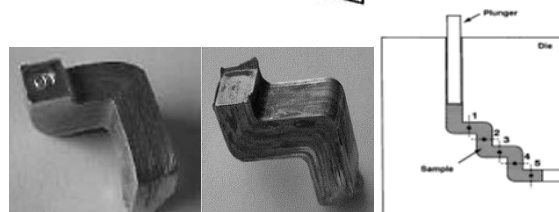
[97]

13 Equal-channel angular pressing in parallel channels



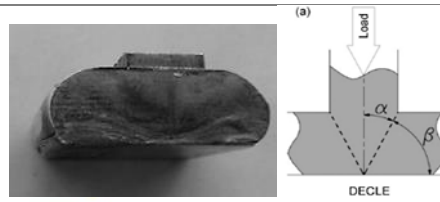
[98]

14 Multi turn/pass ECAP (3D ECAP)



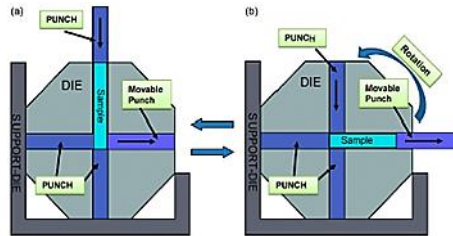
[99,100,80]

15 Dual equal channel lateral extrusion (DECLE)



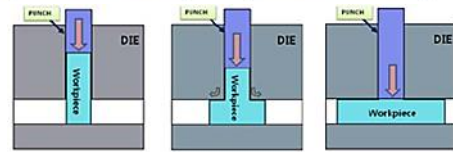
[101]

16 Rotary-fie equal channel angular pressing



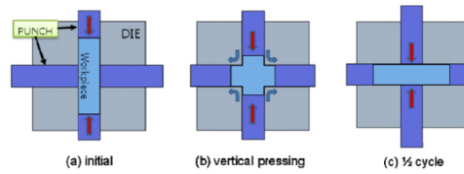
[102,103]

17 T-shaped equal channel angular pressing



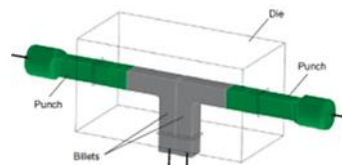
[104,105]

18 Cross-equal channel angular pressing (firstly named as cross-channel extrusion)



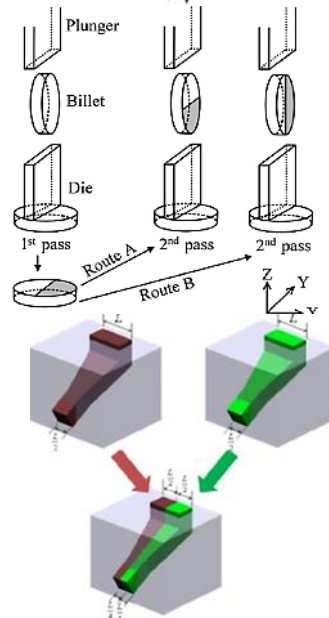
[106,107]

19 ECAP with converging billets



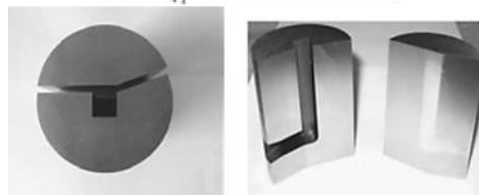
[108]

20 Repetitive upsetting



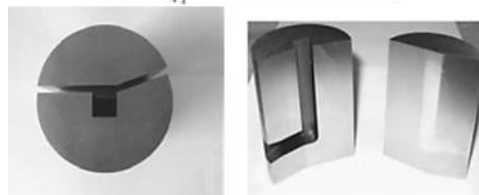
[109]

21 Half channel angular extrusion (HCAE)



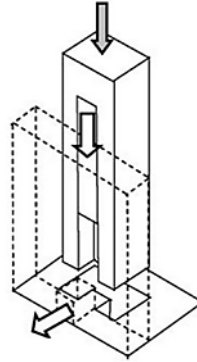
[110]

22 ECAP (New design1)



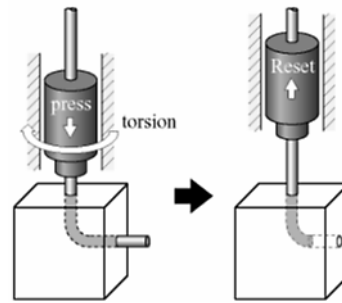
[111]

23 ECAP (New design2)



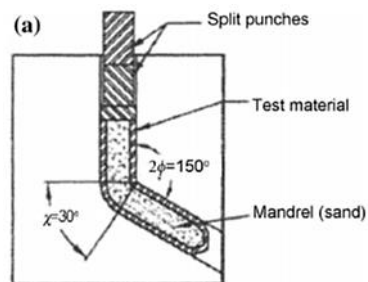
[112]

24 Modified ECAP



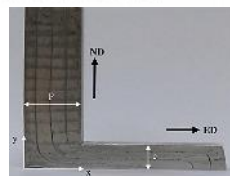
[113]

25 ECAP for processing of tubular samples



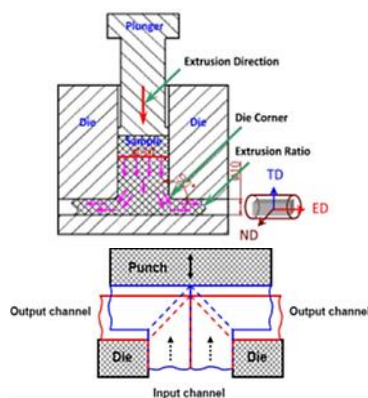
[114,115]

26 Non-equal channel angular pressing / channel angular deformation (CAD)



[116,117]

27 Double change channel angular pressing



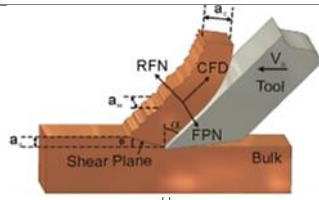
[118]

28 Incremental Angular Splitting



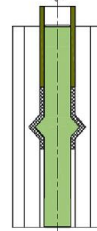
[119]

29 Large machining strain



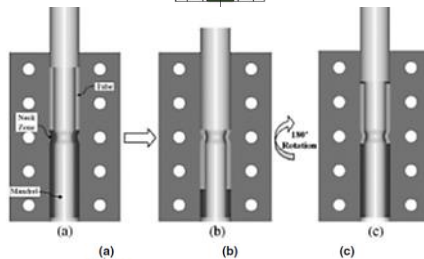
[120,79]

30 Tubular channel angular pressing (TCAP)



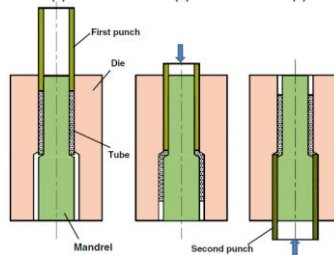
[121]

31 Tube channel pressing (TCP)



[122,123]

32 Parallel tubular channel angular pressing (PTCAP)



[124]

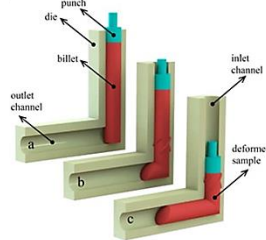
33 Single-roll angular-rolling (SRAR)



[125]

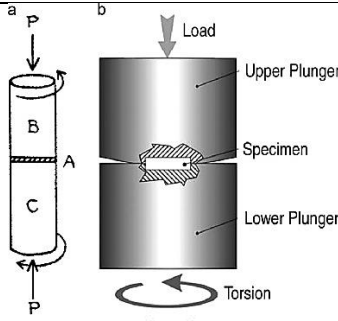
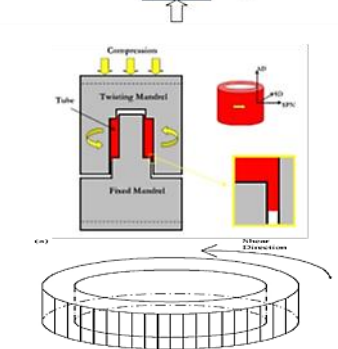
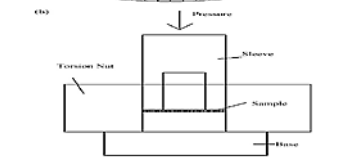
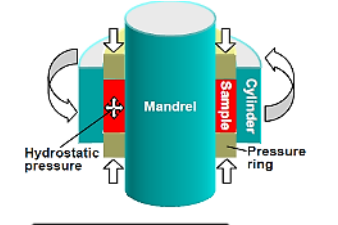
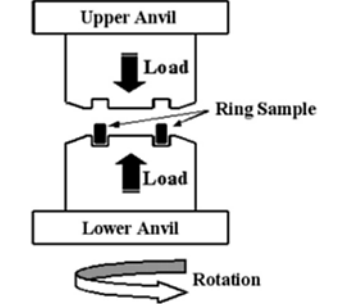
Spiral equal channel

34 angular extrusion (Sp-ECAE)

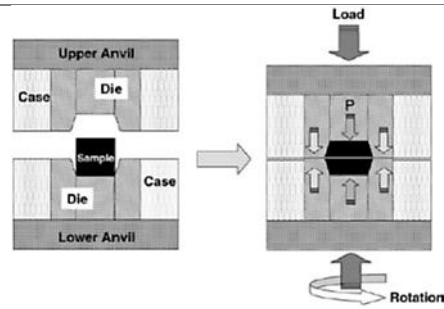


[126]

Table 3. Summary of different SPD techniques based on application of torsion/shear (under high pressure)

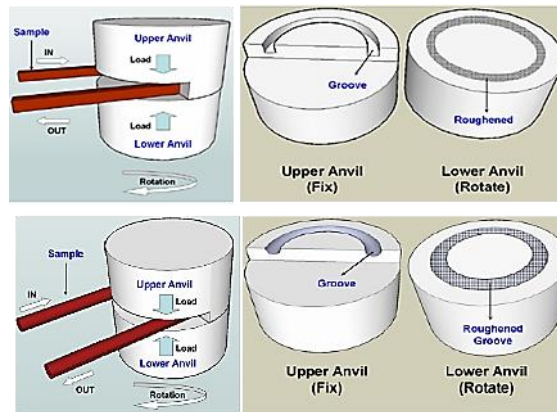
SPD technique	Illustration	[Ref.]
1 High-pressure torsion (HPT)	 <p>The diagram shows a cylindrical specimen placed between an upper plunger and a lower plunger. A downward arrow labeled 'Load' is applied to the upper plunger, and an upward arrow labeled 'P' is applied to the lower plunger. A circular arrow labeled 'Torsion' indicates the direction of twisting. A cross-section of the specimen is shown with regions B, A, and C. Below this, a more detailed view shows the specimen on a mandrel, with a 'right disc' on the left and a 'sample' on the right, all within a 'Compression machine'.</p>	[13,127]
2 High pressure tube twisting (HPTT)	 <p>The diagram illustrates a tube being twisted between a 'Twisting Mandrel' and a 'Fixed Mandrel'. A 'Compression' force is applied to the tube. A 'right disc' is shown on the left, and a 'sample' is on the right. Below, a cross-section of the tube is shown with 'Shear Directions' indicated by arrows. A 'Torsion Notch' is also shown on the tube.</p>	[128,129]
3 Rotation torsion	 <p>The diagram shows a sample placed between a 'Torsion Notch' and a 'Groove'. A 'Pressure' is applied to the sample. A 'Notch' is also shown on the sample.</p>	[130]
4 High-pressure shearing (t-HPS)	 <p>The diagram shows a sample placed between a 'Mandrel' and a 'Cylinder'. 'Hydrostatic pressure' is applied to the sample. A 'Pressure ring' is also shown on the sample.</p>	[131]
5 HPT for ring specimens	 <p>The diagram shows a 'Ring Sample' placed between an 'Upper Anvil' and a 'Lower Anvil'. A 'Load' is applied to the upper anvil, and an upward 'Load' is applied to the lower anvil. A 'Rotation' arrow is shown below the ring sample.</p>	[132]

6 High pressure torsion for bulk samples



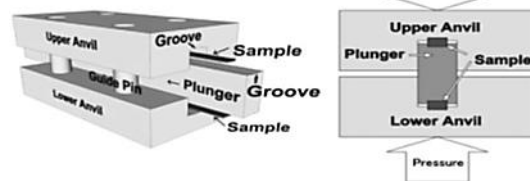
[28]

7 Continuous high-pressure torsion for bars/rods



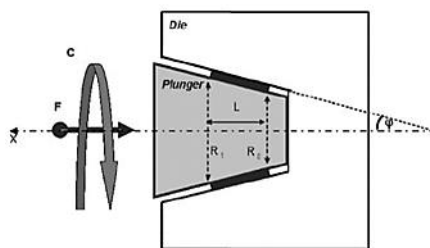
[29,133]

8 High pressure sliding



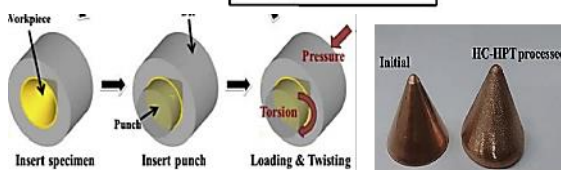
[134]

9 Cone-cone method



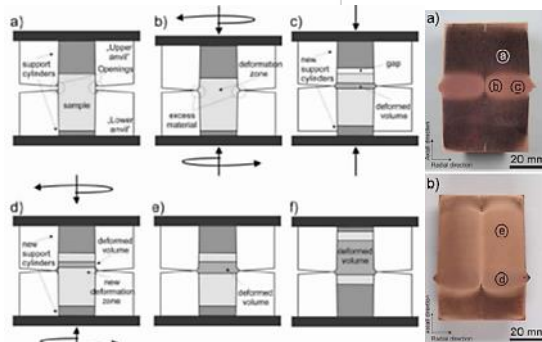
[135]

10 Hollow cone high-pressure torsion



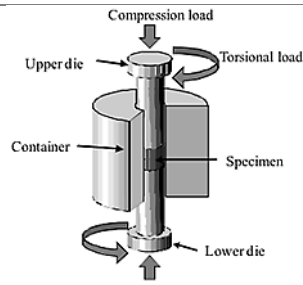
[136]

11 Incremental high pressure torsion



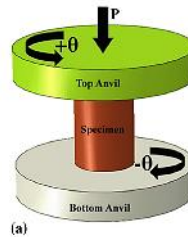
[137]

12 Compressive torsion processing



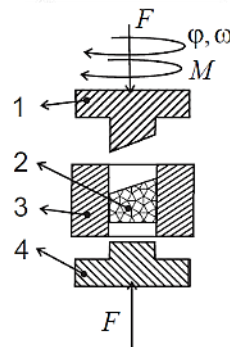
[138]

13 High pressure double torsion (HPDT)



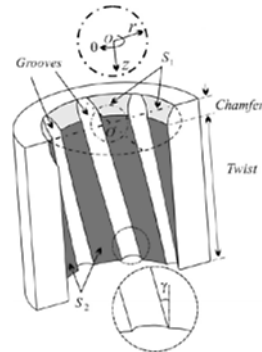
[139]

14 High pressure torsion-cylindrical segment (HPT-CS)



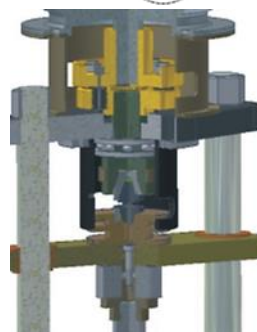
[140]

15 Axi-symmetric forward spiral extrusion (AFSE)



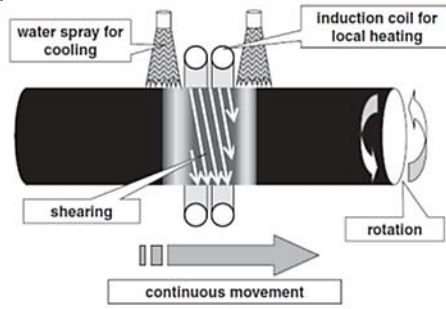
[141]

16 High-speed high pressure torsion (HS-HPT)



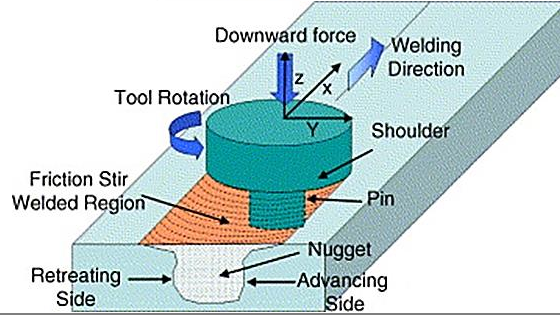
[142]

17 Severe torsion straining (STS)



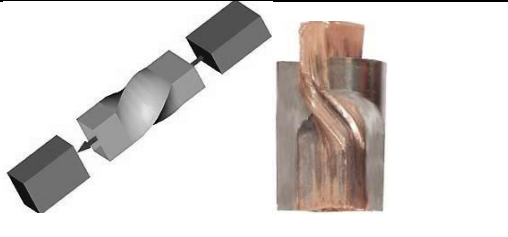
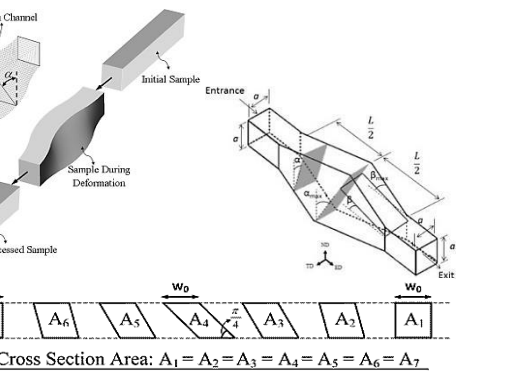
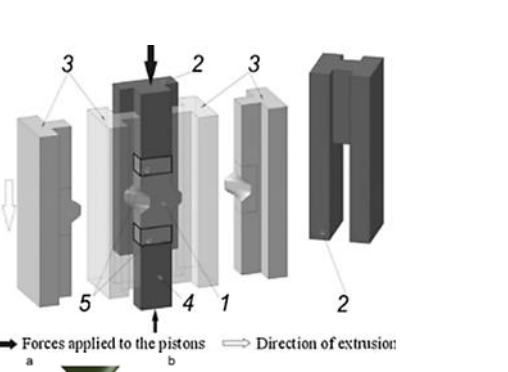
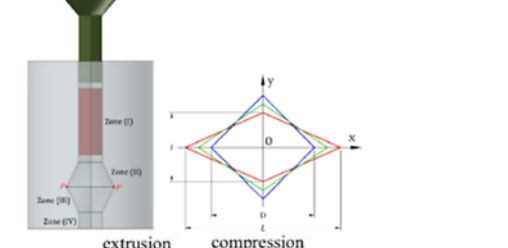
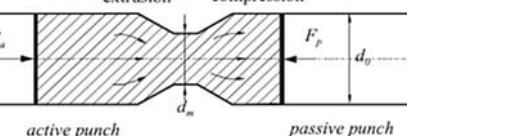
[143]

18 Friction stir processing (FSP)

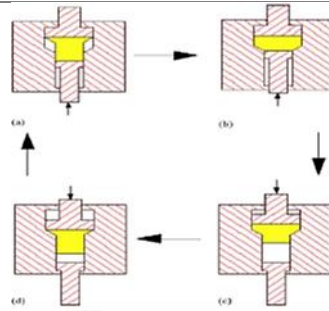


[144,145]

Table 4. Summary of different SPD techniques based on direct/indirect extrusion

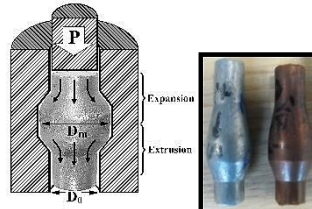
SPD technique	Illustration	[Ref.]
1 Twist extrusion (TE)		[159-166]
2 Simple shear extrusion (SSE)		[146,148]
3 Planar twist extrusion (PTE) (similar to SSE)		[167]
4 Pure shear Extrusion (PSE)		[168]
5 Cyclic extrusion-compression (CEC)		[169]

6 Repetitive upset extrusion (RUE)



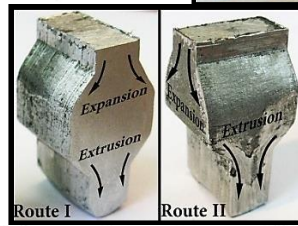
[170-174]

7 Cyclic expansion-extrusion (CEE)



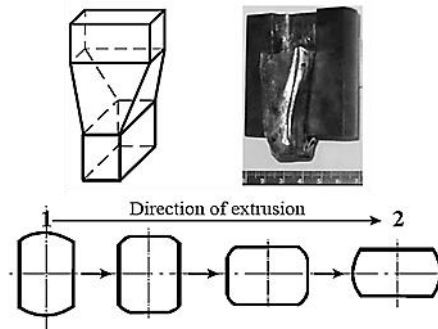
[175,176]

8 Cyclic expansion extrusion (CEE) for rectangular samples



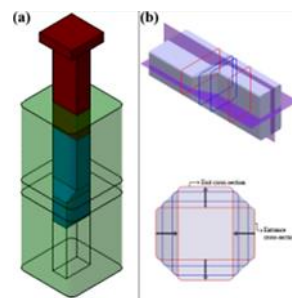
[177]

9 Spread extrusion



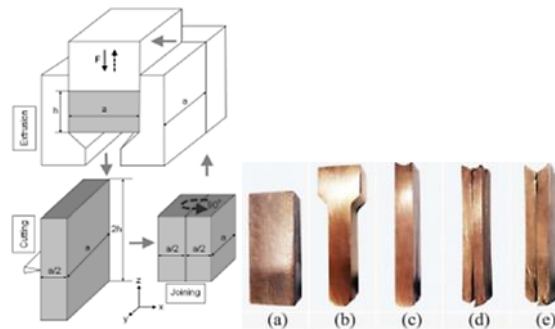
[178]

10 Equal channel forward extrusion (ECFE) (similar to spread extrusion)



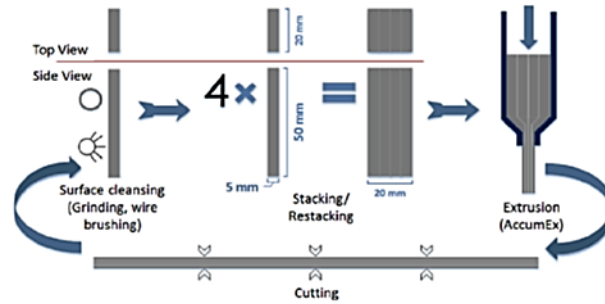
[179]

11 Multiple direct extrusion



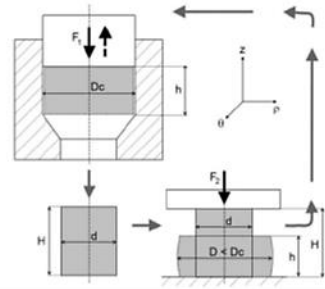
[180]

12 Accumulated extrusion (AccumEx)



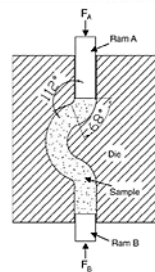
[181]

13 Repetitive extrusion and upsetting



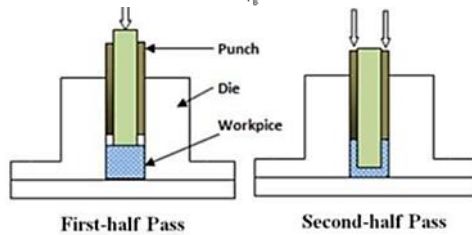
[173]

14 C shape equal channel reciprocating extrusion (CECRE)



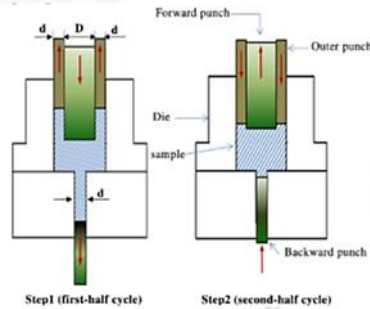
[182]

15 Accumulative back extrusion (ABE)



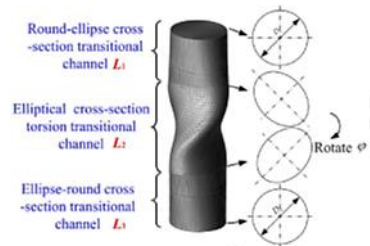
[183]

16 Cyclic forward-backward extrusion



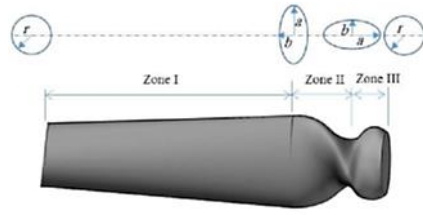
[184]

17 Elliptical cross-section spiral equal-channel extrusion (ECSEE)

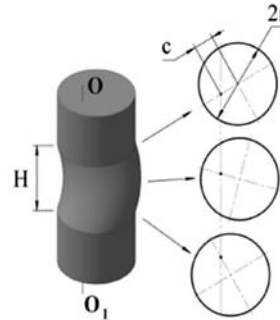


[185]

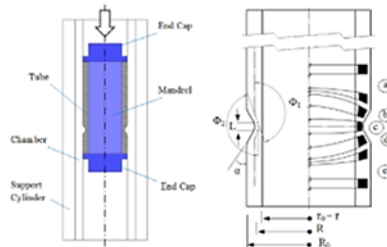
18 Nonlinear rotary extrusion (NRE) (similar to ECSEE) [148]



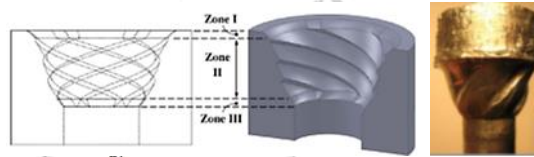
19 Off-axis twist extrusion [186]



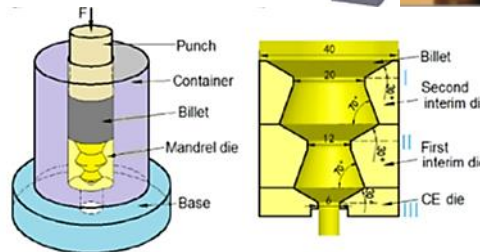
20 Tube cyclic extrusion-compression (TCEC) [187]



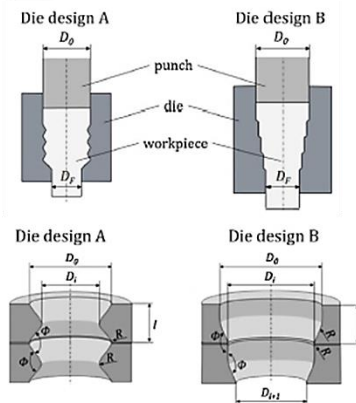
21 Vortex extrusion (VE) [188,189]



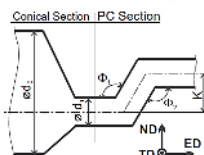
22 Variable cross-section direct extrusion (CVCDE) [190,191]



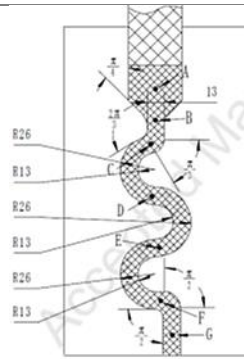
23 Gradation extrusion [192,193]



24 Integrated extrusion [194]

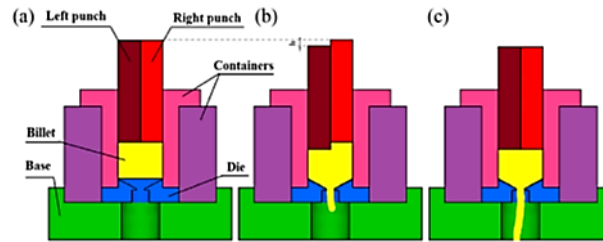


25 Compound
extrusion



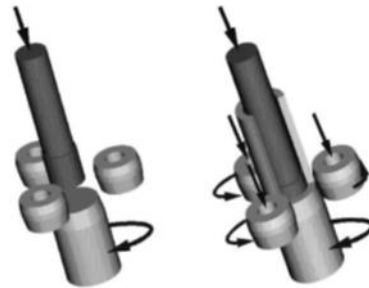
[195]

26 Alternate
extrusion (AE)



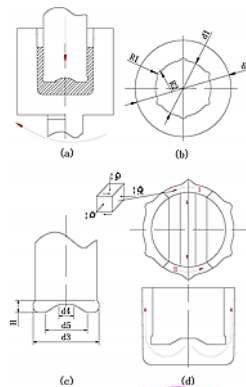
[196]

27 Spin
extrusion



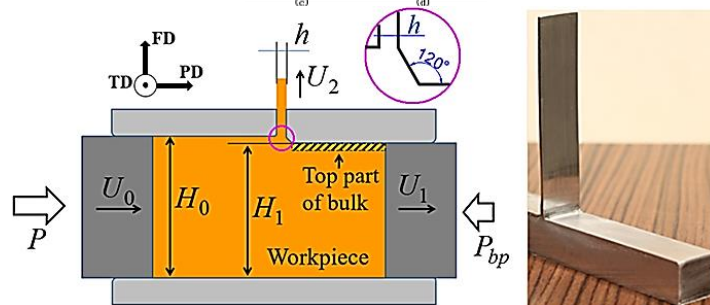
[197]

28 Rotary
extrusion (RT)



[198]

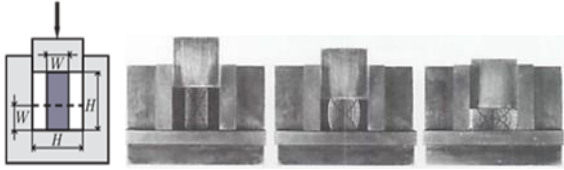
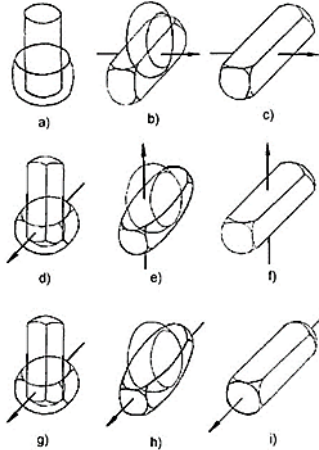
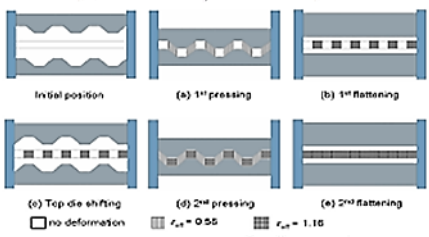
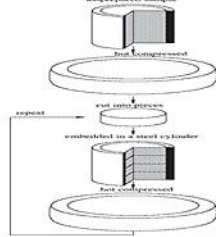
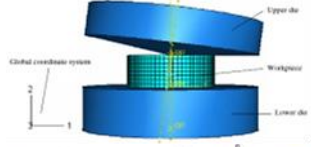
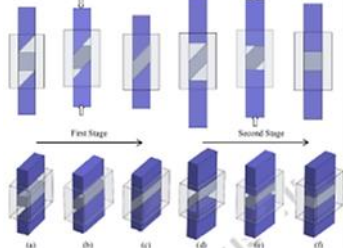
29 Plastic flow
machining (PFM)



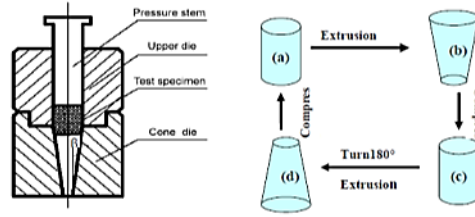
[199]



Table 5. Summary of different SPD techniques based on pressing/forging

	SPD technique	Illustration	[Ref.]
1	Multi axial forging/compression; Cyclic closed-die forging(CCDF)		[200-202]
2	Multi axial forging (open die)		[203-206]
3	Constrained groove pressing (CGP)		[207-209]
4	Cylinder covered compression (CCC)		[210]
5	Orbital rotary forging		[211,212]
6	Repetitive forging (RF)		[213]

7 Continuous variable cross-section Recycled extrusion (CVCE)



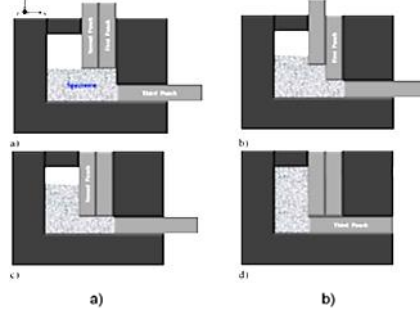
[214]

8 MAX strain (multi-axis deformation system)



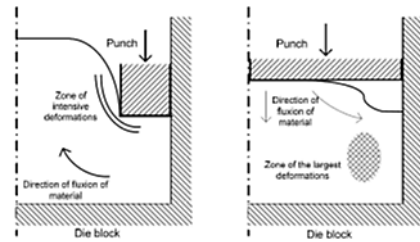
[88,215]

9 Multi-axial incremental forging & shearing (MAIFS)



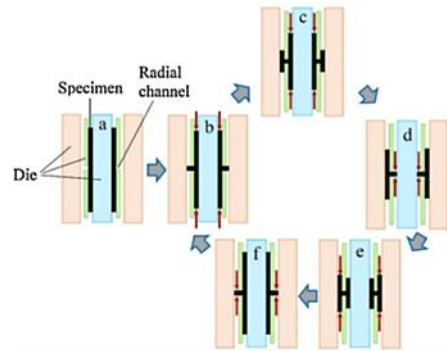
[216]

10 Alternate pressing & multi-axial compression



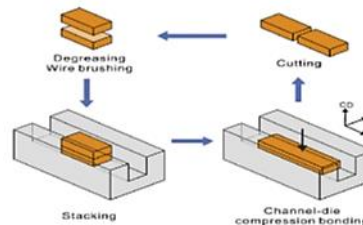
[217]

11 H-tube pressing (HTP)



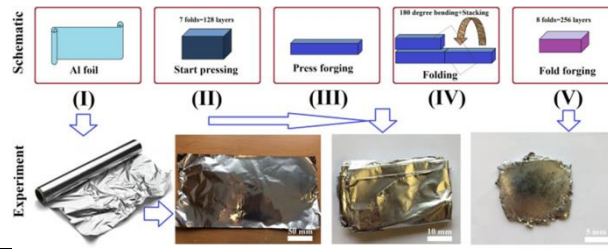
[218]

12 Accumulative channel-die compression bonding (ACCB)



[219]

13 Accumulative fold-
forging (AFF)

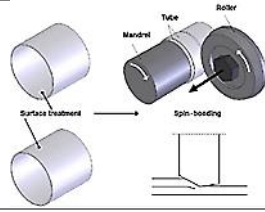


[220]

Table 6. Summary of different SPD techniques based on rolling

SPD technique	Illustration	[Ref.]
1 Accumulative roll-bonding (ARB)		[14]
2 Repetitive corrugation & straightening (RCS)		[221]
3 Repetitive corrugation & straightening by rolling		[222]
4 Continuous cyclic bending (CCB)		[223]
5 Asymmetric rolling		[224,225]
6 New asymmetrical rolling		[226]

7 Accumulative
spin bonding
(ASB)



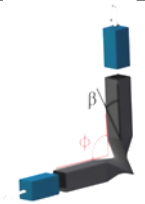
[227]

Table 7. Combined SPD techniques

	SPD technique	Illustration	[Ref.]
1	Torsional-equal channel angular pressing (T-ECAP) {ECAP+Torsion}		[228]
2	Twist channel angular pressing (TCAP) {ECAP+TE}		[229,230]
3	ECAP forward extrusion (ECAP-FE)		[231]
4	Forward extrusion ECAP (FE-ECAP)		[232]
5	Twist channel multi-angular pressing (TCMAP) {TE+MECAP}		[233]
6	Planar twist channel angular extrusion (PTCAE) {ECAP+SSE}		[234]

7

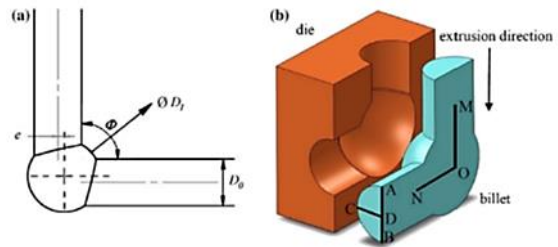
Symmetrical channels angular pressing (SCAP) {TE+ECAP+TE}



[235]

8

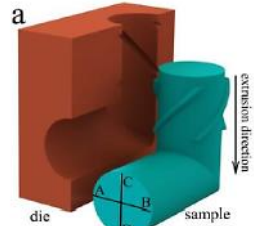
Expansion equal channel angular extrusion {ECAP+CEE}



[236]

9

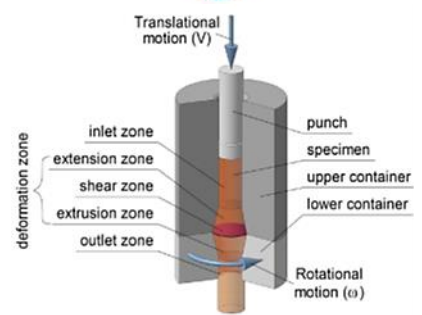
Spiral equal channel angular extrusion (Sp-ECAE)



[126]

10

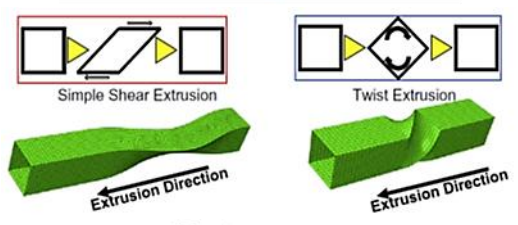
High pressure torsion extrusion {CEE+HPT}



[237]

11

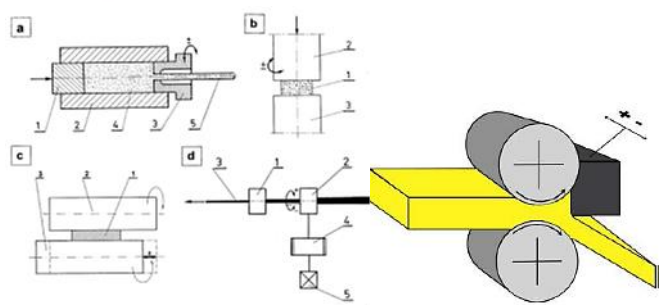
Tandem process of simple shear extrusion & twist extrusion (TST)



[157]

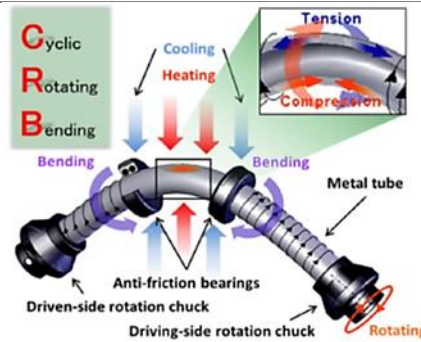
12

KOBO method



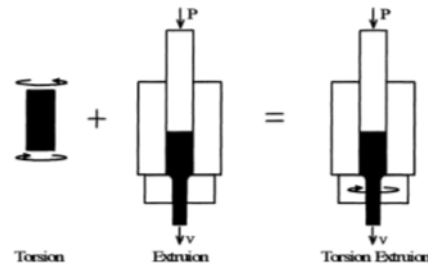
[238]

13 Cyclic rotating bending (CRB)



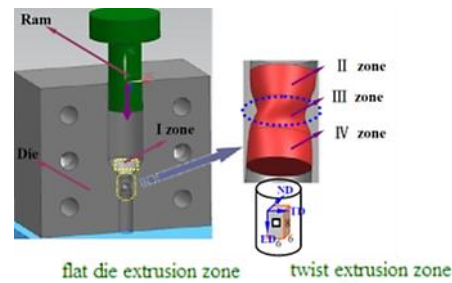
[239]

14 Torsion extrusion



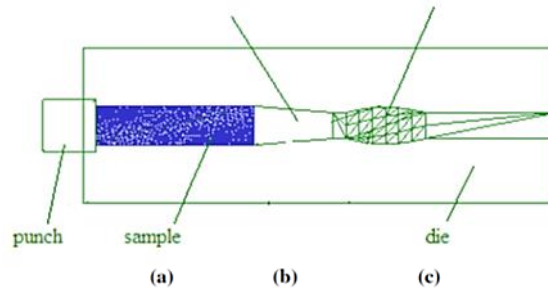
[240,241]

15 Integrated forward extrusion & torsion deformation method



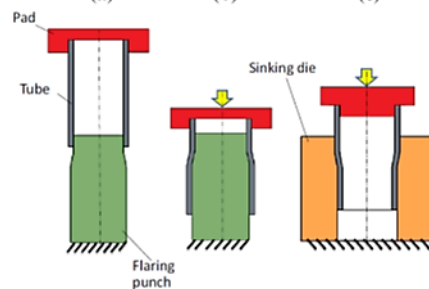
[242]

16 Compound twist extrusion/C-TE (TE+Ext.)



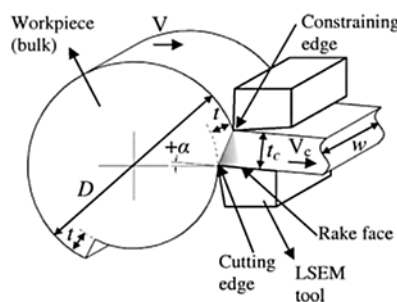
[243]

17 Cyclic flaring and sinking (CFS)



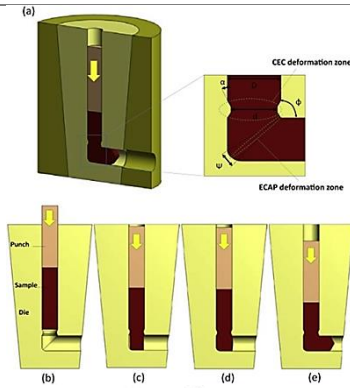
[244]

18 Large strain extrusion machining (LSEM)



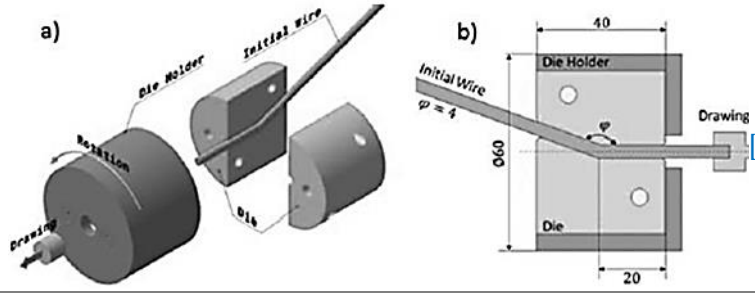
[245]

19 Cyclic extrusion
compression
angular pressing
(CECAP)



[246]

20 Equal channel
angular torsion
drawing
(ECATD)



[247]